Extracellular Electron Transfer of Lactococcus lactis

Fundamentals and Applications

Gu, Liuyan

Publication date:
2023

Document Version
Publisher's PDF, also known as Version of record

Extracellular Electron Transfer of *Lactococcus lactis*: Fundamentals and Applications

PhD thesis

Liuyan Gu

Technical University of Denmark

National Food Institute

Microbial Biotechnology and Biorefining

October, 2023

Extracellular Electron Transfer of *Lactococcus lactis*:

Fundamentals and Applications

PhD thesis

October 2023

Liuyan Gu

liugu@food.dtu.dk

Main supervisor:

Assoc. Prof. Christian Solem

Co-supervisors:

Prof. Sang Yup Lee

Senior Researcher Jianming Liu

Preface

This dissertation serves as a partial fulfillment of the requirements for obtaining the doctor's degree of philosophy at the PhD School of the Technical University of Denmark. The work was carried out in the Research Group for Microbial Biotechnology and Biorefining at the National Food Institute, Technical University of Denmark, under the supervision of Assoc. Prof. Christian Solem, Prof. Sang Yup Lee and Senior Researcher Jianming Liu. During the PhD project, three months were spent at Helmholtz Centre for Environmental Research-UFZ, Germany. In this project, the fundamentals and applications of extracellular electron transfer in *Lactococcus lactis* were investigated. The project was funded by a DTU PhD scholarship and the Otto Mønsted foundation.

Liuyan Gu

October 2023

Table of contents

Summary

The Gram-positive bacterium, *Lactococcus lactis*, plays an immensely important industrial role in food fermentation processes. *L. lactis* normally relies on a fermentative metabolism under anaerobic conditions, where NADH generated by glycolysis is re-oxidized into NAD^+ by the lactate dehydrogenase, converting more than 90% of the metabolized sugar into lactate. Despite of its fermentative metabolism, *L. lactis* can also use oxygen as an electron acceptor. There are two ways, in which oxygen can serve as an electron acceptor to oxidize NADH: through the H_2O-forming NADH oxidase (NoxE), or via respiration in the presence of heme, its precursor protoporphyrin IX or hemin. When *L. lactis* grows with respiration, less ATP is spent on generating the essential proton electrochemical gradient, which increases the biomass yield. For this reason, starter culture manufacturers often harness respiration when culturing *L. lactis*. However, the use of animal blood, as a source of heme, in microbial food cultures can be unwanted for some customers. Moreover, there are challenges associated with using oxygen as electron acceptor, e.g. its low solubility in the fermentation broth can be a major limitation for microbial growth and production, microorganisms can be oxidatively stressed by it, and supplying oxygen/air is costly as pumping and stirring oxygen into the fermentation broth requires a lot of electrical energy.

The aim of this PhD project was to investigate the possibility of replacing oxygen with an alternative electron acceptor for regeneration of NAD^+, which has been termed extracellular electron transfer (EET). First, we explored the effects of extracellular electron acceptor ferricyanide on the wild-type *L. lactis* MG1363 and a mutant of *L. lactis*, CS4363, blocked in NAD^+ regeneration. We tested the electron acceptor ferricyanide, which supported good growth of CS4363, which has not been reported previously. When growth was facilitated by EET, we observed that cell morphology was altered from the normal coccoid to a more rod-shaped appearance, and acid resistance was increased. By electrochemical analysis and knock-out of possible relevant genes in EET, we found that the NADH dehydrogenase and 2-amino-3-carboxy-1,4-naphthoquinone (ACNQ) were important in EET. To enhance the capacity of EET, adaptive laboratory evolution (ALE) was performed for CS4363, and EET-enhanced mutant CS4363-F2 was further characterized physiologically.

To figure out the underlying mechanism of the enhanced capacity for EET in mutant CS4363-F2, the strain was whole-genome sequenced and a comparative transcriptomics analysis was carried out. It was found that the amino acid metabolism and nucleotide metabolism had changed significantly in CS4363-F2. The gene *noxB*, encoding NADH dehydrogenase, was found to be most upregulated ($log_2FC=3.56$), and the reason for this was a single-nucleotide variation (SNV) in its promoter region. NoxB was found to differ from the other NADH dehydrogenase, NoxA, of *L. lactis*, and was demonstrated to be a novel type II NADH dehydrogenase solely involved in EET. A bioinformatics study revealed that NoxB-type NADH dehydrogenases could be found widely distributed in other *L. lactis* strains and members of the gut microbiota.

Finally, we explored whether it was possible to support the growth of CS4363 and its EET-enhanced mutant by an anode in a bioelectrochemical system (BES) setup. The ALE mutant CS4363-F2 displayed a remarkable performance, producing a high-yield bulk chemical 2,3-butanediol and achieving a record high current density of 0.809 ± 0.051 mA/cm^2.

This study has shed light on the fundamental mechanism of EET in *L. lactis*, and has revealed the feasibility of using anodic electro-fermentation (AEF) to grow *L. lactis*, thereby demonstrating the enormous potential of AEF in the fermentation industry.

Dansk resume

Den Gram-positive bakterie, *Lactococcus lactis*, spiller en enormt vigtig rolle i fødevarefermenteringsprocesser. *L. lactis* er i besiddelse af en fermentativ metabolisme under anaerobe forhold, hvor NADH genereret i glykolysen re-oxidiseres til NAD^+ af laktat dehydrogenase hvilket resulterer omdanner mere end 90% af den metaboliserede sukker til laktat. På trods af sin fermentative metabolisme kan *L. lactis* også bruge ilt som elektronacceptor. Der er to måder, hvorpå ilt kan fungere som elektronacceptor således at NADH kan blive oxideret: via den H_2O-dannende NADH-oxidase (NoxE) eller via respirationen i nærværelse af hæm, protoporphyrin IX eller hæmin. Når *L. lactis* vokser respiratorisk bruges der mindre ATP på at generere den essentielle protongradient, hvilket øger biomassen. Af denne grund udnytter startkultureproducenter ofte respiration, når de dyrker *L. lactis*. Dog kan brugen af animalsk blod som en kilde til hæm i mikrobielle fødevarekulturer være uønsket for nogle kunder. Der er dog udfordringer forbundet med brugen af ilt, såsom dets lave opløselighed i vækstmediet, hvilket kan begrænse mikrobiel vækst og produktion, mikroorganismer kan lide overlast pga. oxidativt stress påført af ilt og der er omkostninger forbundet med at belufte vækstmediet da der skal bruges energi til at pumpe luft/it samt til omrøring.

Målet med dette ph.d.-projekt var at undersøge muligheden for at erstatte ilt med alternative elektronacceptorer til regenerering af NAD^+, hvilket kaldes ekstracellulær elektronoverførsel (EET). Først undersøgte vi virkningerne af elektronacceptoren ferricyanid på vildtypen *L. lactis* MG1363 og mutanten *L. lactis* CS4363, med en blokeret NAD^+ regenerering. Ferricyanid viste sig at understøtte væksten af CS4363, hvilket ikke er demonstreret tidligere. EET med ferricyanid havde nogle uventede effekter, f.eks. ændrede *L. lactis* morfologi fra normal kokformet til et mere stavformet udseende, og tolerance til lavt pH blev øget. Ved elektrokemisk analyse og genetisk arbejde fandt vi ud af, at NADH-dehydrogenase og 2-amino-3-carboxy-1,4-naphtochinon (ACNQ) var vigtige for EET. For at øge kapaciteten til EET blev der udført adaptiv laboratorieevolution (ALE) på CS4363, hvormed dens EET-forbedret mutant CS4363-F2 blev genereret. Denne blev yderligere karakteriseret fysiologisk.

For at finde årsagen til den øgede kapacitet for EET-forbedring i mutanten CS4363-F2, blev dens genom sekventeret og der blev foretaget en transskriptomanalyse hvor mutanten blev sammenlignet med vildtypestammen. Det viste sig at aminosyremetabolismen og

nukleotidmetabolismen havde ændret sig markant i CS4363-F2. Udtrykket af *noxB*, der koder for en NADH-dehydrogenase, viste sig at være mest opreguleret ($log_2FC=3.56$), og årsagen hertil blev fundet at væres en mutation i promoterregionen af *noxB*. Senere blev det vist at NoxB var en ny type II NADH-dehydrogenase der udelukkende var involveret EET, i modsætning til den anden NADH dehydrogenase i *L. lactis*, NoxA der er involveret i ilt-respiration. Ved hjælp af bioinformatikanalyse blev det fundet, at NoxB-type NADH dehydrogenase forekommer i mange organismer, ikke kun i *L. lactis*, men også i mange af de mikroorganisker der findes i tarmen.

Til sidst blev det undersøgt om væksten af CS4363 of dens EET adapterede mutant kunne understøttes af en anode i et bioelektrokemisk system (BES). ALE-mutanten CS4363-F2 udviste en bemærkelsesværdig ydelse, idet den producerede en høj mængde af forbindelsen 2,3-butanediol og opnåede en rekordhøj strømtæthed på 0.809 ± 0.051 mA/cm^2.

Dette studie kaster lys over den grundlæggende mekanisme for EET i *L. lactis* og udforsker potentialet i at benytte anodisk elektrofermentering til at dyrke mikroorganismer (AEF).

Acknowledgments

Time flies, and my doctoral studies are nearing the end. I still remember the excitement I felt one early morning in June 2020 when I opened my email and saw the interview invitation. This short yet enriching journey has been made possible thanks to the support of so many people, and I am truly grateful. It is because of your help that I have been able to complete my PhD study.

First and foremost, I would like to express my gratitude to my main supervisor, Christian Solem. I feel incredibly fortunate to have been given this valuable opportunity to pursue a PhD under his guidance. I learned a lot from him. He always has a wealth of ideas to stimulate my thinking. Moreover, he is always there to encourage and support me. He once told me, “research is re-search, ” and this has left a profound impression on me. Under his guidance, I have come to understand what real research is.

I would also like to thank my co-supervisor, Sang Yup Lee from the Korea Advanced Institute of Science and Technology, whose extensive knowledge has provided me with useful insights into my work. I am grateful to my other co-supervisor, Jianming Liu. When I joined the lab, he offered me valuable advice on research.

Besides my supervisors, I want to extend special thanks to Xinxin Xiao from Aalborg University and Bin Lai from Helmholtz Centre for Environmental Research-UFZ. Xinxin taught me the fundamentals of electrochemistry. Thanks to Bin for hosting me during my external study. I am grateful for his guidance in assembling reactors and for teaching me to analyze electro-fermentation processes through systems biology methods. Their assistance has been indispensable in completing my research, and I am honored to have worked with these two outstanding researchers from whom I have learned so much.

I want to express my gratitude to all the members of the Microbial Biotechnology and Biorefining group. Thank you for our encounters over these three years. Thanks to Peter for building this nice and big group. Thanks to Fa, my lunch companion for most of the time, for the many meaningful and meaningless discussions we've had, and for sending me SALN media when I urgently needed them in Germany. Thanks to Shuangqing, and Belay, for our enjoyable Friday’s meetings and discussions. Thanks to Ge for teaching me genome sequencing analysis. Thanks to Sanne for the warm spring festival greetings every year. Additionally, I want to thank Tine, Hang, Mathieu,

Timothy, Suvasini, Anders, Emmelie, Celia, Mikkel, Blandine, Evangelia, Norbert, Lorenzo, Guillermo, Radhakrishna, Quoc and Hanne.

I want to thank Minmin Pan, Jianqi Yuan and Laura Pause for their help in analytics and lab experiments during my external stay at Helmholtz Centre for Environmental Research–UFZ. Thanks to Paul Kempen from DTU Nanolab for helping me with SEM experiments.

I also want to thank my family and friends for their understanding and support during my studies in a foreign land. Special thanks to Xiyuan for your optimistic attitude and encouragement, which helped me through stressful times.

Lastly, I want to thank myself. Like my *L. lactis*, I also became more and more 'robust' after the adaptive evolution during my PhD study.

"Freedom through truth."

List of publications

Publications in peer-reviewed journals as part of this PhD thesis:

1) **Gu LY**, Xiao XX, Zhao G, Kempen PJ, Zhao SQ, Liu JM, Lee SY, Solem C*. 2023. Rewiring the respiratory pathway of *Lactococcus lactis* to enhance extracellular electron transfer. *Microb Biotechnol* 16 (6):1277-1292.

2) **Gu LY**, Xiao XX, Lee SY, Lai B*, Solem C*.2023. Superior anodic electro-fermentation by enhancing capacity for extracellular electron transfer. *Bioresour Technol* 389: p129813.

3) **Gu LY**, Zhao SQ, Tadesse BT, Zhao G, Solem C*.2023. Scrutinizing a *Lactococcus lactis* strain with enhanced capacity for extracellular electron transfer reveals a unique role for a novel type II NADH dehydrogenase. (in preparation)

Research articles published during the PhD study but not as part of this PhD thesis:

4) **Gu LY**, Tadesse BT, Zhao SQ, Holck J, Zhao G, Solem C*. 2022. Fermented butter aroma for plant-based applications. *FEMS Microbiol Lett* 369:1-7.

5) Zhao G, Kempen PJ, Shetty R, **Gu LY**, Zhao SQ, Jensen PR*, Solem C.2022. Harnessing cross-resistance – sustainable nisin production from low-value food side streams using *a Lactococcus lactis* mutant with higher nisin-resistance obtained after prolonged chlorhexidine exposure. *Bioresour Technol* 348: p126776.

6) Zhao G, Kempen PJ, Zeng T, Jakobsen TH, Zhao SQ, **Gu LY**, Solem C*, Jensen PR*.2022. Synergistic bactericidal effect of nisin and phytic acid against *Escherichia coli* O157:H7. *Food Control* 144(8): p109324.

7) Zhao SQ, Zhao G, **Gu LY**, Solem C*. 2022. A novel approach for accelerating smear development on bacterial smear-ripened cheeses reduces ripening time and inhibits the growth of *Listeria* and other unwanted microorganisms on the rind. *LWT* 170(7): p114109.

8) Zhao G, Zhao SQ, Nielsen LH, Zhou F, **Gu LY**, Tadesse BT, Solem C*. 2023. Transforming acid whey into a resource by selective removal of lactic acid and galactose using optimized food-grade microorganisms. *Bioresour Technol* 387: p129594.

9) Zhao SQ, Dorau R, Tømmerholt L, **Gu LY**, Tadesse BT, Zhao G, Solem C*. 2023. Simple & better – Accelerated cheese ripening using a mesophilic starter based on a single strain with superior autolytic properties. *Int J Food Microbiol* 407(10): p110398.

International conferences:

1) 14th International Symposium on Lactic Acid Bacteria, 27-31 August, 2023, Netherlands. Poster flash. Poster title: Rewiring the respiratory pathway of *Lactococcus lactis* to enhance extracellular electron transfer.

2) Institute Conference Healthy, Safe and Sustainable Food of the Future, 13 October, 2022, Denmark. Oral presentation: Production of food ingredients using novel and more sustainable fermentation technologies.

Outline of the thesis

Chapter 1

Background of the study. This chapter begins with a brief introduction of lactic acid bacteria, especially *L. lactis*, focusing on its respiratory metabolism. This chapter also introduces extracellular electron transfer (EET) and its application as anodic electro-fermentation with different bacteria as examples.

Chapter 2

This chapter consists of the paper "Rewiring the respiratory pathway of *Lactococcus lactis* to enhance extracellular electron transfer". The effects of extracellular electron acceptor ferricyanide on the *L. lactis* MG1363 and its mutant CS4363 which is blocked in NAD^+ regeneration are investigated. By electrochemical analysis and genome engineering, the mechanism of EET is explored. The capacity of EET is enhanced by adaptive laboratory evolution (ALE) and the underlying reason is revealed by whole-genome sequencing.

Chapter 3

This chapter consists of the manuscript "Scrutinizing a *Lactococcus lactis* strain with enhanced capacity for extracellular electron transfer reveals a unique role for a novel type II NADH dehydrogenase". Cell metabolism change is elucidated by comparative transcriptomics analysis. The expression regulation and functions of a novel type-II NADH dehydrogenase are explored.

Chapter 4

This chapter consists of the paper "Superior anodic electro-fermentation by enhancing capacity for extracellular electron transfer". The growth and metabolic profiles of *L. lactis* CS4363 and its ferricyanide adapted version CS4363-F2 in a bioelectrochemical system setup where an anode functions as the electron sink.

Chapter 5

This chapter concludes the results and discusses future perspectives.

Frequently occurred abbreviations

LAB	lactic acid bacteria
L. lactis	*Lactococcus lactis*
IS	insertion sequence
PEP	phosphoenolpyruvate
PTS	phosphotransferase
GAPDH	glyceraldehyde-3-phosphate dehydrogenase
LDH	lactate dehydrogenase
PDHc	pyruvate dehydrogenase complex
NoxE	NADH oxidase
ADHE	alcohol dehydrogenase
PYK	pyruvate kinase
PFL	pyruvate-formate lyase
ALD	acetolactate decarboxylase
ButBA	2,3-butanediol dehydrogenase
MK	menaquinone
ROS	reactive oxygen species
EET	extracellular electron transfer
DET	direct electron transfer
IET	indirect electron transfer
PG	peptidoglycan
WTAs	wall teichoic acids
LTAs	lipoteichoic acids
DMK	demethylmenaquinone
ACNQ	2-amino-3-dicarboxy-1,4-naphthoquinone
DHNA	1,4-dihydroxy-2-naphthoic acid
BES	bioelectrochemical system
AEF	anodic electro-fermentation
CEF	cathodic electro-fermentation

CHAPTER 1. Introduction

1.1 Lactic acid bacteria and their applications

Lactic acid bacteria (LAB) consist of a group of Gram-positive, nonsporulating, catalase-negative, low G+C content, acid-tolerant bacteria that form lactate as the major product of hexose sugar fermentation. Typical LAB belong to the *Lactobacillales* order, but still a few LAB belong to the *Actinobacteria* order (1). *Lactobacillales* order can be further classified into 6 families: *Aerococcaceae, Carnobacteriaceae, Enterococcaceae, Lactobacillaceae, Leuconostocaceae* and *Streptococcaceae*. Detailed taxonomic outline of LAB of the order *Lactobacillales* is listed in **Table 1.1**. Although LAB consist of 33 genera, LAB can be grouped as either homofermenters or heterofermenters based on the final products. In homofermentation, lactate is the major product. While in heterofermention, in addition to lactate, acetate, ethanol, CO_2 or aroma compounds can be produced (2).

Table 1.1 Taxonomic outline of LAB of the order *Lactobacillales* in the *Clostridium* branch.

Family	Genus
Aerococcaceae	*Abiotrophia, Aerococcus, Dolosicoccus, Eremococcus, Facklamia, Globicatella , Ignavigranum*
Carnobacteriaceae	*Alkalibacterium, Allofustis, Alloiococcus, Atopobacter, Atopococcus, Atopostipes, Carnobacterium, Desemzia, Dolosigranulum, Granulicatella, Isobaculum, Marinilactibacillus, Trichococcus*
Enterococcaceae	*Enterococcus, Melissococcus, Tetragenococcus, Vagococcus*
Lactobacillaceae	*Lactobacillus, Paralactobacillus, Pediococcus*
Leuconostocaceae	*Leuconostoc, Oenococcus, Weissella*
Streptococcaceae	*Lactococcus, Lactovum, Streptococcus*

LAB are widespread in various environments with a rich nutrition supply, such as plants (cabbage, corn, barley, grapes, mashes), meat, and dairy. Besides, mucosal surfaces, particularly the gastrointestinal tract, are also the habitats (3). LAB contain valuable nonpathogenic microorganisms associated with food fermentations, some strains even are probiotics. However, some pathogens for human or animals (e.g. some *Enterococcus* species) are also involved in LAB (4, 5).

The nonpathogenic LAB make great contributions to the fermentation and preservation of food (6, 7) **(Fig. 1.1)**. Due to the characteristic of lactic acid production, the most common application of LAB is as starter cultures in fermented dairy products (e.g. cheese, fermented milk, and yogurt), fermented fish, fermented meat, picked vegetables and cereal products. LAB can also be used as secondary cultures or adjunct cultures which are added at some point in the fermentation process to contribute to the extra values (e.g. flavor, nutrition, and texture) of fermented products. For example, a non-starter culture LAB with a comprehensive proteinase/peptidase system play a key role in the flavor development of cheese (8). Some LAB can work as probiotics contributing a beneficial effect to the health of the host animals. The most extensively studied species of LAB probiotics include *Lacticaseibacillus casei*, *Lactiplantibacillus plantarum*, *Lactobacillus acidophilus*, *Limosilactobacillus reuteri*, *Lactococcus lactis*, *Leuconostoc mesenteroides*, etc (9). These LAB probiotics show good impacts in various aspects, such as allergies, cholesterol assimilation, obesity treatment, and so on (10–12). In addition, LAB are widely used in biopreservation to prolong the shelf life and enhance food safety. LAB with antimicrobial properties usually can produce antimicrobial active metabolites such as organic acids (mainly lactic acid and acetic acid), hydrogen peroxide, bacteriocins and antifungal peptides. A natural biopreservative nisin is the best-known bacteriocin and is licensed in more than 50 countries, making a significant contribution to the food industry (13). Currently, the use of nisin has been further expanded to biomedical applications (14).

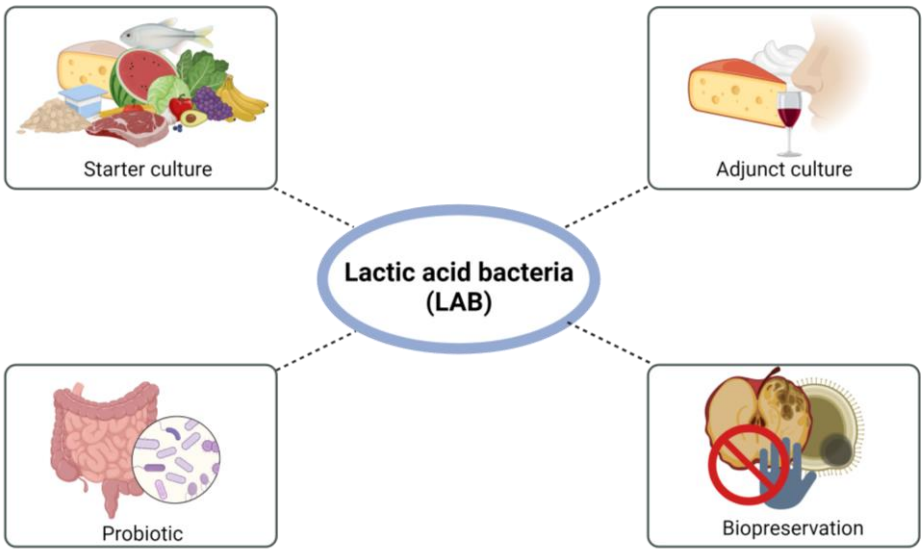

Fig. 1.1 The applications of nonpathogenic LAB. Created with BioRender.com.

1.2 *Lactococcus lactis*

Lactococcus lactis, a representative member of LAB, has been used in food fermentation for centuries. It is Generally Recognized as Safe (GRAS) status by the Food and Drug Administration (FDA) and Qualified Presumption Safety (QPS) status by the European Food Safety Authority (EFSA). The cell morphology of lactococci is usually spherical or ovoid with a diameter of 0.5-1.5 μm. The temperature for growth usually can range from 10 to 40°C, while the optimal growth temperature is 30°C (15). With the development of system biology, the understanding of *L. lactis* physiology and metabolism is becoming clearer (16).

1.2.1 Classifications and Genomics

1.2.1.1 Classifications

L. lactis can be classified within the *Streptoccaceae* family and has four subspecies: *L. lactis* subsp. *lactis* (including *lactis* biovar diacetylactis), *L. lactis* subsp. *cremoris*, *L. lactis* subsp. *hordniae* and *L. lactis* subsp. *tructae* (15). Among them, *L. lactis* subsp. *lactis* and *L. lactis* subsp. *cremoris* are the main well-studied subspecies and they are estimated to diverge around 17 million years ago based on 16sRNA gene sequences. The traditional differentiation between these two subspecies relies on phenotypic traits and their adaptive stress response. These distinctions include the ability of *L. lactis* subsp. *lactis* to produce ammonia from arginine, it's tolerant to higher temperatures and salt concentrations, and the presence of glutamate decarboxylase (GAD) activity. Conversely, *L. lactis* subsp. *cremoris* lacks these characteristics and demonstrates lower tolerance to elevated temperatures and salt levels. Additionally, their adaptive responses to stress factors such as lethal pH, bile-salt and cold stress are also different, with *L. lactis* subsp. *lactis* exhibiting greater adaptability (17, 18). However, some isolates of *L. lactis* subsp. *cremoris* also exhibit the traits of the *L. lactis* subsp. *lactis*. For example, a well-known *L. lactis* subsp. *cremoris* MG1363 is defined as *L. lactis* subsp. *cremoris* type-strain-like-genotype and *L. lactis* subsp. *lactis* phenotype (15).

1.2.1.2 Genome sequences

In 2022, there were 269 *L. lactis* genome assemblies in the National Center for Biotechnology Information (NCBI) database and around 80% of them have been partially sequenced. Among the assemblies, submissions of *L. lactis* subsp. *lactis* and *L. lactis* subsp. *cremoris* are 85 and 69,

respectively. The two most well-researched organisms are *L. lactis* subsp. *cremoris* MG1363 and *L. lactis* subsp. *lactis* IL1403. The genome of IL1403 was first sequenced and was published in 2001 (19). The main genome features of *L. lactis* MG1363 and *L. lactis* IL1403 are concluded in **Table 1.2** (19, 20). Usually, the range of genome size of *L. lactis* assemblies is from 1.71 to 2.96 Mbp and the G+C content is from 34.5% to 38.6% (15).

Table 1.2 The main genome features of strains *L. lactis* MG1363 and *L. lactis* IL1403. Reprint with permission from (21).

	L. lactis MG1363	*L. lactis* IL1403
Size (Mbp)	2.53	2.37
Open reading frames (ORFs)	~ 2500	~ 2310
Total G+C mol%	35.8	35.4
ORFs G+C mol%	36.7	36.1
Phage DNA (kbp)	134	293
Phage genes	~ 200	293
Insertion sequence (IS) elements	92	52

1.2.1.3 Insertion sequence

Insertion sequence (IS) elements are the simplest type of mobile genetic elements, which play an important role in the evolutionary adaption of their hosts. The existence of IS elements can cause the activation or inactivation of genes and rearrangements of the genome to benefit hosts during evolution (22). *L. lactis* MG1363 contains 11 different IS elements, while *L. lactis* IL1403 only has 6 different IS elements. Detailed IS elements information can be found in the **Table 1.3** (20). An interesting example of IS-mediated adaptive evolution occurs in an *L. lactis* MG1363 derivative, which is unable to utilize cellobiose. However, this strain recovers the ability to metabolize cellobiose under selection pressure. The insertion of IS*981* or IS*905* in a transcriptional repressor activates the expression of a novel cellobiose-specific transporter and leads to the bacterial growth on cellobiose (23).

Table 1.3 Number of IS elements of strains *L. lactis* MG1363 and *L. lactis* IL1403. Reprint with permission from (20).

IS element	*L. lactis* MG1363	*L. lactis* IL1403
IS*904*	9	9
IS*1077*	9	7
IS*905*	14	1
IS*981*	16	10
IS*982*	2	1
IS*983*	/	15
IS*712*	8	/
IS-*LL6*	9	/
IS*946*	1	/
IS*1216*	1	/
IS*1297*	1	/
IS*1675*	1	/
Total	71	43

1.2.1.4 Pseudogenes

Pseudogenes, i.e. genes that have lost their function during the course of evolution, are very common in *L. lactis.* Especially, there is a high proportion of pseudogenes in genomes of the subsp. *cremoris* (24). For MG1363, around 3% of genes are found to be pseudogenes. These pseudogenes originate from genes of transposition, genes with putative transport functions, and genes with regulatory roles (20).

1.2.2 Metabolism

1.2.2.1 Glycolysis

Due to the lack of a complete tricarboxylic acid (TCA) cycle, *L. lactis* gains energy by substrate-level phosphorylation. Through glycolysis, *L. lactis* can form 2 mol NADH and 2 mol ATP per glucose by converting sugars to pyruvate (25). There are three major sugar uptake systems: 1) the phosphoenolpyruvate (PEP): carbohydrate phosphotransferase (PTS) system; 2) an ion gradient driven sugar transport; 3) ABC transport system. Most sugars end up in glucose 6-phosphate (G6P) and further enter into the glycolytic pathway (26). For glucose used in our research, the transport systems of glucose uptake in *L. lactis* can be PEP: PTS system (mannose-PTS and cellobiose-PTS) or proton motive force dependent GlcU permease (27). Some work about the control of the glycolytic flux in *L. lactis* MG1363 has been performed. Andersen et al. found that lactate dehydrogenase (LDH) had no control on the glycolytic flux in *L. lactis* MG1363 (28). In another research, except LDH, some other glycolytic enzymes phosphofructokinase (PFK), glyceraldehyde-3-phosphate dehydrogenase (GAPDH) and pyruvate kinase (PYK) have also been proven to have no significant control on the glycolysis of exponential growing *L. lactis* MG1363 (29). By constructing *L. lactis* MG1363 mutants with different GAPDH activities, Solem et al. found that the control of GAPDH over the glycolysis was close to zero whether cells were growing or nongrowing (30). The glycolysis flux can be controlled by an ATP-consuming process. Koebmann et al. found that the introduction of an extra ATP-consuming reaction by overexpressing the F_1 domain of F_1F_0-ATPase can stimulate the glycolytic flux in nongrowing *L. lactis* MG1363 cells, while no increase in flux was observed in growing cells (31). Ana Rute et al. reported that the content of ATP/ADP/inorganic phosphate (Pi) also could be the key factor for the control of glycolysis (32).

1.2.2.2 Pyruvate metabolism

The detailed pathways downstream of pyruvate produced by glycolysis can be found in **Fig.1.2**. Homolactic fermentation of *L. lactis* is commonly used in dairy fermentation. Under anaerobic conditions, more than 90% of sugar is converted into lactate because 2 mol NADH generated by glycolysis is re-oxidized into NAD^+ by LDH to achieve the redox balance (33).

Homolactic fermentation can be shifted to mixed acid fermentation (formate, acetate and ethonal) when the uptake rate of sugar is limited to be slow. The shift was first observed in glucose-limited chemostats and the changes were relevant to the fructose 1,6-diphosphate (FDP) concentration and the level of LDH (34). Besides, growing on slowly fermentable sugars such as maltose or galactose

can shift the most of pyruvate flux to mixed acids. The ratio of NADH/NAD^+ is reported to control the fermentation shift in *L. lactis*. With slow metabolized sugars, the flux of glycolysis and NADH/NAD^+ ratio are reduced, resulting in lower LDH activity and higher pyruvate-formate lyase (PFL) activity under anaerobic conditions (35). In another paper, it has been reported that LDH has a negative control on the flux towards formate which indicates the inhibition of LDH helps the occurrence of mix-acid fermentation (28).

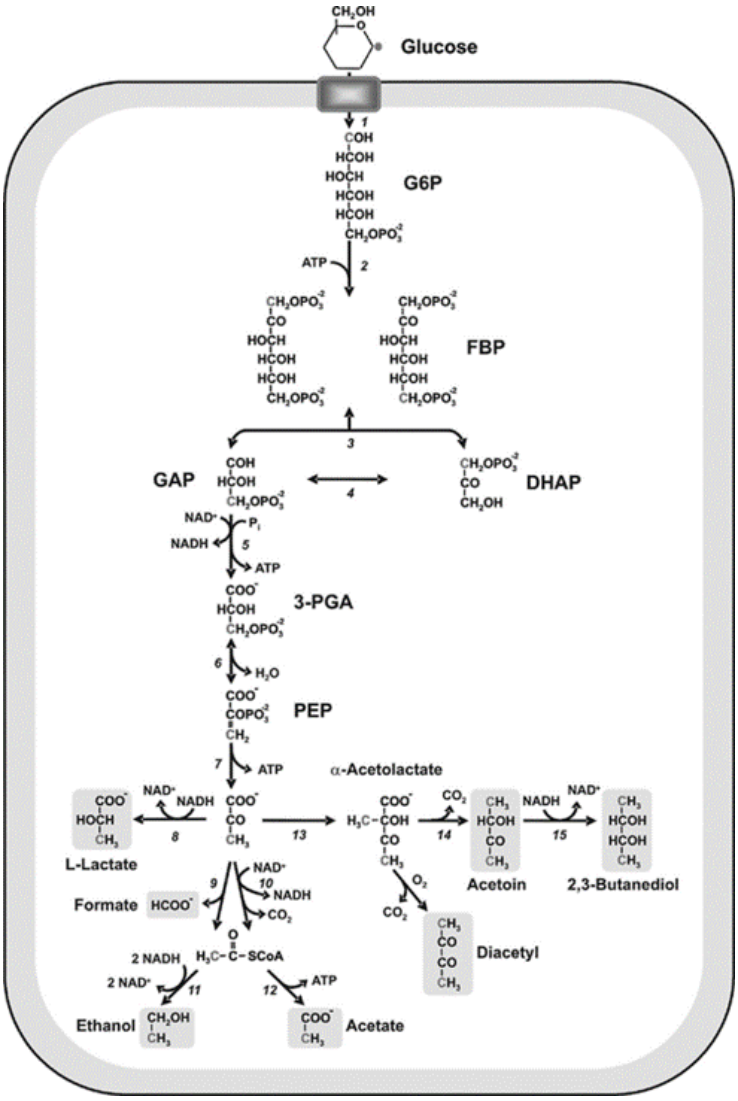

Fig. 1.2 Fermentation pathways in *L. lactis*. 1. phosphoenolpyruvate: carbohydrate phosphotransferase system (PTS, *ptnABCD*) or/and non-PTS permeases (genes unknown)/glucokinase (*glk*) system; 2. phosphoglucose isomerase (*pgi*) and 6-phosphofructo-1-kinase (*pfk*); 3. fructose 1,6-bisphosphate aldolase (*fba*); 4. triosephosphate isomerase (*tpi*); 5. glyceraldehyde 3-phosphate dehydrogenase (*gapB*) and phosphoglycerate kinase (*pgk*); 6. phosphoglyceromutase (*pmg*) and enolase (*enoA*); 7. pyruvate kinase (*pyk*); 8. lactate dehydrogenase (*ldh*); 9. pyruvate-formate lyase (*pfl*);

10. pyruvate dehydrogenase complex (*pdhABCD*); 11. acetaldehyde dehydrogenase (*adhE*) and alcohol dehydrogenase (*adhE*); 12. phosphotransacetylase (*pta*) and acetate kinase (*ackA*); 13. α-acetolactate synthase (*als*); 14. α-acetolactate decarboxylase (*aldB*); 15. 2,3-butanediol dehydrogenase (*butBA*). Reprint with permission from (26).

Furthermore, under certain conditions, pyruvate can also enter the flavor-forming pathway, where α-acetolactate synthase (ALS) further transforms pyruvate into α-acetolactate that can decompose into either diacetyl or acetoin **(Fig. 1.2)**. When O_2 is present, extra NADH can be produced from pyruvate by pyruvate dehydrogenase complex (PDHc) (36), whereas PFL is inactivated due to its sensitivity to O_2 (37). Besides, NADH can be re-oxidized into NAD^+ by H_2O-forming NADH oxidase (NoxE), altering the redox state. With the increased aeration, the composition of by-products shifts from formate and ethanol to acetate, CO_2 and acetoin (33). The decrease in ethanol is probably due to the affinity for NADH of NoxE is higher than alcohol dehydrogenase (ADHE) (38). Furthermore, by overexpressing NoxE, pyruvate can be mostly converted into acetoin or diacetyl through α-acetolactate rather than acetate (39). It also has been reported that *L. lactis* subsp. *lactis* biovar diacetylactis can metabolize citrate (40). The citrate metabolism is important for the production of buttery flavor (diacetyl and acetoin) in food fermentation (41). When citrate exists in the medium, it can be transported into cells by the citrate transporter (CitP), and further be cleaved into oxaloacetate and acetate by citrate lyase (CL). Subsequently, oxaloacetate can be converted into pyruvate and CO_2 by oxaloacetate decarboxylase (OAD) (42). ALS further transforms pyruvate into α-acetolactate, which subsequently decomposes into diacetyl and acetoin **(Fig. 1.3)**. When acetolactate decarboxylase (ALD) is deficient and the activity of LDH is low, the main products are proved to be α-acetolactate and diacetyl under aerobic condition (43). A nonengineered mutant *L. lactis* subsp. *lactis* biovar diacetylactis RD1M5, deficient in LDH activity, is reported to produce acetoin from lactose and citrate contained in dairy waste (44).

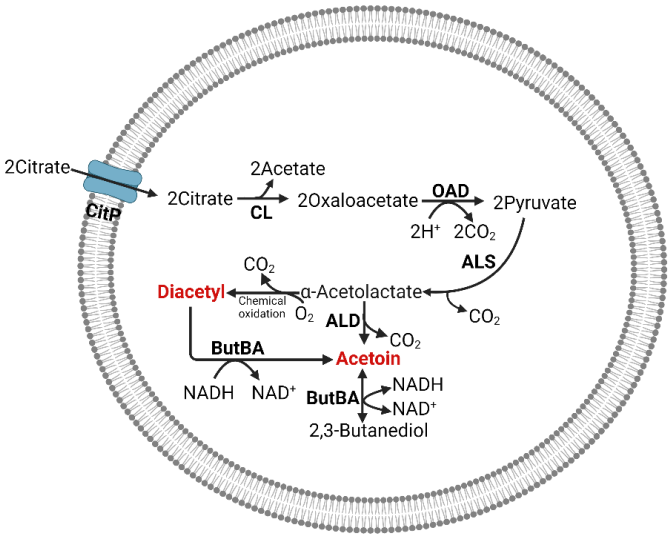

Fig. 1.3 Citrate metabolism in *L. lactis* subsp. *lactis* biovar diacetylactis. CitP, citrate transporter; CL, citrate lyase; OAD, oxaloacetate decarboxylase; ALS, α-acetolactate synthase; ALD, α-acetolactate decarboxylase; ButBA, 2,3-butanediol dehydrogenase. Created with BioRender.com.

1.2.2.3 Aerobic respiration

Composition of respiratory chain

Respiration is a predominant pathway for cells to generate ATP through oxidative phosphorylation in many bacteria. However, due to the lack of a complete pathway for the biosynthesis of heme for respiration, ATP is usually derived from substrate-level phosphorylation in *L. lactis*, resulting in a high glycolytic flux (45). Usually, a respiration chain consists of three parts: 1) type-II NADH dehydrogenases for the supply of electron donor; 2) menaquinones (MKs) for promotion of electron transfer; 3) cytochrome *bd* oxidase donates the electrons to the final electron acceptor oxygen (46, 47) **(Fig. 1.4)**.

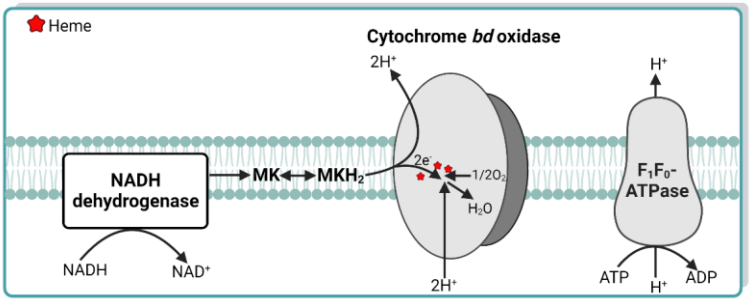

Fig. 1.4 The respiratory chain of *L. lactis*.MK: menaquinone; MKH_2: reduced menaquinone. Created with BioRender.com.

In *L. lactis*, there are two adjacent putative NADH dehydrogenase genes (*llmg_1735 noxA* and *llmg_1734 noxB*) in the genome. NoxA has been shown to be involved in respiration in *L. plantarum*, while the role of NoxB is unknown (48). However, there is no clear study on the specific function of these two enzymes in *L. lactis*. Usually when describing the respiratory chain, both enzymes are mentioned at the same time (49, 50). *L. lactis* carries the complete biosynthesis pathway of menaquinones. Menaquinones can have different numbers of isoprenoid units attached, and how many are attached depends on the growth conditions. Under respiratory conditions, there are from 3 to 10 units attached (46). The cytochrome *bd* oxidase is encoded by the *cyd*ABCD operon. In this operon, *cydA* and *cydB* encode for the structural subunits, while *cydC* and *cydD* encoding ABC transporter are used for the assembly of the *bd*-type cytochrome (46). This two-subunit integral membrane cytochrome *bd* oxidase needs three hemes, b_{558}, b_{595} and *d*, and heme b_{558} and *d* can form a di-heme site for the reduction of O_2 (51). However, *L. lactis* lacks the ability to synthesize heme, and to activate respiration either heme, its precursor protoporphyrin IX or hemin (ferric chloride heme) needs to be added to the culture medium (46).

Heme homeostasis

Heme homostasis is very important for respiration due to the toxicity of heme (52). HrtRBA and menaquinone play central roles in the heme homeostasis in *L. lactis*. Menaquinone favors the accumulation of the reduced heme in the membrane. The accumulation of the reduced heme in the membrane explains why heme can be toxic, as a redox cycle between heme and menaquinone generates semi-quinones and reduced heme that can result in the production of superoxides that can lead to lipid oxidation and other oxidative damage of cell components (53). This toxicity can be regulated with HrtRBA which transports toxic heme back to the medium (54). Thus, HrtRBA is a heme efflux system in *L. lactis*. When heme is present, it can bind and modify the conformation of the HrtR repressor, which is an important intracellular heme sensor. When HrtR binds heme it is released from its target *hrtRBA* promoter region, activating the expression of the HrtBA transporter that pumps out heme (55) **(Fig. 1.5)**.

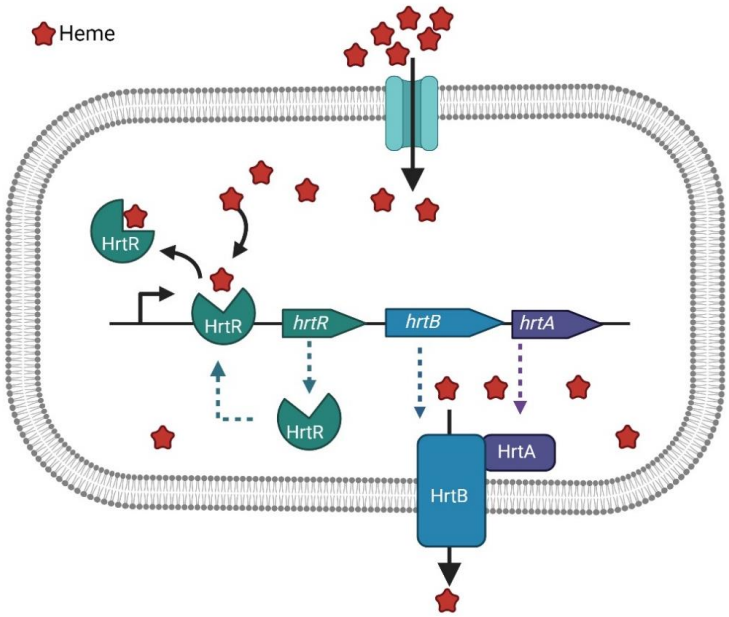

Fig. 1.5 The heme homeostasis regulated by HrtBA-mediated efflux. Created with BioRender.com.

Impacts of respiration

Respiration brings benefits to the growth and survival of *L. lactis*, greatly improving its robustness for industrial applications (56). Under respiratory conditions, NADH is reoxidized to NAD^+ by the respiration chain rather than by LDH. So less lactate is formed and the acid stress is alleviated (57). Compared with fermentation, the respiration process is energetically more efficient. When cytochrome *bd* oxidase transfers electrons to oxygen, protons are released to the exterior, protons which otherwise have to be pumped out by the F_1F_0-ATPase at the cost of ATP (58). Thus, ATP is saved when respiration is active, and this increases biomass yield (45). However, the reverse function of F_1F_0-ATPase, i.e. ATP production, has not been demonstrated until now. Respiration can also reduce oxidative stress and thereby improve the long-term survival of *L. lactis*. Reactive oxygen species (ROS), e.g. O_2^-, H_2O_2 and OH^o, are well-known toxic by-products caused by O_2. ROS can lead to the damage of DNA, proteins and lipids, etc. Besides, *L. lactis* is catalase-negative and is thus poorly equipped to detoxify H_2O_2 (59). The last component cytochrome *bd* oxidase can reduce O_2 into the neutral H_2O to limit the formation of ROS (57).

Furthermore, respiration is also associated with changes in carbon and nitrogen metabolism. Respiration has been reported to take place in the late exponential phase, while fermentation occurs in the initial growth. Due to the activity of the respiratory chain, pyruvate is rerouted to acetoin

and acetate along with the lower LDH activity (56). The accumulation of acetoin and acetate is also accompanied by a slight increase in the expression of PDHc and α-acetolactate synthase (ALS) (60). Another unexpected observation is the induction of *pepO1* under respiration conditions, while it is usually repressed during the fermentation. The gene *pepO1* encoding PepO1 peptidase is involved in the proteolytic system and can cleave the proline-rich peptides. This probably is also the reason for the accumulation of proline in the respiration cultures (60).

The number of isoprene units attached to the MK depends on the growth conditions. Long-chain MKs are more efficient in the respiratory chain, while short-chain MKs are preferred for extracellular electron transfer or reaction with O_2 (61).

Applications of respiration

From an industrial perspective, oxidative stress and acid stress are very common problems. Respiration growth is widely applied for the preparation of starter cultures to alleviate these problems, leading to increased biomass yield and prolonged survival (47, 56, 57). Acetoin and diacetyl (chemical oxidation of α-acetolactate) are important volatile compounds, providing butter aroma for dairy products, bread, wine and beer. Respiration can alter the pyruvate metabolism to the production of these volatile compounds with a good yield (62). The heme-inducible system during respiration can also be developed into a tool for regulating the expression of proteins (63). *L. lactis*, as the producer of MKs, can be the source of MKs in the host and is also used for the preparation of MKs-enriched food products (64, 65). The longer chain lengths of MKs, mainly produced under respiration, are important for health because they are more easily absorbed and utilized by the human body (66). Besides, respiration can help promote the mutually beneficial symbiosis between plants and lactococci. For example, nodules in the roots of leguminous plants can produce heme-rich leghemoglobin (67), which can activate the respiration of *L. lactis*. In turn, with respiration, *L. lactis* can produce acetoin and it can stimulate the growth of plants (68).

However, exogenous heme is usually required to be added for the activation of respiration in the food industry. Usually, the resource of heme is animal blood and including animal blood is not accepted by some customers. The heme can also be toxic to human health because heme-rich red meat is proven to promote colon cancer (69). But from another perspective, the toxicity caused by free heme in the gut can be alleviated by LAB respiratory utilization.

1.3 Extracellular electron transfer

1.3.1 Introduction

Extracellular electron transfer (EET) is usually defined as the electron exchange reaction between microbial cells and extracellular solid materials, including naturally-occurring metal compounds and artificial electrodes (70, 71). The previous applications of EET are more about diverse biotechnologies, including microbial electrochemical systems, bioremediation of toxic metals, biocorrosion, and recovery of useful metals (71). Recently, the reach of EET has been expanded to microbial survival in the mammalian gut (72, 73) **(Fig. 1.6)**, suggesting that EET plays an increasingly important role in different environments.

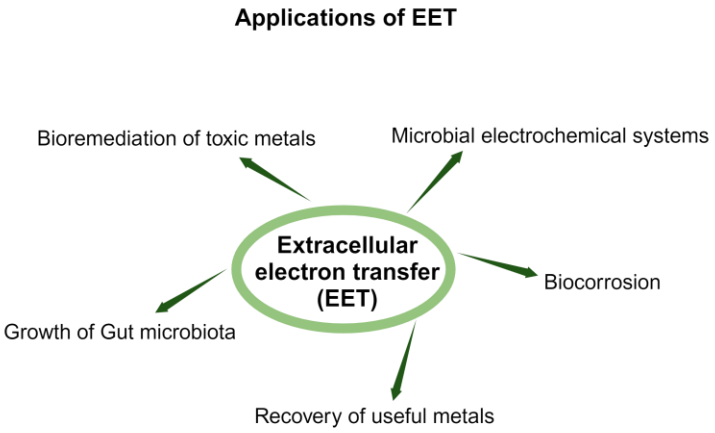

Fig. 1.6 Schematic showing the various applications of EET. Created with BioRender.com.

1.3.2 Mechanisms of EET

EET can be divided into outward EET and inward EET which depends on the direction of electron transfer. For outward EET, electrons are transferred from cells to the electron acceptors, while inward EET proceeds in the opposite direction (74). Outward EET will be referred to as EET here, unless otherwise stated. The mechanisms of EET can be categorized into two main types: direct electron transfer (DET) and indirect electron transfer (IET) (75–77). In DET, electron transfer is accomplished via self-assembled appendages called nanowires or outer membrane cytochromes. In IET, a redox mediator that acts as a shuttle to transfer electrons to cells is a common way. By-products can also participate in IET. It is worth mentioning that extracellular polymeric substances (EPS) can act as transient media for electron hopping as the prevailing pathway for the above EET pathways (78) **(Fig. 1.7)**.

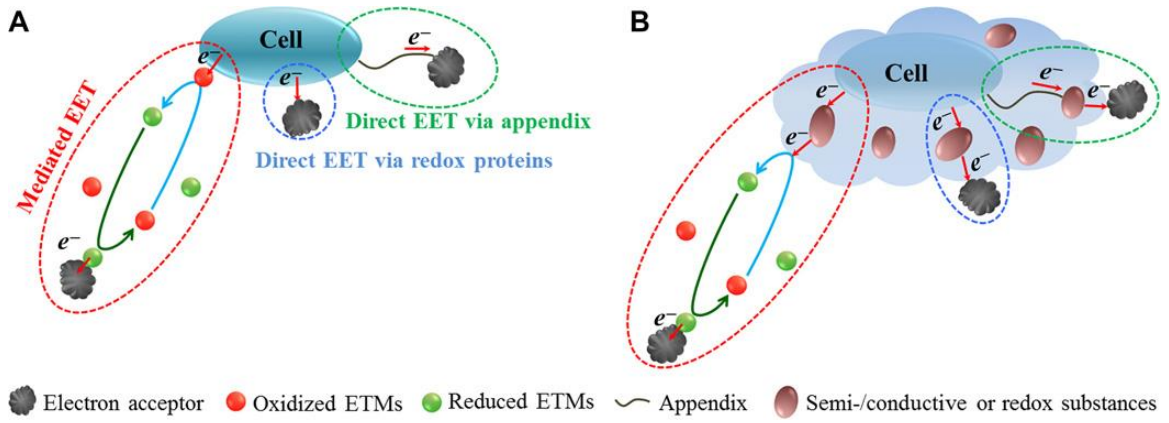

Fig. 1.7 Pathways of outward EET with the microorganism as the electron donor. (A) DET and IET. (B) EPSs are transient media for EET. ETMs, electron transfer mediators. Reprint with permission from (78).

1.3.2.1 DET

For short-range DET, multihaem *c*-type cytochromes (*c*-Cyts) are the major electron carrier proteins for the Gram-negative bacteria *Shewanella* and *Geobacter*, which are the most extensively studied microorganisms for EET. Cytochromes OmcE and OmcS of *Geobacter* and MtrC and OmcA of *Shewanella* have been shown to mediate EET (79). These *c*-Cyts are strategically located in the bacterial cell envelope to facilitate the electron transfer from the quinone/quinol pool in the inner membrane (IM) to the periplasm (PS) and then to the outer membrane (OM) where they are positioned to transfer electrons to the metal oxides **(Fig. 1.8)**.

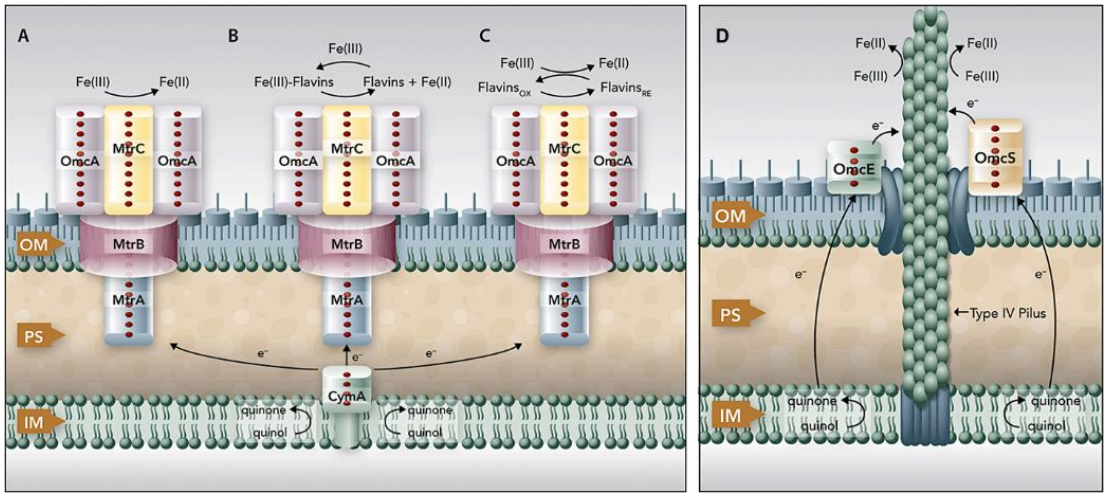

Fig. 1.8 The roles of *c*-Cyts in *Shewanella* and *Geobacter*-mediated extracellular reduction of Fe(III) oxides. (A,B,C) roles of MtrC and OmcA in *Shewanella*; (D) roles of OmcE and OmcS in *Geobacter*. Reprint with permission from (79).

For long-range DET, the formation of nanowires allows the microbes to transfer electrons to electron acceptors that are physically distant from microbes (80). Based on the composition and structure, microbial nanowires (MNWs) can be divided into three main types: 1) type IV pili (TFP); 2) a concoction of periplasmic proteins and outer membrane cytochromes (e.g. MtrC, OmcA); 3) consist of an unknown type protein (GenBank: CAO90693.1). The mechanisms of electron transfer in MNWs have been widely studied in *Geobacter sulfurreducens* and *Shewanella oneidensis*. One is the metallic-like conductivity model and another is the electron hopping model. The hopping mechanism is believed to occur in both organisms, while the metallic-like conductivity model only has been proposed for *G. sulfurreducens* MNWs. Aromatic amino acids have been proved unambiguously that they are indispensable in *G. sulfurreducens* MNWs, whereas, for *S. oneidensis* MNWs, cytochromes play an important role (81).

1.3.2.2 IET

Due to the lack of a mechanism for DET in many microbes, a proper electron mediator is commonly used for IET. The electrons from the bacterial cells can be transferred to an electron acceptor via this redox mediator. During this process, the mediator changes between the oxidized and reduced states. A good mediator should possess the following characteristics: 1) good solubility; 2) proper redox potential; 3) high stability; 4) reusable; 5) readily available. The sources of mediators can either be endogenous or exogenous. Endogenous mediators are usually metabolites produced by the cells, such as phenazines (82–84), quinones (85, 86), pyocyanins (87, 88) and flavins (89–91). Using the exogenous mediators is the norm when exoelectrogen microbes are not yet known in early research. Common exogenous mediators include neutral red (92), potassium ferricyanide (93), humic acid (94), and anthraquinone-2,6-disulfonate (95). In addition to the above electron mediators, reduced metabolites secreted by the microbes can also be used for IET. However, this type of IET is only applicable to fermentative microorganisms and yeasts (77). Normally, the fermentative pathway that produces organic acids can generate the secreted metabolites (96).

1.3.3 EET in Gram-positive bacteria

Gram-negative mesophilic bacteria, especially the model organisms *Geobacter* and *Shewanella*, are well-studied electroactive organisms. However, for several years, Gram-positive bacteria were

considered to exhibit weaker electrochemical activity than Gram-negative bacteria due to their thick, non-conductive cell wall (97).

1.3.3.1 The cell wall of Gram-positive bacteria

A general scheme of the structure of the cell wall of Gram-positive and Gram-negative bacteria can be found in **Fig. 1.9**. Due to the lack of an outer membrane with redox-active proteins, e.g. cytochrome proteins, it is difficult for direct physical contact with the external conductive surface. Gram-positive bacteria also have a 30-100 nm thick peptidoglycan (PG) layer, while it is only a 2-7 nm thick layer in Gram-negative bacteria (98). The main structures of PG are linear glycan strands cross-linked by short peptides. Glycan strands are made up of N-acetylglucosamine (GlcNAc) and N-acetylmuramic acid (MurNAc) residues in β-1,4-linkage. This non-conducting polymer PG prevents or hinders EET processes in Gram-positive bacteria. Compared to Gram-negative bacteria, there are more cross-links in the PG in Gram-positive bacteria (98). The porous structure forms numerous pores in the cell wall and this allows high molecular weight polymeric mediators to pass through for EET (99, 100).

In addition, anionic glycopolymers, which tunnel the PG meshwork, are another feature of the cell wall of Gram-positive bacteria. Anionic glycopolymers can be divided into two classes: wall teichoic acids (WTAs), which are covalently attached to PG, and lipoteichoic acids (LTAs), which are anchored in the bacterial membrane via a glycolipid (101). Together with PG, these polymers can make up a polyanionic continuum. This polyanionic continuum has ion-exchange properties, which are not only important for maintaining metal cation homeostasis but also assisting the trafficking of ions, nutrients, antibiotics and proteins (102). For example, WTAs can bind extracellular metal cations (103) and protons. By governing the abundance of protons in the cell wall, WTAs can control the autolysin (104). Some cell wall-associated proteins can be covalently attached to PG or non-covalently bound via ionic interactions with teichoic acids (105, 106). These cell wall-associated proteins play a key role in the interactions of host-symbiont or host-pathogen (101, 107).

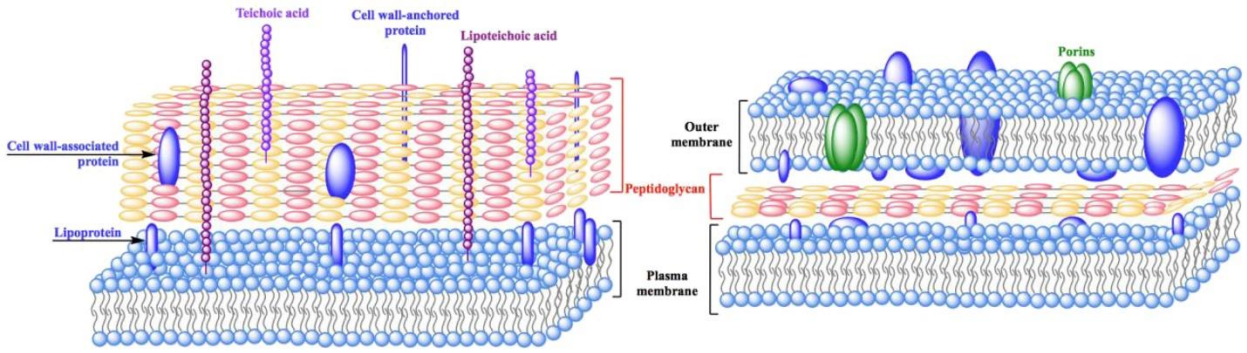

Fig. 1.9 Structures of a typical Gram-positive (left) and Gram-negative (right) cell envelope. Reprint with permission from (108).

1.3.3.2 Common Gram-positive electroactive bacteria

So far, 40 Gram-positive electroactive bacteria have been reported. These bacteria can be classified into three phyla: firmicutes (33 strains), actinobacteria (6 strains) and chloroflexi (1 strain) **(Fig. 1.10)**. Most Gram-positive electroactive bacteria belong to the bacilli and clostridia classes. Several bacteria in the *Lactobacillales* order of bacilli class, such as *Enterococccus faecalis*, *Enterococccus avium, Lactobacillus plantarum* and *L. lactis* have been reported to be electroactive. We will briefly introduce the research progress on EET for these electroactive bacteria of *Lactobacillales* order.

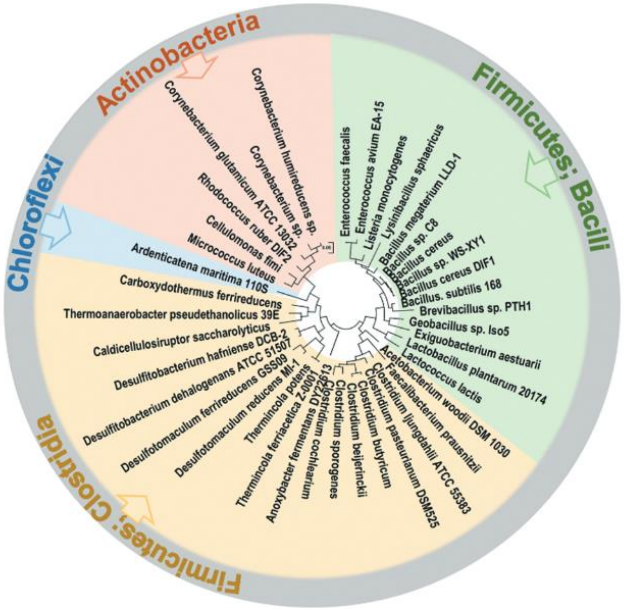

Fig. 1.10 Cladogram of Gram-positive electroactive bacteria. Reprint with permission from (109).

Enterococccus faecalis

E. faecalis, a commensal bacterium in the gut of mammals, has been proven to transfer the electrons generated in fermentation metabolism to electrodes via riboflavin (110), osmium redox polymer (OsRP) (99, 111, 112) or ferricyanide (111, 112). Demethylmenaquinone (DMK) is demonstrated to be crucial for both OsRP and ferricyanide as mediators in EET. When the electrode is coated by OsRP, electrons generated in fermentation metabolism can be transferred from a type II NADH dehydrogenase to DMK, and then be directly transferred to the electrode. OsRP on the electrode is positively charged and probably intercalates with the abundant negatively charged teichoic acids (TAs) in the cell envelope to reach positions close to the membrane. This allows efficient EET from reduced DMK to the electrode. During this progress, cytochrome *bd* oxidase is found to attenuate EET (111). When EET is mediated by ferricyanide, a novel Type-II NADH dehydrogenase Ndh3 and an uncharacterized membrane protein EetA are important for EET (112), consistent with findings in *Listeria monocytogenes* (where the orthologue is Ndh2) (91). However, EET mediated with OsRP is found to be independent of this Ndh3, this indicates that another two NADH dehydrogenases Ndh and Ndh2 of *E. faecalis* may be involved in this process (112). Heme also affects the EET ability of *E. faecalis*. In the absence of heme, LDH promotes EET through iron-augmented energy production and biofilm formation (113). Besides, *E. faecalis* endocarditis and biofilm-associated pili (Edp) are important in mediating iron-dependent biofilm growth and contributing to EET which in turn promotes iron acquisition (114).

Enterococccus avium

An EET-capable *E. avium*, which is known as a rare human pathogen, has been isolated from the human gut by using an electrochemical enrichment method. After replacing the spent medium with fresh medium, a decrease in the current level was observed for a short period and gradually recovered to the current level before the exchange of medium. This indicates that the soluble electron carriers make a low contribution to EET. Besides, cellular attachment on the electrode surface was observed, suggesting EET of *E. avium* is mainly mediated by redox proteins, but the protein type is still unknown (115).

Lactococcus lactis

L. lactis is known to produce DMKs, which are essential electron shuttles for the reduction of iron and copper (116). When tetrazolium violet (TV) is an electron acceptor, different experimental conditions (plate or liquid test) show different reduction sites of the EET chain in *L. lactis*. For the plate test, MKs are essential for TV reduction and membrane NADH dehydrogenases are partly involved in EET to MKs. During the liquid test, TV is directly reduced by NADH dehydrogenase (117). 2-amino-3-dicarboxy-1,4-naphthoquinone (ACNQ), a soluble redox mediator with the presence of a carboxyl group, has been shown to be important for electron transfer to the anode (86) and ferricyanide (118). Besides, riboflavin and derivate flavin mononucleotide (FMN) can be the exogenous redox mediators for the anodic electron transfer, while flavin adenine dinucleotide (FAD) is not, possibly due to the lack of a specific transporter of FAD (90).

Lactobacillus plantarum

L. plantarum is commonly found in the human gut and used in food fermentations. This microbe can perform EET when an exogenous quinone, 1,4-dihydroxy-2-naphthoic acid (DHNA), or riboflavin is provided. The roles of these two different redox-active small molecules in EET have been shown to be different. They can independently support EET but differ in the extent to which they support iron reduction and anode reduction **(Fig. 1.11)**. DHNA-dependent iron reduction largely relies on a type II NADH dehydrogenase (Ndh2) and a flavin mononucleotide (FMN) cofactor (PplA), while flavin-dependent iron reduction relies on Ndh2 and EetA proteins. In contrast to iron reduction, the DHNA-dependent pathway is more efficient for the electron transfer to an anode than the flavin-dependent pathway. It is found that DHNA-dependent anode reduction requires Ndh2 and PplA, while flavin-dependent anode reduction requires Ndh2, PplA and EetA (119). Besides, except DHNA, ACNQ, 1,4-naphthoquinone and menadione can also be used for EET reduction of insoluble iron by *L. plantarum.* Quinone-producing *L. lactis* and *Leuconostoc mesenteroides* can be a source of these electron shuttles to stimulate EET of *L. plantarum* in food fermentations (120).

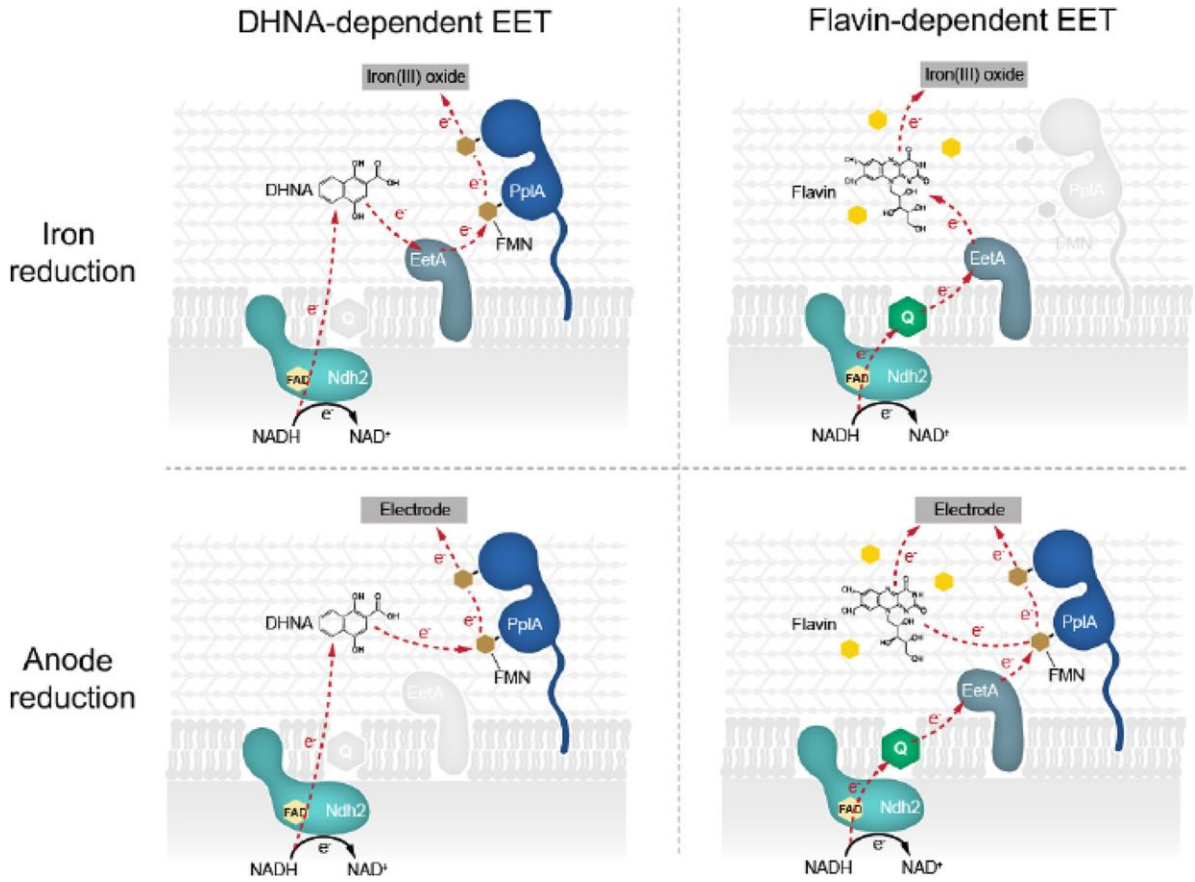

Fig. 1.11 Proposed working model of DHNA- and flavin-dependent EET routes in *L. plantarum*. Reprint with permission from (119).

1.4 Anodic electro-fermentation

1.4.1 Introduction

A bioelectrochemical system (BES) is a type of bioreactor in which both biological and electrochemical processes can take place to generate electricity, hydrogen, or other products of interest. Previous BES research mainly focused on the production of electricity in microbial fuel cells (MFCs), hydrogen production in microbial electrolysis cells (MECs), chemical production from CO_2 reduction in microbial electrosynthesis (MES) and water desalination in microbial desalination cells (MDCs). Based on the knowledge from these previous technologies, electro-fermentation, a novel type of BES that involves the use of electrochemical means to steer and control fermentative processes, is proposed (96). In electro-fermentation, inexhaustible electrodes serve as electron acceptors (i.e., anodic electro-fermentation, AEF) or donors (i.e., cathodic electro-fermentation, CEF), and can be used to control the metabolism of microbes. As a third option, electrodes can be used to control the oxidation-reduction potential (ORF) of the

fermentation broth, which affects the metabolic activity of microbial cells and, in turn, the redistribution of fermentation products **(Fig. 1.12)** (121).

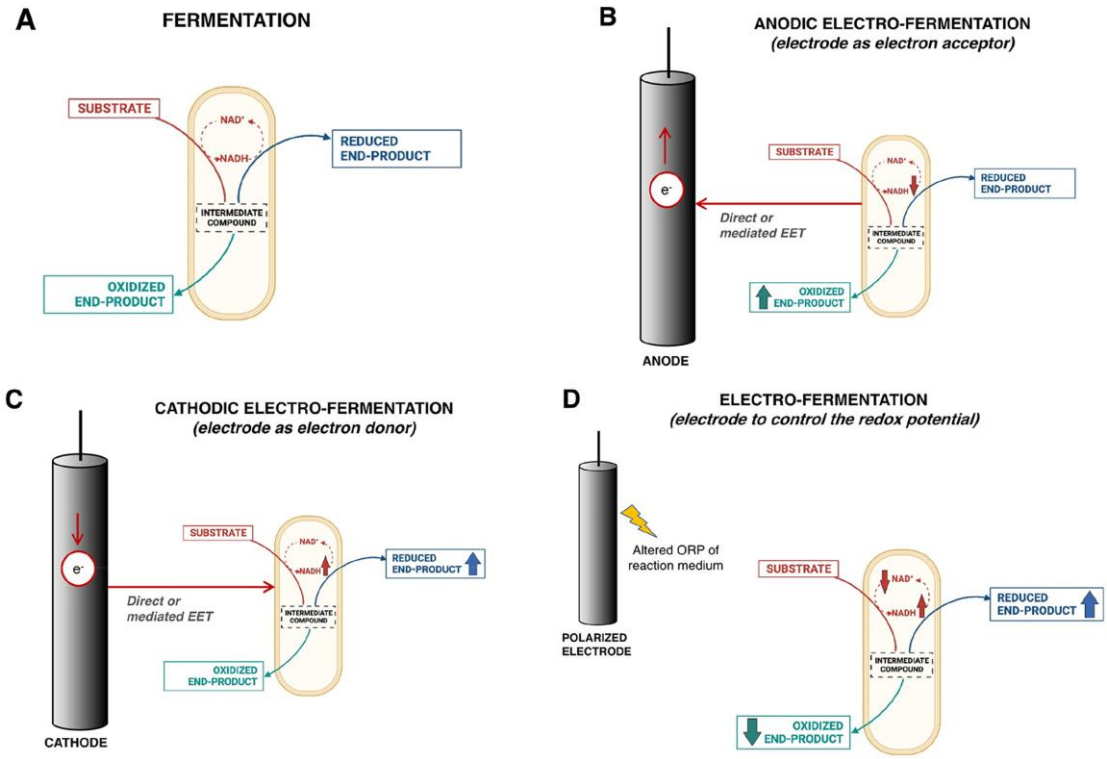

Fig. 1.12 Anaerobic fermentation (A), electro-fermentation with anode serving as electron acceptor (B), electro-fermentation with cathode serving as electron donor (C), electron-fermentation with electrode controlling the ORF of reaction environment (D). Reprint with permission from (121).

AEF provides a promising and novel approach that can combine the benefits of aerobic and anaerobic processes and eliminate their disadvantages **(Fig. 1.13)**. The specific reasons can be explained by the microbiological production process under aerobic and anaerobic processes. For many industrial microorganisms, oxygen is essential as the terminal electron acceptor to generate energy for cell growth and balance the metabolic redox state. The energy conservation of aerobic respiration can reach −2870 kJ per mol glucose, which is much higher than fermentation ($\Delta G° \approx -218$ kJ per mol glucose). Only 2 mol ATP per mol glucose generated by substrate-level phosphorylation in fermentation results in low biomass production compared to aerobic respiration (122). So, under fermentative conditions, the synthesis of reduced products is used for the regeneration of cofactors and stabilization of redox state. These reduced products normally are by-products and lead to the low yield of the target product under fermentative conditions. Although

the aerobic process can produce high biomass via oxidative phosphorylation, the yield of the target product can be low because of the substrate loss for the formation of biomass and CO_2 (123). Furthermore, the low solubility of oxygen in aqueous media makes it challenging to transfer oxygen, and further restricts the upscale of bioreactors, resulting in higher costs (124). The addition of antifoaming agents to prevent foam generation is another extra cost (125). A continuous supply of oxygen also needs a high energy input (123). In AEF, by replacing oxygen with a non-depletable electron acceptor anode, less energy is available for biomass formation, and less substrate is oxidized into CO_2, resulting in a high yield of product. Besides, AEF makes it possible for co-factors to be regenerated by transferring electrons to the anode rather than generating unwanted reduced by-products during anaerobic fermentation (122).

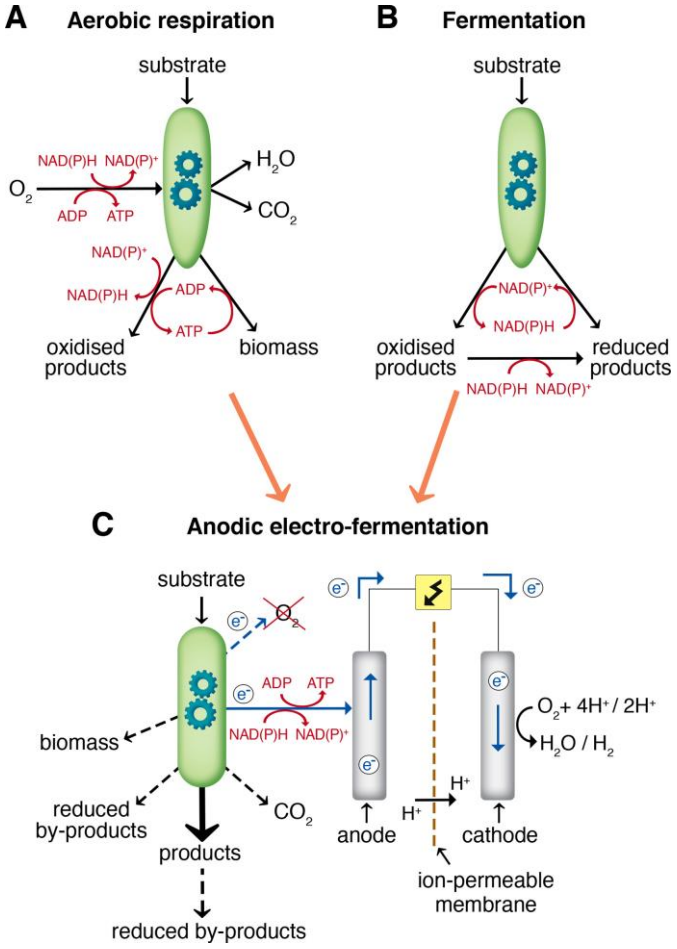

Fig. 1.13 Schematic of substrate conversion into products via aerobic respiration (A), fermentation (B), and anodic electro-fermentation (C). Reprint with permission from (122).

1.4.2 Examples of anodic electro-fermentation

Most previous research efforts on microbial electrophysiology and electroactive microorganisms have focused on anodic interactions and mainly MFC applications. In contrast, less research has dealt with anodic bio-production. Below, a brief review of the efforts on the latter is provided.

Pseudomonas putida

P. putida is a promising platform for producing harsh chemicals, but the applications are greatly limited by its obligate aerobic character. Using an anode as the electron sink and 1 mM ferricyanide as electron mediator, *P. putida* F1 could produce 2-Keto-gluconate (2KGA) with an overall yield of over 90% from glucose. An observed increased adenylate energy charge suggested that cells can produce energy with the anode as a terminal electron acceptor (93). Metabolic engineering was used to optimize another model strain, *P. putida* KT2440, in BES. High electron transfer rate (1.14 ± 0.07 mmol/gCDW/h) and 2KGA productivity (0.25 ± 0.02 mmol/gCDW/h) were achieved in BES with the improved expression of glucose dehydrogenase (GCD) and gluconate dehydrogenase (GAD) (126). Other than glucose, fructose was also tested as a substrate, it can improve the redox status (especially $NADPH/NADP^+$ ratio) of *P. putida* KT2440 in BES (127). Besides, the phenazine-based redox balancing in BES was proved to be possible in *P. putida* KT2440 when a phenazine synthesis pathway from *pseudomonas aeruginosa* was introduced into *P. putida* KT2440 (128).

Bacillus subtilis

B. subtilis, a Generally Regarded As Safe (GRAS) organism, is widely used for the production of vitamins, amino acids, enzymes, etc. *B. subtilis* is electro-active because it can produce electron mediators and form a conductive biofilm (129). Under a limited aeration rate condition, with 1.5 mM ferricyanide as an exogenous mediator, AEF can alter the cofactor levels and steer the product spectrum towards acetoin production with a high yield of 0.78 ± 0.04 $mol_{product}/mol_{glucose}$ (130).

Corynebacterium glutamicum

The Gram-positive bacterium *C. glutamicum* is an important industrial cell factory for the production of amino acids, especially lysine. Using an AEF setup with ferricyanide as mediator, anaerobic cell growth of a *C. glutamicum lysC* feedback-relieved mutant was accomplished, leading to the production of 2.89 mM L-lysine (131). In a previous study where CEF was applied

for *C. glutamicum*, no growth was observed and the titer of L-lysine was low (131). The increased biomass was probably explained by a regulatory process, since only 12.6 % of energy was added by anodic respiration, which only contributed little to the energy balance (131).

Lactobacillus plantarum

In *L. plantarum*, supplemented with DHNA as an electron mediator, energy conservation was found to be significantly increased and a high NAD^+/NADH ratio was achieved under EET. EET also increased the cellular metabolic fluxes and yield of fermentation through substrate-level phosphorylation, probably accounting for the vast majority of the increased energy conservation. However, the biomass yield in BES was quite lower due to more ATP being used by other functions although ATP was produced more efficiently. In BES, lactate, acetate and ethanol were major end-fermentation products and no acetoin or 2,3-butanediol were detected. Besides, in the practical AEF with kale juice as the medium, results similar to the laboratory medium were obtained, indicating that EET can also be used in the complex physiological conditions of fermentation (132).

Vibrio natriegens

V. natriegens is a promising new biotechnological working horse due to a fast growth rate and a doubling time of less than 10 min (133). Recently, it was proved for the first time that electrons from the metabolism of *V. natriegens* can be donated to the anode in a BES via both DET and IET. With mediator ferricyanide, the maximum current density reached 196 $\mu A/cm^2$, while the current density was 6.6 $\mu A/cm^2$ via cytochromes. The low current density by DET to the anode was probably caused by the low surface-to-volume ratio of the anode. The addition of inorganic carbon sources HCO_3^- and CO_2 had a good impact on microbial growth and the current density (134).

1.5 Objectives

L. lactis plays an immensely important industrial role in food fermentation processes. Normally, it relies on a typical fermentative metabolism. Under anaerobic conditions, NADH regenerated by glycolysis is re-oxidized into NAD^+ by LDH, converting more than 90% sugar into lactate. The low pH caused by lactate hampers its growth, in particular when pH is lower than 5 (135), which is not good for the production of starter cultures requiring large biomass. Under aerobic conditions, O_2 can shift the pyruvate metabolism away from homolactic fermentation to other products like

acetoin and acetate. Challenges caused by O_2, e.g. its low solubility in the fermentation broth, foaming problems and oxidative stress, can limit microbial growth and in addition, aeration is costly. With the addition of heme, acid stress and oxidative stress can be alleviated due to activation of respiration. However, heme used in the food industry usually comes from animal blood, which is not acceptable to some customers.

Thus, the aim of this project is to explore and develop a novel and more sustainable fermentation technology for *L. lactis*. The specific objectives of this project can be divided into two main parts (fundamentals and applications): 1) the fundamental research about the mechanism and regulation of EET in *L. lactis* by utilizing system biology methods (e.g. adaptive laboratory evolution, genome engineering and next-generation sequencing) and bioelectrochemical means; 2) the application research about AEF of *L. lactis* and deep understanding this novel fermentative process by metabolic engineering principles.

1.6 References

1. König H, Fröhlich J. 2017. Lactic acid bacteria, p. 3–41. *In* König, H, Unden, G, Fröhlich, J (eds.), Biology of Microorganisms on Grapes, in Must and in Wine. Springer International Publishing, Cham.

2. Zarour K, Vieco N, Pérez-Ramos A, Nácher-Vázquez M, Mohedano ML, López P. 2017. Chapter 4 - Food Ingredients synthesized by lactic acid bacteria, p. 89–124. *In* Holban, AM, Grumezescu, AM (eds.), Microbial Production of Food Ingredients and Additives. Academic Press.

3. Carr FJ, Chill D, Maida N. 2002. The lactic acid bacteria: a literature survey. Crit Rev Microbiol 28:281–370.

4. Ben Braïek O, Smaoui S. 2019. Enterococci: Between emerging pathogens and potential probiotics. Biomed Res Int 2019:e5938210.

5. Axelsson A von W Lars. 2019. Lactic acid bacteria: An introduction, p. 1–16. *In* Lactic Acid Bacteria, 5th ed. CRC Press.

6. Reis JA, Paula AT, Casarotti SN, Penna ALB. 2012. Lactic acid bacteria antimicrobial compounds: characteristics and applications. Food Eng Rev 4:124–140.

7. Bintsis T. 2018. Lactic acid bacteria: their applications in foods. J Bacteriol Mycol 6:89–94.

8. Gobbetti M, De Angelis M, Di Cagno R, Mancini L, Fox PF. 2015. Pros and cons for using non-starter lactic acid bacteria (NSLAB) as secondary/adjunct starters for cheese ripening. Trends Food Sci 45:167–178.

9. Holzapfel WH, Haberer P, Geisen R, Björkroth J, Schillinger U. 2001. Taxonomy and important features of probiotic microorganisms in food and nutrition. Am J Clin Nutr 73:365s–373s.

10. Pereira DIA, Gibson GR. 2002. Cholesterol assimilation by lactic acid bacteria and bifidobacteria isolated from the human gut. Appl Environ Microbiol 68:4689–4693.

11. Żukiewicz-Sobczak W, Wróblewska P, Adamczuk P, Silny W. 2014. Probiotic lactic acid bacteria and their potential in the prevention and treatment of allergic diseases. Cent Eur J Immunol 39:104–108.

12. Evivie SE, Huo G-C, Igene JO, Bian X. 2017. Some current applications, limitations and future perspectives of lactic acid bacteria as probiotics. Food Nutr Res 61:1318034.

13. de Arauz LJ, Jozala AF, Mazzola PG, Vessoni Penna TC. 2009. Nisin biotechnological production and application: a review. Trends Food Sci 20:146–154.

14. Shin JM, Gwak JW, Kamarajan P, Fenno JC, Rickard AH, Kapila YL. 2016. Biomedical applications of nisin. J Appl Microbiol 120:1449–1465.

15. Kazou M. 2022. Lactic Acid Bacteria: *Lactococcus lactis*, p. 218–225. *In* McSweeney, PLH, McNamara, JP (eds.), Encyclopedia of Dairy Sciences (Third Edition). Academic Press, Oxford.

16. Liu J, Chan SHJ, Chen J, Solem C, Jensen PR. 2019. Systems biology – a guide for understanding and developing improved strains of Lactic Acid Bacteria. Front Microbiol 10.

17. Kim WS, Ren J, Dunn NW. 1999. Differentiation of *Lactococcus lactis* subspecies *lactis* and subspecies *cremoris* strains by their adaptive response to stresses. FEMS Microbiol Lett 171:57–65.

18. Nomura M, Kimoto H, Someya Y, Suzuki I. 1999. Novel characteristic for distinguishing *Lactococcus lactis* subsp. *lactis* from subsp. *cremoris*. Int J Syst Evol Microbiol 49:163–166.

19. Bolotin A, Wincker P, Mauger S, Jaillon O, Malarme K, Weissenbach J, Ehrlich SD, Sorokin A. 2001. The complete genome sequence of the lactic acid bacterium *Lactococcus lactis* ssp. *lactis* IL1403. Genome Res 11:731–753.

20. Wegmann U, O'Connell-Motherway M, Zomer A, Buist G, Shearman C, Canchaya C, Ventura M, Goesmann A, Gasson MJ, Kuipers OP, van Sinderen D, Kok J. 2007. Complete genome sequence of the prototype lactic acid bacterium *Lactococcus lactis* subsp. *cremoris* MG1363. J Bacteriol 189:3256–3270.

21. Kok J, Buist G, Zomer AL, van Hijum SAFT, Kuipers OP. 2005. Comparative and functional genomics of lactococci. FEMS Microbiol Rev 29:411–433.

22. Schneider D, Lenski RE. 2004. Dynamics of insertion sequence elements during experimental evolution of bacteria. Res Microbiol 155:319–327.

23. Solopova A, Kok J, Kuipers OP. 2017. Disruption of a transcriptional repressor by an insertion sequence element integration leads to activation of a novel silent cellobiose transporter in *Lactococcus lactis* MG1363. Appl Environ Microbiol 83:e01279-17.

24. Kelleher P, Bottacini F, Mahony J, Kilcawley KN, van Sinderen D. 2017. Comparative and functional genomics of the *Lactococcus lactis* taxon; insights into evolution and niche adaptation. BMC Genom 18:267.

25. Papagianni M. 2012. Recent advances in engineering the central carbon metabolism of industrially important bacteria. Microb Cell Factories 11:50.

26. Neves AR, Pool WA, Kok J, Kuipers OP, Santos H. 2005. Overview on sugar metabolism and its control in *Lactococcus lactis*— The input from in vivo NMR. FEMS Microbiol Rev 29:531–554.

27. Castro R, Neves AR, Fonseca LL, Pool WA, Kok J, Kuipers OP, Santos H. 2009. Characterization of the individual glucose uptake systems of *Lactococcus lactis*: mannose-PTS, cellobiose-PTS and the novel GlcU permease. Mol Microbiol 71:795–806.

28. Andersen HW, Pedersen MB, Hammer K, Jensen PR. 2001. Lactate dehydrogenase has no control on lactate production but has a strong negative control on formate production in *Lactococcus lactis*. Eur J Biochem 268:6379–6389.

29. Koebmann BJ, Andersen HW, Solem C, Jensen PR. 2002. Experimental determination of control of glycolysis in *Lactococcus lactis*. Antonie Van Leeuwenhoek 82:237–248.

30. Solem C, Koebmann BJ, Jensen PR. 2003. Glyceraldehyde-3-Phosphate dehydrogenase has no control over glycolytic flux in *Lactococcus lactis* MG1363. J Bacteriol 185:1564–1571.

31. Koebmann BJ, Solem C, Pedersen MB, Nilsson D, Jensen PR. 2002. Expression of genes encoding F1-ATPase results in uncoupling of glycolysis from biomass production in *Lactococcus lactis*. Appl Environ Microbiol 68:4274–4282.

32. Neves AR, Ventura R, Mansour N, Shearman C, Gasson MJ, Maycock C, Ramos A, Santos H. 2002. Is the glycolytic fux in *Lactococcus lactis* primarily controlled by the redox charge? J Biol Chem 277:28088–28098.

33. Nordkvist M, Jensen NBS, Villadsen J. 2003. Glucose metabolism in *Lactococcus lactis* MG1363 under different aeration conditions: requirement of acetate to sustain growth under microaerobic conditions. Appl Environ Microbiol 69:3462–3468.

34. Thomas TD, Ellwood DC, Longyear VMC. 1979. Change from homo- to heterolactic fermentation by *Streptococcus lactis* resulting from glucose limitation in anaerobic chemostat cultures. J Bacteriol 138:109–117.

35. Garrigues C, Loubiere P, Lindley ND, Cocaign-Bousquet M. 1997. Control of the shift from homolactic acid to mixed-acid fermentation in *Lactococcus lactis*: predominant role of the NADH/NAD^+ ratio. J Bacteriol 179:5282–5287.

36. Snoep JL, de Graef MR, Westphal AH, de Kok A, Joost Teixeira de Mattos M, Neijssel OM. 1993. Differences in sensitivity to NADH of purified pyruvate dehydrogenase complexes of *Enterococcus faecalis*, *Lactococcus lactis*, *Azotobacter vinelandii* and *Escherichia coli*: Implications for their activity in vivo. FEMS Microbiol Lett 114:279–283.

37. Cocaign-Bousquet M, Even S, Lindley ND, Loubière P. 2002. Anaerobic sugar catabolism in *Lactococcus lactis*: genetic regulation and enzyme control over pathway flux. Appl Microbiol Biotechnol 60:24–32.

38. Jensen NBS, Melchiorsen CR, Jokumsen KV, Villadsen J. 2001. Metabolic behavior of *Lactococcus lactis* MG1363 in microaerobic continuous cultivation at a low dilution rate. Appl Environ Microbiol 67:2677–2682.

39. Lopez de Felipe F, Kleerebezem M, de Vos WM, Hugenholtz J. 1998. Cofactor engineering: a novel approach to metabolic engineering in *Lactococcus lactis* by controlled expression of NADH oxidase. J Bacteriol 180:3804–3808.

40. Hugenholtz J, Perdon L, Abee T. 1993. Growth and energy generation by *Lactococcus lactis* subsp. *lactis* biovar diacetylactis during citrate metabolism. Appl Environ Microbiol 59:4216–4222.

41. Hugenholtz J. 1993. Citrate metabolism in lactic acid bacteria. FEMS Microbiol Rev 12:165–178.

42. Magni C, de Mendoza D, Konings WN, Lolkema JS. 1999. Mechanism of citrate metabolism in *Lactococcus lactis*: resistance against lactate toxicity at low pH. J Bacteriol 181:1451–1457.

43. Monnet C, Aymes F, Corrieu G. 2000. Diacetyl and α-acetolactate overproduction by *Lactococcus lactis* subsp. *lactis* biovar diacetylactis mutants that are deficient in α-acetolactate decarboxylase and have a low lactate dehydrogenase activity. Appl Environ Microbiol 66:5518–5520.

44. Liu J-M, Chen L, Dorau R, Lillevang SK, Jensen PR, Solem C. 2020. From waste to taste—efficient production of the butter aroma compound acetoin from low-value dairy side streams using a natural (nonengineered) *Lactococcus lactis* dairy isolate. J Agric Food Chem 68:5891–5899.

45. Koebmann B, Blank LM, Solem C, Petranovic D, Nielsen LK, Jensen PR. 2008. Increased biomass yield of *Lactococcus lactis* during energetically limited growth and respiratory conditions. Biotechnol Appl Biochem 50:25–33.

46. Brooijmans R, Smit B, Santos F, van Riel J, de Vos WM, Hugenholtz J. 2009. Heme and menaquinone induced electron transport in lactic acid bacteria. Microb Cell Factories 8:28.

47. Pedersen MB, Gaudu P, Lechardeur D, Petit M-A, Gruss A. 2012. Aerobic respiration metabolism in lactic acid bacteria and uses in biotechnology. Annu Rev Food Sci Technol 3:37–58.

48. Brooijmans R, WM, Vos, J., Hugenholtz. 2009. *Lactobacillus plantarum* WCFS1 electron transport chains. Appl Environ Microbiol 75:3580–3585.

49. Liu J, Wang Z, Kandasamy V, Lee SY, Solem C, Jensen PR. 2017. Harnessing the respiration machinery for high-yield production of chemicals in metabolically engineered *Lactococcus lactis*. Metab Eng 44:22–29.

50. Brooijmans RJW, Poolman B, Schuurman-Wolters GK, de Vos WM, Hugenholtz J. 2007. Generation of a membrane potential by *Lactococcus lactis* through aerobic electron transport. J Bacteriol 189:5203–5209.

51. Borisov VB, Gennis RB, Hemp J, Verkhovsky MI. 2011. The cytochrome *bd* respiratory oxygen reductases. Biochim Biophys Acta Bioenerg 1807:1398–1413.

52. Kumar S, Bandyopadhyay U. 2005. Free heme toxicity and its detoxification systems in human. Toxicol Lett 157:175–188.

53. Wakeman CA, Hammer ND, Stauff DL, Attia AS, Anzaldi LL, Dikalov SI, Calcutt MW, Skaar EP. 2012. Menaquinone biosynthesis potentiates haem toxicity in *Staphylococcus aureus*. Mol Microbiol 86:1376–1392.

54. Joubert L, Derré-Bobillot A, Gaudu P, Gruss A, Lechardeur D. 2014. HrtBA and menaquinones control haem homeostasis in *Lactococcus lactis*. Mol Microbiol 93:823–833.

55. Lechardeur D, Cesselin B, Liebl U, Vos MH, Fernandez A, Brun C, Gruss A, Gaudu P. 2012. Discovery of intracellular heme-binding protein HrtR, which controls heme efflux by the conserved HrtB-HrtA transporter in *Lactococcus lactis*. J Biol Chem 287:4752–4758.

56. Duwat P, Sourice S, Cesselin B, Lamberet G, Vido K, Gaudu P, Le Loir Y, Violet F, Loubière P, Gruss A. 2001. Respiration capacity of the fermenting bacterium *Lactococcus lactis* and its positive effects on growth and survival. J Bacteriol 183:4509–4516.

57. Rezaïki L, Cesselin B, Yamamoto Y, Vido K, Van West E, Gaudu P, Gruss A. 2004. Respiration metabolism reduces oxidative and acid stress to improve long-term survival of *Lactococcus lactis*. Mol Microbiol 53:1331–1342.

58. Blank LM, Koebmann BJ, Michelsen O, Nielsen LK, Jensen PR. 2001. Hemin reconstitutes proton extrusion in an H^+-ATPase-negative mutant of *Lactococcus lactis*. J Bacteriol 183:6707–6709.

59. Miyoshi A, Rochat T, Gratadoux J-J, Le Loir Y, Oliveira SC, Langella P, Azevedo V. 2003. Oxidative stress in *Lactococcus lactis*. Genet Mol Res 2:348–359.

60. Vido K, le Bars D, Mistou M-Y, Anglade P, Gruss A, Gaudu P. 2004. Proteome analyses of heme-dependent respiration in *Lactococcus lactis*: involvement of the proteolytic system. J Bacteriol 186:1648–1657.

61. Liu Y, Charamis N, Boeren S, Blok J, Lewis AG, Smid EJ, Abee T. 2022. Physiological roles of short-chain and long-chain menaquinones (vitamin K2) in *Lactococcus cremoris*. Front Microbiol 13:823623.

62. Kaneko T, Takahashi M, Suzuki H. 1990. Acetoin fermentation by citrate-positive *Lactococcus lactis* subsp. *lactis* 3022 grown aerobically in the presence of hemin or Cu^{2+}. Appl Environ Microbiol 56:2644–2649.

63. Pedersen MB, Garrigues C, Tuphile K, Brun C, Vido K, Bennedsen M, Møllgaard H, Gaudu P, Gruss A. 2008. Impact of aeration and heme-activated respiration on *Lactococcus lactis* gene expression: identification of a heme-responsive operon. J Bacteriol 190:4903–4911.

64. Bøe CA, Holo H. 2020. Engineering *Lactococcus lactis* for increased vitamin K2 production. Front Bioeng Biotechnol 8:1–14.

65. Conly JM, Stein K, Worobetz L, Rutledge-Harding S. 1994. The contribution of vitamin K2 (menaquinones) produced by the intestinal microflora to human nutritional requirements for vitamin K. Am J Gastroenterol 89:915–923.

66. Schurgers LJ, Teunissen KJF, Hamulyák K, Knapen MHJ, Vik H, Vermeer C. 2006. Vitamin K–containing dietary supplements: comparison of synthetic vitamin K1 and natto-derived menaquinone-7. Blood 109:3279–3283.

67. Appleby CA. 1984. Leghemoglobin and rhizobium respiration. Annu Rev Plant Physiol 35:443–478.

68. Ryu C-M, Farag MA, Hu C-H, Reddy MS, Wei H-X, Paré PW, Kloepper JW. 2003. Bacterial volatiles promote growth in *Arabidopsis*. Proc Natl Acad Sci USA 100:4927–4932.

69. Corpet DE. 2011. Red meat and colon cancer: should we become vegetarians, or can we make meat safer? Meat Sci 89:310–316.

70. Hernandez ME, Newman DK. 2001. Extracellular electron transfer. Cell Mol Life Sci 58:1562–1571.

71. Kato S. 2015. Biotechnological aspects of microbial extracellular electron transfer. Microbes Environ 30:133–139.

72. Saunders SH, Newman DK. 2018. Extracellular electron transfer transcends microbe-mineral interactions. Cell Host Microbe 24:611–613.

73. Wang W, Du Y, Yang S, Du X, Li M, Lin B, Zhou J, Lin L, Song Y, Li J, Zuo X, Yang C. 2019. Bacterial extracellular electron transfer occurs in mammalian gut. Anal Chem 91:12138–12141.

74. Shi L, Dong H, Reguera G, Beyenal H, Lu A, Liu J, Yu H-Q, Fredrickson JK. 2016. Extracellular electron transfer mechanisms between microorganisms and minerals. 10. Nat Rev Microbiol 14:651–662.

75. Yang Y, Xu M, Guo J, Sun G. 2012. Bacterial extracellular electron transfer in bioelectrochemical systems. Process Biochem 47:1707–1714.

76. Choi O, Sang B-I. 2016. Extracellular electron transfer from cathode to microbes: application for biofuel production. Biotechnol Biofuels 9:11.

77. Aiyer KS. 2020. How does electron transfer occur in microbial fuel cells? World J Microbiol Biotechnol 36:19.

78. Xiao Y, Zhang E, Zhang J, Dai Y, Yang Z, Christensen HEM, Ulstrup J, Zhao F. 2017. Extracellular polymeric substances are transient media for microbial extracellular electron transfer. Sci Adv 3:e1700623.

79. Shi L, Richardson DJ, Wang Z, Kerisit SN, Rosso KM, Zachara JM, Fredrickson JK. 2009. The roles of outer membrane cytochromes of *Shewanella* and *Geobacter* in extracellular electron transfer. Environ Microbiol Rep 1:220–227.

80. Reguera G, McCarthy KD, Mehta T, Nicoll JS, Tuominen MT, Lovley DR. 2005. Extracellular electron transfer via microbial nanowires. Nature 435:1098–1101.

81. Sure S, Ackland ML, Torriero AAJ, Adholeya A, Kochar M. 2016. Microbial nanowires: an electrifying tale. Microbiol 162:2017–2028.

82. Franco A, Elbahnasy M, Rosenbaum MA. Screening of natural phenazine producers for electroactivity in bioelectrochemical systems. Microb Biotechnol 16:579–594.

83. Pham TH, Boon N, Aelterman P, Clauwaert P, De Schamphelaire L, Vanhaecke L, De Maeyer K, Höfte M, Verstraete W, Rabaey K. 2008. Metabolites produced by *Pseudomonas* sp. enable a Gram-positive bacterium to achieve extracellular electron transfer. Appl Microbiol Biotechnol 77:1119–1129.

84. Pierson LS, Pierson EA. 2010. Metabolism and function of phenazines in bacteria: impacts on the behavior of bacteria in the environment and biotechnological processes. Appl Microbiol Biotechnol 86:1659–1670.

85. Xia X, Cao X, Liang P, Huang X, Yang S, Zhao G. 2010. Electricity generation from glucose by a *Klebsiella* sp. in microbial fuel cells. Appl Microbiol Biotechnol 87:383–390.

86. Freguia S, Masuda M, Tsujimura S, Kano K. 2009. *Lactococcus lactis* catalyses electricity generation at microbial fuel cell anodes via excretion of a soluble quinone. Bioelectrochemistry 76:14–18.

87. Pham TH, Boon N, De Maeyer K, Höfte M, Rabaey K, Verstraete W. 2008. Use of *Pseudomonas* species producing phenazine-based metabolites in the anodes of microbial fuel cells to improve electricity generation. Appl Microbiol Biotechnol 80:985–993.

88. Rabaey K, Boon N, Höfte M, Verstraete W. 2005. Microbial phenazine production enhances electron transfer in biofuel cells. Environ Sci Technol 39:3401–3408.

89. Marsili E, Baron DB, Shikhare ID, Coursolle D, Gralnick JA, Bond DR. 2008. *Shewanella* secretes flavins that mediate extracellular electron transfer. Proc Natl Acad Sci USA 105:3968–3973.

90. Masuda M, Freguia S, Wang Y-F, Tsujimura S, Kano K. 2010. Flavins contained in yeast extract are exploited for anodic electron transfer by *Lactococcus lactis*. Bioelectrochemistry 78:173–175.

91. Light SH, Su L, Rivera-Lugo R, Cornejo JA, Louie A, Iavarone AT, Ajo-Franklin CM, Portnoy DA. 2018. A flavin-based extracellular electron transfer mechanism in diverse Gram-positive bacteria. 7725. Nature 562:140–144.

92. Park DH, Zeikus JG. 2000. Electricity generation in microbial fuel cells using neutral red as an electronophore. Appl Environ Microbiol 66:1292–1297.

93. Lai B, Yu S, Bernhardt PV, Rabaey K, Virdis B, Krömer JO. 2016. Anoxic metabolism and biochemical production in *Pseudomonas putida* F1 driven by a bioelectrochemical system. Biotechnol Biofuels 9:39.

94. Lovley DR, Coates JD, Blunt-Harris EL, Phillips EJP, Woodward JC. 1996. Humic substances as electron acceptors for microbial respiration. 6590. Nature 382:445–448.

95. Min D, Liu D-F, Wu J, Cheng L, Zhang F, Cheng Z-H, Li W-W, Yu H-Q. 2021. Extracellular electron transfer via multiple electron shuttles in waterborne *Aeromonas hydrophila* for bioreduction of pollutants. Biotechnol Bioeng 118:4760–4770.

96. Moscoviz R, Toledo-Alarcón J, Trably E, Bernet N. 2016. Electro-fermentation: How to drive fermentation using electrochemical systems. Trends Biotechnol 34:856–865.

97. Doyle LE, Marsili E. 2018. Weak electricigens: A new avenue for bioelectrochemical research. Bioresour Technol 258:354–364.

98. Vollmer W, Blanot D, De Pedro MA. 2008. Peptidoglycan structure and architecture. FEMS Microbiol Rev 32:149–167.

99. Pankratova G, Szypulska E, Pankratov D, Leech D, Gorton L. 2019. Electron transfer between the Gram-positive *Enterococcus faecalis* bacterium and electrode surface through osmium redox polymers. ChemElectroChem 6:110–113.

100. Pankratova G, Pankratov D, Milton RD, Minteer SD, Gorton L. 2019. Following nature: bioinspired mediation strategy for Gram-positive bacterial cells. Adv Energy Mater 9:1900215.

101. Brown S, Santa Maria JP, Walker S. 2013. Wall teichoic acids of Gram-positive bacteria. Annu Rev Microbiol 67:313–336.

102. Neuhaus FC, Baddiley J. 2003. A continuum of anionic charge: structures and functions of d-alanyl-teichoic acids in Gram-positive bacteria. Microbiol Mol Biol Rev 67:686–723.

103. Kern T, Giffard M, Hediger S, Amoroso A, Giustini C, Bui NK, Joris B, Bougault C, Vollmer W, Simorre J-P. 2010. Dynamics characterization of fully hydrated bacterial cell walls by solid-state NMR: evidence for cooperative binding of metal ions. J Am Chem Soc 132:10911–10919.

104. Biswas R, Martinez RE, Göhring N, Schlag M, Josten M, Xia G, Hegler F, Gekeler C, Gleske A-K, Götz F, Sahl H-G, Kappler A, Peschel A. 2012. Proton-binding capacity of *Staphylococcus aureus* wall teichoic acid and its role in controlling autolysin activity. PLoS One 7:e41415.

105. Dramsi S, Magnet S, Davison S, Arthur M. 2008. Covalent attachment of proteins to peptidoglycan. FEMS Microbiol Rev 32:307–320.

106. Bierne H, Cossart P. 2007. *Listeria monocytogenes* surface proteins: from genome predictions to function. Microbiol Mol Biol Rev 71:377–397.

107. Navarre WW, Schneewind O. 1999. Surface proteins of Gram-positive bacteria and mechanisms of their targeting to the cell wall envelope. Microbiol Mol Biol Rev 63:174–229.

108. Pankratova G, Hederstedt L, Gorton L. 2019. Extracellular electron transfer features of Gram-positive bacteria. Analytica Chimica Acta 1076:32–47.

109. Chen L, Li Y, Tian X, Zhao F. 2020. Electron transfer in Gram-positive electroactive bacteria and its application. Prog Chem 32:1557–1563.

110. Zhang E, Cai Y, Luo Y, Piao Z. 2014. Riboflavin-shuttled extracellular electron transfer from *Enterococcus faecalis* to electrodes in microbial fuel cells. Can J Microbiol 60:753–759.

111. Pankratova G, Leech D, Gorton L, Hederstedt L. 2018. Extracellular electron transfer by the Gram-positive bacterium *Enterococcus faecalis*. Biochemistry 57:4597–4603.

112. Hederstedt L, Gorton L, Pankratova G. 2020. Two routes for extracellular electron transfer in *Enterococcus faecalis*. J Bacteriol 202:e00725-19.

113. Keogh D, Lam LN, Doyle LE, Matysik A, Pavagadhi S, Umashankar S, Low PM, Dale JL, Song Y, Ng SP, Boothroyd CB, Dunny GM, Swarup S, Williams RBH, Marsili E, Kline KA. 2018. Extracellular electron transfer powers *Enterococcus faecalis* biofilm metabolism. mBio 9:e00626-17.

114. Lam LN, Wong JJ, Matysik A, Paxman JJ, Chong KKL, Low PM, Chua ZS, Heras B, Marsili E, Kline KA. 2019. Sortase-assembled pili promote extracellular electron transfer and iron acquisition in *Enterococcus faecalis* biofilm. bioRxiv.

115. Naradasu D, Miran W, Sakamoto M, Okamoto A. 2019. Isolation and characterization of human gut bacteria capable of extracellular electron transport by electrochemical techniques. Front Microbiol 9:1–9.

116. Rezaïki L, Lamberet G, Derré A, Gruss A, Gaudu P. 2008. *Lactococcus lactis* produces short-chain quinones that cross-feed Group B Streptococcus to activate respiration growth. Mol Microbiol 67:947–957.

117. Tachon S, Michelon D, Chambellon E, Cantonnet M, Mezange C, Henno L, Cachon R, Yvon M. 2009. Experimental conditions affect the site of tetrazolium violet reduction in the electron transport chain of *Lactococcus lactis*. Microbiology 155:2941–2948.

118. Yamziki S, Kaneko T, Taketomo N, Kano K, Ikeda T. 2002. Glucose metabolism of lactic acid bacteria changed by quinone-mediated extracellular electron transfer. Biosci Biotechnol Biochem 66:2100–2106.

119. Tolar JG, Li S, Ajo-Franklin CM. 2022. The differing roles of flavins and quinones in extracellular electron transfer in *Lactiplantibacillus plantarum*. Appl Environ Microbiol 0:e01313-22.

120. Stevens ET, Beeck WV, Blackburn B, Tejedor-Sanz S, Rasmussen ARM, Mevers E, Ajo-Franklin CM, Marco ML. 2023. *Lactiplantibacillus plantarum* uses ecologically relevant, exogenous quinones for extracellular electron transfer. bioRxiv.

121. Virdis B, D. Hoelzle R, Marchetti A, Boto ST, Rosenbaum MA, Blasco-Gómez R, Puig S, Freguia S, Villano M. 2022. Electro-fermentation: Sustainable bioproductions steered by electricity. Biotechnol Adv 59:107950.

122. Vassilev I, Averesch NJH, Ledezma P, Kokko M. 2021. Anodic electro-fermentation: Empowering anaerobic production processes via anodic respiration. Biotechnol Adv 48:107728.

123. Weusthuis RA, Lamot I, van der Oost J, Sanders JPM. 2011. Microbial production of bulk chemicals: development of anaerobic processes. Trends Biotechnol 29:153–158.

124. Garcia-Ochoa F, Gomez E. 2009. Bioreactor scale-up and oxygen transfer rate in microbial processes: An overview. Biotechnol Adv 27:153–176.

125. Delvigne F, Lecomte J. 2010. Foam formation and control in bioreactors, p. 1–13. *In* Encyclopedia of Industrial Biotechnology. John Wiley & Sons, Ltd.

126. Yu S, Lai B, Plan MR, Hodson MP, Lestari EA, Song H, Krömer JO. 2018. Improved performance of *Pseudomonas putida* in a bioelectrochemical system through overexpression of periplasmic glucose dehydrogenase. Biotechnol Bioeng 115:145–155.

127. Nguyen AV, Lai B, Adrian L, Krömer JO. 2021. The anoxic electrode-driven fructose catabolism of *Pseudomonas putida* KT2440. Microb Biotechnol 14:1784–1796.

128. Schmitz S, Nies S, Wierckx N, Blank LM, Rosenbaum MA. 2015. Engineering mediator-based electroactivity in the obligate aerobic bacterium *Pseudomonas putida* KT2440. Front Microbiol 6.

129. Nimje VR, Chen C-Y, Chen C-C, Jean J-S, Reddy AS, Fan C-W, Pan K-Y, Liu H-T, Chen J-L. 2009. Stable and high energy generation by a strain of *Bacillus subtilis* in a microbial fuel cell. J Power Sources 190:258–263.

130. Sun Y, Kokko M, Vassilev I. 2023. Anode-assisted electro-fermentation with *Bacillus subtilis* under oxygen-limited conditions. Biotechnol Biofuels Bioprod 16:6.

131. Vassilev I, Gießelmann G, Schwechheimer SK, Wittmann C, Virdis B, Krömer JO. 2018. Anodic electro-fermentation: Anaerobic production of L-Lysine by recombinant *Corynebacterium glutamicum*. Biotechnol Bioeng 115:1499–1508.

132. Tejedor-Sanz S, Stevens ET, Li S, Finnegan P, Nelson J, Knoesen A, Light SH, Ajo-Franklin CM, Marco ML. 2022. Extracellular electron transfer increases fermentation in lactic acid bacteria via a hybrid metabolism. eLife 11:e70684.

133. Xu J, Yang S, Yang L. 2022. *Vibrio natriegens* as a host for rapid biotechnology. Trends Biotechnol 40:381–384.

134. Gemünde A, Gail J, Holtmann D. 2023. Anodic respiration of *Vibrio natriegens* in a bioelectrochemical system. ChemSusChem 1–8.

135. Harvey RJ. 1965. Damage to *Streptococcus Lactis* resulting from growth at low pH. J Bacteriol 90:1330–1336.

CHAPTER 2. Investigating effects of electron acceptor ferricyanide on *L. lactis* and enhancing extracellular electron transfer capacity by adaptive laboratory evolution

Published in Microbial Biotechnology, 2023, 16 (6):1277-1292.DOI: 10.1111/1751-7915.14229.
Reprint with permission.

Received: 1 November 2022 | Accepted: 22 January 2023

DOI: 10.1111/1751-7915.14229

MICROBIAL BIOTECHNOLOGY Applied Microbiology International

RESEARCH ARTICLE

Rewiring the respiratory pathway of *Lactococcus lactis* to enhance extracellular electron transfer

Liuyan Gu[1] | Xinxin Xiao[2] | Ge Zhao[1] | Paul Kempen[3,4] | Shuangqing Zhao[1] | Jianming Liu[1] | Sang Yup Lee[5] | Christian Solem[1]

2.1 Abstract

Lactococcus lactis, a lactic acid bacterium with a typical fermentative metabolism, can also use oxygen as an extracellular electron acceptor. Here we demonstrate, for the first time, that *L. lactis* blocked in NAD^+ regeneration can use the alternative electron acceptor ferricyanide to support growth. By electrochemical analysis and characterization of strains carrying mutations in the respiratory chain, we pinpoint the essential role of the NADH dehydrogenase and 2-amino-3-carboxy-1,4-naphthoquinone (ACNQ) in extracellular electron transfer (EET) and uncover the underlying pathway systematically. Ferricyanide respiration has unexpected effects on *L. lactis*, e.g. we find that morphology is altered from the normal coccoid to a more rod-shaped appearance, and that acid resistance is increased. Using adaptive laboratory evolution (ALE), we successfully enhance the capacity for EET. Whole-genome sequencing reveals the underlying reason for the observed enhanced EET capacity to be a late-stage blocking of menaquinone biosynthesis. The perspectives of the study are numerous, especially within food fermentation and microbiome engineering, where EET can help relieve oxidative stress, promote growth of oxygen sensitive microorganisms and play critical roles in shaping microbial communities.

2.2 Introduction

L. lactis is a Gram-positive lactic acid bacterium (LAB) used in various food fermentations, in particular within the dairy segment (1). When grown anaerobically, NADH generated in glycolysis is re-oxidized into NAD^+ by the lactate dehydrogenase, and usually >90% of the sugar metabolized ends up as lactic acid **(Fig. 2.1a)**. Despite of its fermentative metabolism, *L. lactis* can be cultivated with aeration, which usually has an effect on the composition of products formed. Most *L. lactis* strains are equipped with a H_2O-forming NADH oxidase (NoxE), which uses oxygen to regenerate NAD^+ **(Fig. 2.4a)**, and when grown with aeration, significant amounts of acetate and acetoin are formed in addition to lactic acid (2). Furthermore, *L. lactis* has been demonstrated to have a fully functional respiratory pathway in the presence of heme, its precursor protoporphyrin IX or hemin (ferric chloride heme). *L. lactis* is equipped with type II NADH dehydrogenase (NoxAB, non-proton pumping) and a heme-dependent cytochrome *bd* oxidase and is also able to synthesize menaquinones (MK) **(Fig. 2.4a)** (3). The cytochrome *bd* oxidase has a high affinity for oxygen and catalyzes the four-electron reduction of oxygen into water (4). The oxygen reduction process drives protons outside the membrane, similar to the process that occurs in a proton pump, leading

to a proton motive force (PMF) across the cell membrane (4). As a consequence, the need for proton pumping by the ATP driven F_1F_0-ATPase is reduced, which helps save ATP for growth, thereby increasing biomass yield (5). An additional benefit of having an active respiration is that it alleviates oxidative stress (6). For these reasons, the starter culture industry frequently uses aerobic respiratory conditions when producing food cultures, and use fish blood as a source of heme.

In food fermentations, it may be undesirable to introduce heme derived from animal blood and in particular oxygen, as oxygen is a strong oxidant that can cause lipid oxidation (7) and promote unwanted microbial growth (8). A promising alternative is to rely on alternative electron acceptors to oxygen for regenerating NAD^+, which has been termed extracellular electron transfer (EET) (9). Certain microbial species, e.g. *Geobacter* and *Shewanella*, rely on EET to reduce minerals and sustain growth, which has important biotechnological applications within bioremediation and biomining. EET can also be harnessed for producing biofuels and nanomaterials (10). In recent years, EET has received increasing attention due to its important role in microbial fuel cells (MFCs), a promising technology for generating renewable bioelectricity from various biomasses (11). Furthermore, EET appears to play a role for growth of certain bacteria in the mammalian gut (12–14). For example, the human pathogen *Listeria monocytogenes* relies on a flavin-based EET (FLEET) pathway to confer anaerobic growth advantages in the mouse intestinal lumen (15). Recent studies on EET in LAB have focused on species such as *Enterococcus faecalis* (16–18), *Lactiplantibacillus plantarum* (19) and *L. lactis* (20, 21). For the opportunistic human pathogen *E. faecalis*, it was proposed that demethylmenaquinone (DMK)-mediated EET takes place (16), and in this particular species a specific NADH dehydrogenase (Ndh3) and an EetA protein appear to be involved in EET (17, 18). In *L. plantarum*, FLEET also occurs, leading to increased NAD^+/NADH ratio and enhanced ATP formation. It has also been mentioned that *L. lactis* contains the FLEET genes except for *pplA* (19). For *L. lactis*, studies have shown that EET can alter product formation, and that the compound 2-amino-3-carboxy-1,4-naphthoquinone (ACNQ) can mediate EET when ferricyanide ($[Fe(CN)_6]^{3-}$) is used as the final electron acceptor (21). ACNQ, a soluble quinone, has been shown to be endogenously produced from DHNA, a menaquinone precursor (20). However, there are still many aspects of ACNQ-mediated EET that remain unresolved, which makes it difficult to come up with strategies to improve the capacity for EET in *L. lactis* and other LAB.

In this work, we start out by characterizing the effect of ferricyanide, a model electron acceptor in the field of bioelectrochemistry (22, 23), on the wild-type *L. lactis* strain MG1363. Subsequently, we study how ferricyanide affects a derivative of MG1363 whose NAD^+ regeneration pathways have been partly blocked due to gene deletions in *adhE* (encoding alcohol dehydrogenase), *pta* (encoding phosphate acetyltransferase) and *ldh* (encoding lactate dehydrogenase). We substantiate that ACNQ is involved in EET and manage to enhance EET by blocking menaquinone biosynthesis. Finally, we perform adaptive laboratory evolution (ALE) to obtain mutants with enhanced EET capacity, which are characterized physiologically and by whole-genome sequencing.

2.3 Materials and Methods

2.3.1 Bacterial strains and medium

All the constructed strains and plasmids are listed in **Table 2.1**. For molecular cloning, *E. coli* strains were aerobically grown at 30°C in Luria-Bertani (LB) broth (Sigma-Aldrich, USA) supplemented with 0.2% glucose (Sigma-Aldrich, USA). *L. lactis* was cultured at 30°C in M17 broth (Thermo Fisher Scientific, USA) supplemented with 1% glucose (GM17). When required, antibiotics were added with the following concentrations: erythromycin: 200 μg/mL for *E. coli* and 5 μg/mL for *L. lactis*. 2.5 μg/mL hemin (Sigma-Aldrich, USA) was added to activate respiration.

Table 2.1 Strains and plasmids used in the study.

Name	Genotype or description	Reference
L. lactis strains		
CS4363	MG1363 *Δ[3]ldh Δpta ΔadhE*	(32)
CS4363-F1	CS4363 adapted on ferricyanide about 300 generations	This work
CS4363-F2	CS4363 adapted on ferricyanide about 600 generations	This work
AceN	MG1363 *Δ[3]ldh Δpta ΔadhE ΔbutBA ΔnoxE*	(33)
AceN-F	AceN adapted on ferricyanide	This work
CS4363-MA	MG1363 *Δ[3]ldh Δpta ΔadhE ΔmenA*	This work
CS4363-MB	MG1363 *Δ[3]ldh Δpta ΔadhE ΔmenB*	This work
CS4363-NAB	MG1363 *Δ[3]ldh Δpta ΔadhE ΔnoxAB*	This work
CS4363-UE	MG1363 *Δ[3]ldh Δpta ΔadhE ΔubiE*	This work
Plasmids		

pCS1966	*oroP*-based selection/counters election vector, Em^R	(25)
pCS1966menA	Plasmid used for deleting *menA*	This work
pCS1966menB	Plasmid used for deleting *menB*	This work
pCS1966noxAB	Plasmid used for deleting *noxAB*	This work
pCS1966ubiE	Plasmid used for deleting *ubiE*	This work

2.3.2 Cultivation conditions and adaptive laboratory evolution (ALE)

In general, for growth experiments, cells from frozen glycerol stocks were streaked on GM17 agar and incubated overnight at 30°C. Single colonies were inoculated into 25 mL GM17 broth in a 300 mL shake flask aerobically at 30°C overnight to obtain the pre-culture. The pre-culture was inoculated into 2 mL fresh GM17 broth supplemented with different concentrations of ferricyanide in a 2 mL Eppendorf tube (Eppendorf, Germany) and the initial OD_{600} was 0.05. All tube cultivations were done statically (sealed tubes, no active aeration) at 30°C in an incubator.

The ALE was carried out in 15 mL tubes containing 15 mL GM17 medium with 50 mM ferricyanide (Thermo Fisher Scientific, USA) under static conditions in a 30°C incubator. After reaching the stationary phase, 1.5 mL of the culture was transferred into a fresh medium. The ALE of CS4363 was continued for about 6 months (approximately 600 generations). The ALE of AceN was carried out for approximately 3 months.

2.3.3 DNA techniques

To prepare electrocompetent cells of *L. lactis*, cells were grown in GM17 to OD_{600} of 0.5 to 0.8 and then inoculated (1%) into 25 mL GM17 containing 0.5 M sucrose (SGM17) supplemented with 1% glycine. The cells were harvested at OD_{600} of 0.2 to 0.7 by centrifugation at 4 °C, 4,000 × *g* for 10 minutes. After washing twice in ice-cold 0.5 M sucrose containing 10% glycerol, the cells were suspended in 250 µL washing solution and the solution was divided into small portions by 50 µL. Then the cells were stored at -80°C until use (24). One shot™ top10 chemically competent *Escherichia coli* (Thermo Fisher Scientific, USA) was used for storing recombinant plasmids. Phusion high-fidelity DNA polymerase (Thermo Fisher Scientific, USA) was used for PCR amplification. Gibson assembly HiFi master mix (Thermo Fisher Scientific, USA) was used for assembling gene fragments. DreamTaq Hot Start DNA polymerase (Thermo Fisher Scientific, USA) was used for PCR verification. Monarch plasmid miniprep kit (New England Biolabs, USA)

was used for plasmid extraction from *E. coli*. The DNA sequencing was performed by Macrogen (South Korea).

2.3.4 Construction of knock-out plasmids and strains

PCR primers used are shown in **Table S2.1**. The plasmid pCS1966 was used for knocking out genes in *L. lactis* (25). Derivatives of pCS1966 for deleting *menA, menB, noxAB* and *ubiE* were constructed as described below. When constructing knock-out plasmids: pCS1966menA, pCS1966menB, pCS1966noxAB and pCS1966ubiE, ~1000 bp regions upstream and downstream of the deleted genes were amplified by Phusion high-fidelity DNA polymerase. The primers used for amplifying upstream and downstream of the deleted genes: 2-up-F/R (*menA-upstream*), 3-up-F/R (*menB-upstream*), 4-up-F/R (*noxAB-upstream*), 7-up-F/R (*ubiE-upstream*), 2-down-F/R (*menA-downstream*), 3-down-F/R (*menB-downstream*), 4-down-F/R (*noxAB-downstream*) and 7-down-F/R (*ubiE-downstream*). Phusion high-fidelity DNA polymerase was also used to generate linearized versions of plasmid pCS1966. Primers 2-plas-F/R, 3-plas-F/R, 4-plas-F/R and 7-plas-F/R were used for corresponding genes. To insert upstream and downstream sequence in multiple cloning site (MCS) of pCS1966, upstream, downstream and linearized plasmid were assembled by using the Gibson assembly HiFi master mix. The recombinant plasmids were introduced into prepared *L. lactis* competent cells by electroporation using a MicroPulser Electroporator (Bio-Rad, Hercules, USA). The electroporation condition: voltage 2.0 kV, resistance 200 Ω and time constants of 4.5 to 5 ms (24). The successful integration resulted in erythromycin resistance. 5-fluoroorotic acid (Thermo Fisher Scientific, USA) was used for the counter selection (25). Deletions were verified using primers 2-F/R (*menA*), 3-F/R (*menB*), 4-F/R (*noxAB*) and 7-F/R (*ubiE*) with DreamTaq Hot Start DNA polymerase.

2.3.5 Measurement of cell growth

Cell growth was measured by recording the time profile of optical density at 600 nm (OD_{600}). Since the medium changed color during growth, cells were harvested by centrifugation (14,000 rpm, 2 minutes), washed and re-suspended in dH_2O prior to measurements. dH_2O was used as reference. Specific growth rates were calculated as described by Widdel (26).

2.3.6 Quantification of fermentation metabolites

Quantification of metabolites (glucose, pyruvate, acetoin, 2,3-butanediol) was carried out by high-performance liquid chromatography (HPLC) using an Aminex HPX-87H column (Bio-Rad, Hercules, USA). 5 mM H_2SO_4 was used as the mobile phase at a flow rate of 0.5 mL/min. The temperature of the column oven was set to 60^{o}C. Glucose, acetoin, and 2,3-butanediol were quantified using an RI detector, while pyruvate was quantified using a UV detector at the wavelength of 210 nm. The samples for HPLC analysis were filtered using 0.22 μM filters (Labsolute) immediately after sampling and were stored at -20^{o}C.

2.3.7 Quantification of ACNQ and DHNA

Quantification of ACNQ and DHNA was carried out by HPLC equipped with the HC-C18 column (Agilent, USA). ACNQ standard (ALB Technology, Hong Kong) and DHNA standard (Sigma-Aldrich, USA) were used to prepare standard curves. The mobile phase was a 23:77 mixture of acetonitrile and 0.2% acetic acid, respectively. The temperature of the column oven was set at 40^{o}C and the flow rate was 0.5 mL/min. The concentration of ACNQ and DHNA was measured using UV detector at the wavelength of 269 nm.

2.3.8 Determination of pH change

An iCinac instrument (KPM Analytics, USA) was used to determine pH profiles. The overnight seed culture was inoculated in fresh GM17 medium with different concentrations of ferricyanide to reach an initial OD_{600} of 0.05. The total volume was set to 40 mL in a 50 mL centrifuge tube. After inserting the pH-electrode the tube was almost completely filled. The tubes were sealed with sterilized laboratory wrapping film (parafilm, Bemis, USA). The centrifuge tubes were placed in a 30^{o}C water bath. Immediately after the addition of the cells, pH recording was initiated.

2.3.9 Measurement of NADH/NAD^+ ratio

Samples were taken from exponentially growing cultures of *L. lactis*. Then samples were rapidly chilled down by centrifugation at 4^{o}C, 14,000 rpm for 2 minutes and the supernatants were discarded. The pellets were quenched quickly with liquid nitrogen and subsequently stored at -20^{o}C before measuring. The extraction and quantification of NADH/NAD^+ were performed using the NAD^+/NADH-Glo^{TM} Assay kit (Promega, Madison), following the instructions from the

supplier. The cell dry weight (CDW) was calculated by using equation: CDW (g/L) = 0.37 g/L × OD_{600} (27).

2.3.10 Scanning electron microscopy (SEM) of cell morphology

CS4363 cells were cultured with/without ferricyanide until the stationary phase. Then cells were collected by centrifugation and the supernatants were removed. The pellets were washed and re-suspended in 100 mM phosphate-buffered saline (PBS) buffer (pH 7.4). An equal volume of fixative, consisting of 4% glutaraldehyde and 8% paraformaldehyde in water, was added to the cell suspension and maintained at room temperature for 1 hour. After that, the samples were kept at 4°C until imaging. The morphology was observed by using 5kV in an FEI Quanta FEG 200 Environmental SEM.

2.3.11 Wavelength scan and detection of ferricyanide and ferrocyanide

Wavelength scan of 100 µl 8 mM ferricyanide (dissolved in GM17), 8 mM ferricyanide (dissolved in GM17), and empty GM17 medium separately were conducted by Infinite 200 PRO microplate reader (Tecan, Switzerland). The range of wavelength scan was from 315 nm to 500 nm. The calibration curve of ferricyanide and ferrocyanide was measured at 420 nm and at 320 nm. The supernatant of sample was obtained by centrifugation and 100 µl was taken for measurement at 420 nm and 320 nm. The detailed calculation process can be found in **Fig. S2.1**.

2.3.12 Electrochemical measurements

Cyclic voltammetry (CV) was recorded by using a potentiostat (Autolab PGSTAT12, EcoChemie, Netherlands) in a three-electrode setup, using a Ag/AgCl with saturated KCl as the reference electrode, a platinum wire counter electrode, and a glassy carbon working electrodes (GCE) respectively. CVs were usually recorded with a scan rate of 5 mV/s. For CVs of ACNQ, menadione and ferricyanide, different scan rates of 5, 20, 50, 100 and 200 mV/s were used. Before electrochemical measurements, GCEs were polished with 0.1 and 0.05 µm Al_2O_3 slurries sequentially. Then GCEs were sonicated in acetone for 5 minutes twice and subsequently in deionized water for 5 minutes. The electrolyte was GM17 medium. Dissolved oxygen was removed by bubbling argon gas through the medium and argon was maintained above the solution throughout the measurements.

2.3.13 Recovery test of EET ability in knock-out strain CS4363-MB

Overnight pre-cultures of CS4363-MB were inoculated into 2 mL fresh GM17 broth with 50 mM ferricyanide supplemented with different concentrations of DHNA (0.01-0.2 mM), ACNQ (0.01-0.2 mM), menadione (0.05-1 mM) and menaquinone-4 (MK-4) (0.1-1 mM), respectively, in 2 mL Eppendorf tubes and the initial OD_{600} was 0.05. DHNA and ACNQ were dissolved in methanol. Menadione and MK-4 were dissolved in ethanol. Considering that organic solvents may have a negative effect on the growth of the cell, cultures containing the equivalent volume of methanol and ethanol were included as well. The relative OD_{600} = OD_{600} (add ACNQ/DHNA/menadione/MK-4) – OD_{600} (add same volume of methanol/ethanol) was adopted. The samples at 0 h and 12 h were taken for further HPLC analysis.

2.3.14 Complementation assays for multiple strains

Overnight cultures of CS4363, CS4363-MA, and CS4363-MB were streaked on GM17 supplemented with 50 mM ferricyanide using sterile loops. After the plates had been dried on a flow clean bench, they were incubated overnight in the anaerobic tank with an anaerobic bag. Digital photos were taken of plates placed on a lightbox.

2.3.15 Whole genome sequencing

Whole genome sequencing of CS4363, AceN, CS4363-F1, CS4363-F2, and AceN-F was carried out by BGI Europe A/S (Denmark), using PE150 sequencing and the DNBseq tech platform (BGISEQ)(28). After the preparation of short insert fragment library preparation, at least 1Gb data per sample was generated. Geneious Prime (Auckland, New Zealand) was used to analyze the sequencing data, map the genome, and identify variations. The *L. lactis* MG1363 (Genbank accession number: NC009004) genome was used as a reference. Single nucleotide variations (SNVs) were identified based on Bowtie2 assembled data. The SNVs were compared between all ferricyanide adaptive strains and their parental strains. The genome sequencing project has been deposited in the NCBI under the BioProject (https://www.ncbi.nlm.nih.gov/bioproject) accession PRJNA869519. The sequencing data have been deposited in NCBI Sequence Read Archive (SRA; https://www.ncbi.nlm.nih.gov/sra) under the accession numbers of SRR21065319, SRR21065318, SRR21065317, SRR21065316, and SRR21065315.

2.4 Results

2.4.1 Growth and product formation of wild-type *L. lactis* is perturbed by ferricyanide

Ferricyanide is chosen as a model electron acceptor due to its relatively moderate redox potential, which is insensitive to pH changes in the media (29). It can serve as an excellent electron acceptor in EET (30), but has also been reported to be toxic to certain bacteria (31). To determine how *L. lactis* responds to the presence of ferricyanide, we grew the wild-type *L. lactis* MG1363 in rich GM17 medium containing different amounts of ferricyanide. As shown in **Fig. 2.1b**, the growth of MG1363 was somewhat inhibited by ferricyanide, and the specific growth rate decreased to $0.870 \pm 0.006\ h^{-1}$ in the presence of 50 mM ferricyanide, which was 22% below that of MG1363 without ferricyanide. The effect of ferricyanide was directly correlated to the concentration **(Fig. 2.1b)**. Ferricyanide also altered fermentation product composition and promoted the formation of acetate, ethanol and acetoin **(Fig. 2.1c)**, suggesting that ferricyanide indeed was involved in NAD^+ regeneration and EET.

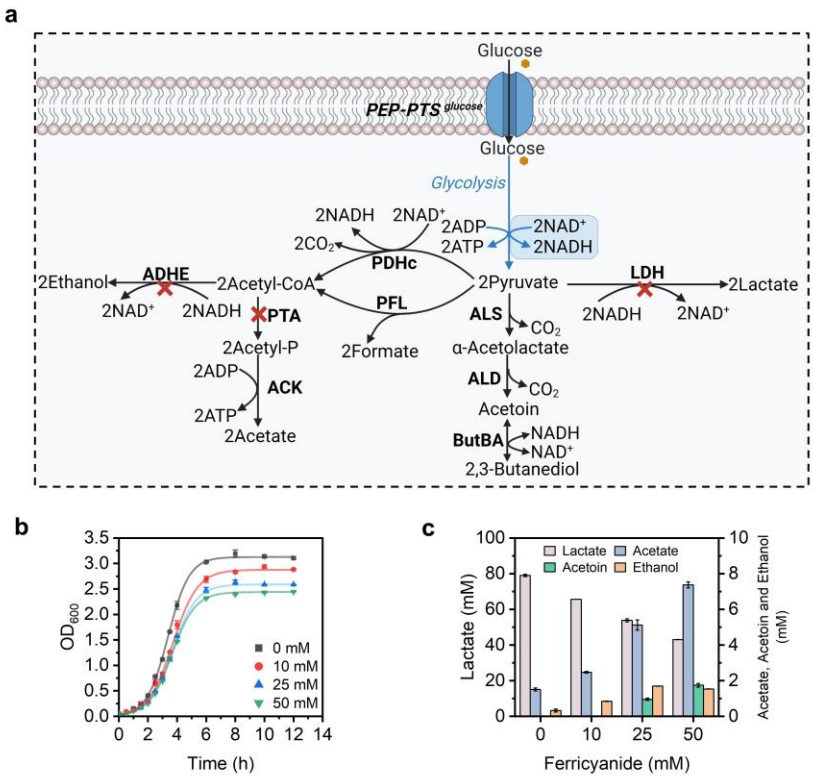

Fig. 2.1 Characterization of growth and product formation of MG1363 in the presence of different concentrations of ferricyanide. (a) Schematic drawing of glycolytic pathway in *L. lactis*. LDH: lactate dehydrogenases; ALS: α-

acetolactate synthase; ALD: α-acetolactate decarboxylase; ButBA: 2,3-butanediol dehydrogenase; PDHc: pyruvate dehydrogenase complex; PFL: pyruvate-formate lyase; ADHE: alcohol dehydrogenase; PTA: phosphate acetyltransferase; ACK: acetate kinase. The red crosses indicate inactivated pathways in CS4363. (b) Growth performance of MG1363 in a time course of 12 h. (c) Metabolite levels of MG1363 at the time point of 12 h. MG1363 was cultured in GM17 (M17+Glucose) supplemented with ferricyanide under relative anaerobic conditions.

2.4.2 Extracellular electron transfer enables growth of an *L. lactis* mutant partly blocked in NAD^+ re-generation

CS4363, a derivative of MG1363, which is partly blocked in NAD^+ regeneration, is unable to grow under strictly anaerobic condition. However, it can grow under aerated conditions where oxygen serve as electron acceptor (32, 33) **(Fig. 2.1a)**. Based on the observations with the wild-type strain MG1363, we speculated that CS4363 might be able to grow under anaerobic (or O_2-limiting) conditions in the presence of ferricyanide, and this was indeed what we found. As the concentration of ferricyanide increased from 25 to 150 mM, the time to reach the stationary phase was shortened from 12 to 8 h **(Fig. 2.2a)**. Without ferricyanide added, limited growth was observed, which was due to small amounts of dissolved oxygen in the medium. At the highest concentration tested (150 mM), the specific growth rate of CS4363 was $0.626 \pm 0.009\ h^{-1}$. The final OD_{600} reached around 2 when the concentration of ferricyanide was in the range 75 to 150 mM, and a similar amount of glucose had been consumed by these cultures **(Fig. 2.2b)**. For all ferricyanide concentrations tested, a small amount of pyruvate was detected, the concentration of which peaked in the late exponential phase and subsequently declined; there was a clear correlation between pyruvate production and ferricyanide concentration **(Fig. 2.2c)**. In conclusion, ferricyanide enabled anaerobic growth of CS4363 with acetoin as the main fermentation product **(Fig. 2.2d)**.

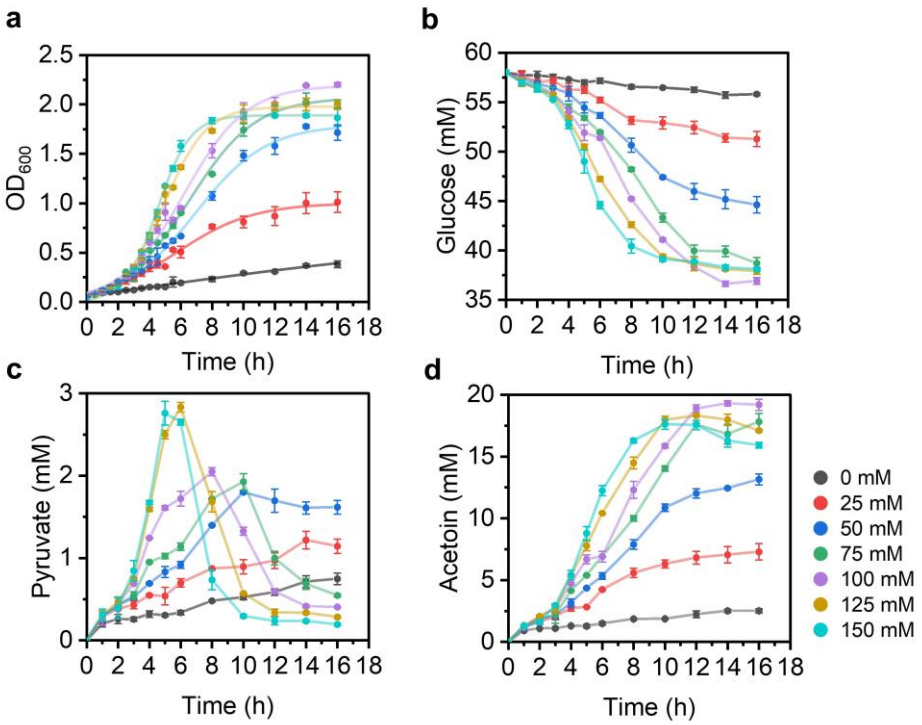

Fig. 2.2 Characterization of growth and product formation of CS4363 in the presence of different concentrations of ferricyanide. (a) Time profiles of growth performance. (b) Glucose consumption. (c) Pyruvate formation. (d) Acetoin formation. CS4363 was cultured in GM17 supplemented with ferricyanide under relative anaerobic conditions.

As CS4363 grew in the medium containing ferricyanide, the color changed due to the reduction of ferricyanide (yellow) to ferrocyanide (colorless) **(Fig. 2.3a)**. At higher concentrations, exceeding 75 mM, the color of the medium became greenish after 12 h, and the pH dropped to approximately 3.8 ± 0.0 in 16 h **(Fig. 2.3b)**. It has been reported that, ferricyanide can decompose in acidic media (pH < 4.0), generating free iron species and finally Prussian blue ($Fe_4[Fe(CN)_6]_3$) (34, 35), which may explain the observed green color. The concentration of ferricyanide and ferrocyanide was quantified by an optical method described by Lai et al (23) **(Fig. S2.1a-d)**. As shown in **Fig. S2.1e-f**, for CS4363, when grown in the presence of 25 or 50 mM ferricyanide, ferricyanide was stoichiometrically reduced to ferrocyanide at 16 h. At ferricyanide concentrations above 75 mM, part of the ferricyanide appeared to decompose into Prussian blue due to the acidic pH, which has been reported previously (35) **(Fig. 2.3b)**.

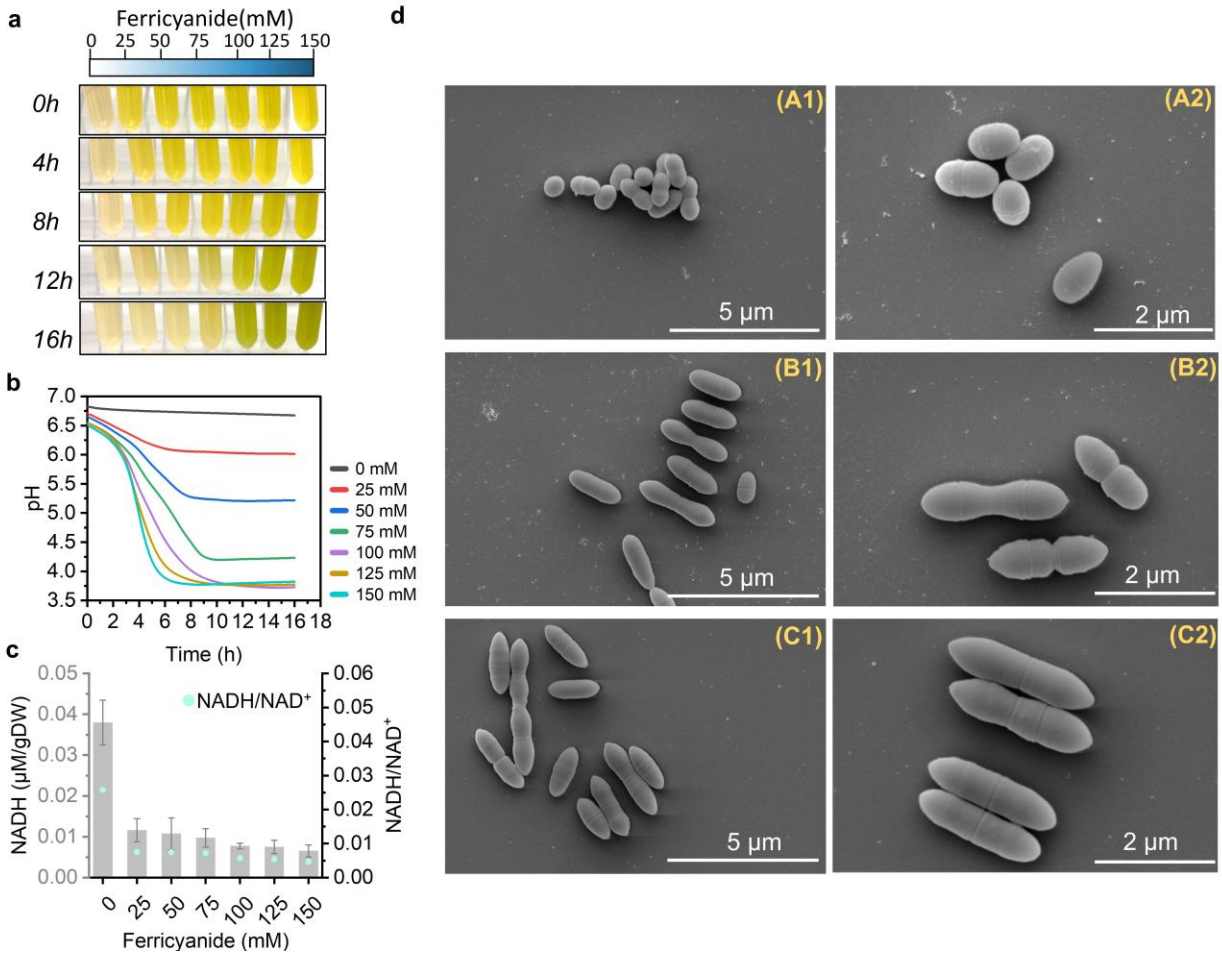

Fig. 2.3 The concentration effect of ferricyanide on CS4363. (a) The color change with time at different concentrations of ferricyanide. (b) The pH change with time at different concentrations of ferricyanide. (c) NADH/NAD^+ ratio changes at different concentrations of ferricyanide at exponential phase. (d) SEM images of CS4363 at stationary phase without ferricyanide (A1, A2), with 50 mM ferricyanide (B1, B2) and 150 mM ferricyanide (C1, C2). CS4363 was cultured in GM17 supplemented with ferricyanide under relative anaerobic conditions.

As can be seen in **Fig. 2.3b**, the pH of the culture medium dropped more quickly with increasing concentrations of ferricyanide, implying that NADH was oxidized more rapidly to NAD^+ thereby leading to quicker acidification of the medium. This could also be seen directly from the trend of the NADH/NAD^+ ratio measured, which decreased from 0.0258 ± 0.0002 (without ferricyanide) to 0.0047± 0.0011 (with 150 mM ferricyanide) **(Fig. 2.3c)**. Besides its growth-stimulating effect on CS4363, ferricyanide also had a clear effect on cell morphology **(Fig. 2.3d)**, and with increasing ferricyanide concentrations the cells became more rod-shaped.

2.4.3 Blocking menaquinone biosynthesis can enhance EET in *L. lactis*

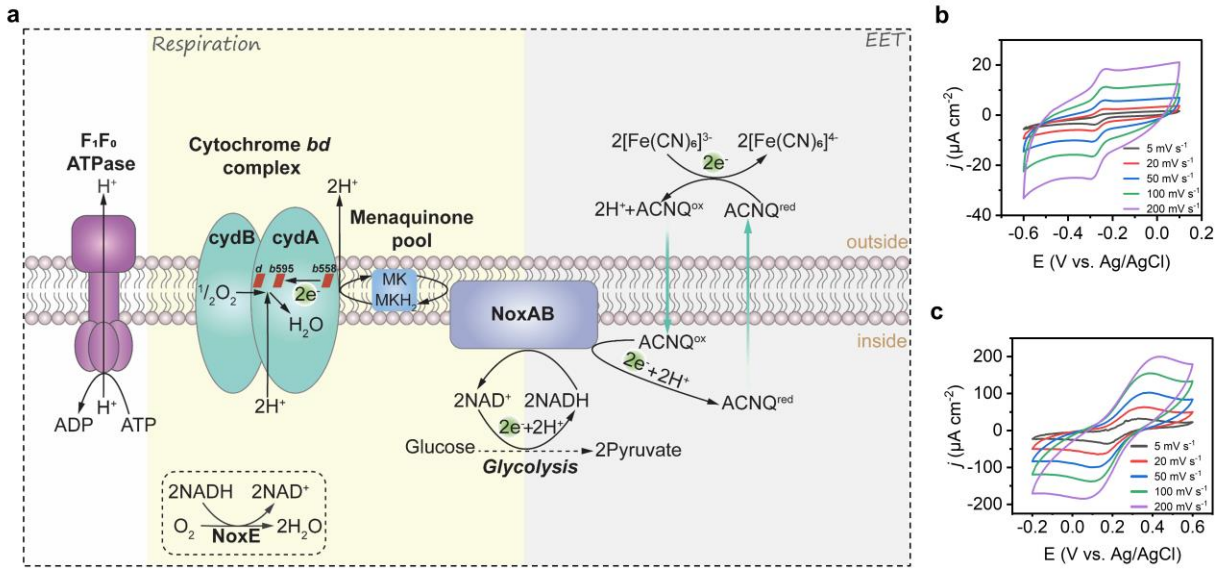

Fig. 2.4 Schematic drawing of pathway for NAD^+ regeneration and cyclic voltamograms (CVs). (a) Respiration and proposed mechanism of ACNQ-mediated ferricyanide reduction. NoxAB: NADH dehydrogenase; NoxE: NADH oxidase; F_1F_0-ATPase: F_1F_0-ATP synthase; MK: menaquinone; MKH_2: menaquinol. CVs of 0.023 mM ACNQ (b), 1 mM ferricyanide (c) at different scan rates.

The role of diaphorase and ACNQ for EET in *L. lactis* has been indicated previously (21). NADH dehydrogenase (NoxAB) is an example of a diaphorase (36). ACNQ was identified to be a soluble analog of menaquinone (MK), which is derived from 1,4-dihydroxy-2-naphthoic acid (DHNA), an intermediary in menaquinone biosynthesis, formed without the participation of enzymes (37). As shown in **Fig. 2.5a**, the menaquinone biosynthesis pathway can be divided into two parts: production of the napthoate ring: DHNA and production of the polyprenyl diphosphate (PPP) chain. The precursors D-erythrose-4-phosphate (E4P) and phosphoenolpyruvate (PEP) are converted to DHNA by shikimate and menaquinone pathways. Acetyl-CoA from glycolysis is converted to PPP chain by mevalonate and polyprenyl pathways. 1,4-dihydroxy-2-naphthoyl-CoA synthase (MenB) is the key enzyme for the formation of DHNA. About 2% of the DHNA pool can be transformed into ACNQ through a chemical reaction with NH_3, and the remaining 98% is converted into DMK by 1,4-dihydroxy-2-naphthoate heptaprenyltransferase (MenA). DMK can further be metabolized into menaquinone (MK), which is important in aerobic respiration, by demethylmenaquinone methyltransferase (UbiE) (37, 38). We determined the standard redox potential (E^0) of ACNQ and ferricyanide in GM17 to be close to -0.26 and 0.24 V vs. Ag/AgCl, respectively **(Fig. 2.4b and**

2.4c), thus thermodynamically ACNQ should be able to transfer electrons to ferricyanide. To verify this proposed EET pathway **(Fig. 2.4a)**, we knocked out the genes encoding NoxAB, MenA, and MenB. The resulting mutants were named CS4363-NAB, CS4363-MA, and CS4363-MB.

When *menA* was knocked out in CS4363, this resulted in faster growth in ferricyanide supplemented GM17, and CS4363-MA grew with a specific growth rate of 0.741 ± 0.027 h^{-1}, approximately 18% faster than CS4363 in the presence of 150 mM ferricyanide, whereas the final cell density remained the same **(Fig. 2.5b (i))**. Likewise, the CS4363-MA acidified the medium more quickly than CS4363 **(Fig. 2.5b (ii))** and the glucose consumption rate was higher than for CS4363 **(Fig. 2.5b (iii))**. In contrast, when *menB* was knocked out, formation of DHNA, and thus of ACNQ, was prevented, and this almost completely eliminated EET. An interesting observation was that CS4363-MB grew slightly better than CS4363 without ferricyanide, which indicated that other compounds besides ACNQ could serve as electron carrier. When the NADH dehydrogenase was eliminated, this also eliminated EET. In the presence of ferricyanide, CS4363-NAB displayed the same poor growth as CS4363 in the absence of ferricyanide, demonstrating that the NADH dehydrogenase (NoxAB) is an essential component for EET in *L. lactis* when using ferricyanide as the terminal electron acceptor.

The *menB* knock-out strain CS4363-MB was then used in complementation studies where the growth stimulatory effect of different quinones was investigated. As shown in **Fig. 2.5c**, supplementation with ACNQ, DHNA, and the DMK analogue menadione was able to restore growth of CS4363-MB, whereas MK-4 failed to do this. The growth stimulatory effect could also be observed on agar plates when CS4363-MB was streaked in close proximity to CS4363 or CS4363-MA **(Fig. S2.2)**, and thus growth stimulating quinones are released to the surroundings by LAB able to synthesize DHNA. Even though the EET ability of CS4363-MB could be restored by adding DHNA **(Fig. 2.5c)**, we were unable to detect DHNA in the culture medium of CS4363-MB, whereas ACNQ was detected after 12 h and the yield was around 2%, which is consistent with previous findings **(Fig. S2.3)**. It has been stated that menadione (Vitamin K_3) can serve the same function as DMK (16). Menadione has a suitably low E^0 (-0.18 V vs. Ag/AgCl, **Fig. S2.4a**), thus enabling it to serve as an electron mediator to ferricyanide, and this compound was also able to restore the EET ability of CS4363-MB. In an attempt to achieve build-up of DMK, which may be able to participate in EET and thus stimulate growth, the gene *ubiE*, coding for the enzyme that

converts DMK into MK, was knocked out. The resulting strain CS4363-UE, however, did not grow better than CS4363 in the presence of 150 mM ferricyanide **(Fig. S2.4b-d)**. These results clearly show that NoxAB and ACNQ are key components of EET when ferricyanide is used as the final electron acceptor.

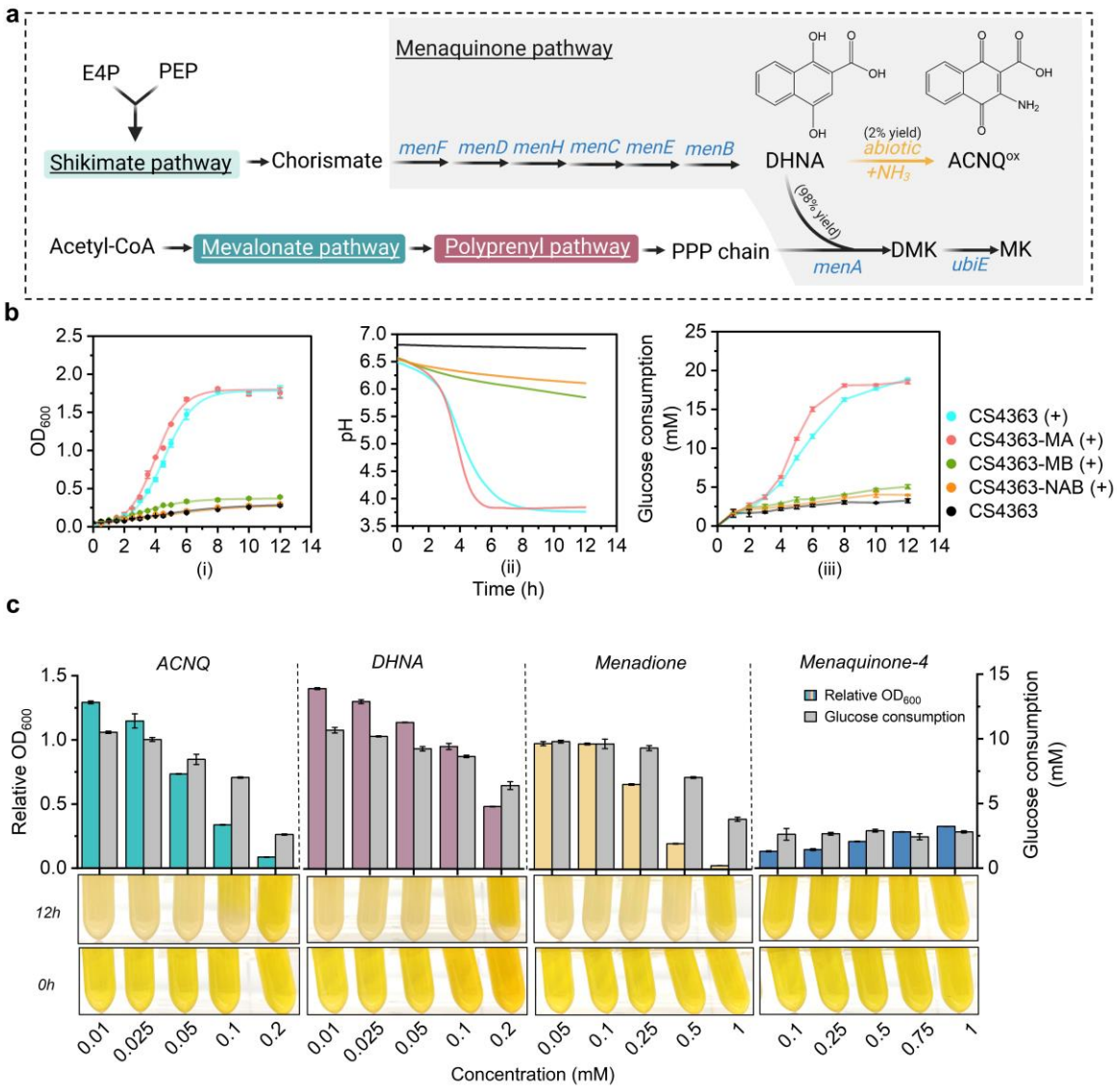

Fig. 2.5 The involvement of NADH dehydrogenase and quinones in EET. (a) The quinone biosynthesis pathway in *L. lactis*. MenF*:* isochorismate synthase; MenD:2-succinyl-5-enolpyruvyl-6-hydroxy-3-cyclohexene-1-carboxylate synthase; MenH: demethylmenaquinone methyltransferase; MenC*:* o-succinylbenzoate synthase; MenE*:* o-succinylbenzoate-CoA ligase; MenB: 1,4-dihydroxy-2-naphthoyl-CoA synthase; MenA: 1,4-dihydroxy-2-naphthoate heptaprenyltransferase; UbiE: demethylmenaquinone methyltransferase; PEP: phosphoenolpyruvate; E4P: D-erythrose-4-phosphate; PPP: polyprenyl diphosphate; DHNA: 1, 4-dihydroxy-2-naphthoate; ACNQ: 2-amino-3-

carboxy-l,4-naphthoquinone; DMK: demethylmenaquinone; MK: menaquinone. (b) The growth curve (i), pH change with time (ii) and glucose consumption change with time (iii) of CS4363 and knock-out strains with 150 mM ferricyanide. (+) indicates the addition of 150 mM ferricyanide. (c) The relative OD_{600} and glucose consumption of CS4363-MB with different concentrations of ACNQ, DHNA, DMK analogue menadione, and MK-4 with 50 mM ferricyanide. The color change at 0 and 12 h (the bottom row). The relative OD_{600} = OD_{600} (add ACNQ/DHNA/menadione/MK-4) – OD_{600} (add same volume of methanol/ethanol) was presented. CS4363 and knock-out strains were cultured in GM17 supplemented with ferricyanide under relative anaerobic condition.

2.4.4 Using adaptive laboratory evolution to enhance extracellular electron transfer capacity of *L. lactis*

The growth stimulatory effect of ferricyanide on CS4363 was found to be directly correlated with the concentration of ferricyanide **(Fig. 2.2a)**. To improve the capacity for EET of *L. lactis* at lower concentrations of ferricyanide, CS4363 was adaptively evolved in the presence of 50 mM ferricyanide anaerobically. The rationale was that faster-growing mutants might be better at doing EET. After around 300 generations of growth, the faster-growing isolate CS4363-F1 was obtained, which had a specific growth rate of 0.744 ± 0.002 h^{-1} as compared to 0.419 ± 0.006 h^{-1} for CS4363 **(Fig. 2.6a)**. Where the main fermentation product of CS4363 was acetoin, CS4363-F1 almost exclusively produced 2,3-butanediol **(Fig. 2.6b)**. The enzyme 2,3-butanediol dehydrogenase (ButBA) catalyzes the reduction of acetoin into 2,3-butanediol, a process which consumes NADH, and thus helps regenerate NAD^+ **(Fig. 2.1a)**. The adaptation was continued for an additional 300 generations, which resulted in CS4363-F2, which grew even faster ($\mu_{max} = 0.896 \pm 0.020$ h^{-1}). CS4363-F1 and CS4363-F2 reached the same high cell density, OD_{600} of 2.8 **(Fig. 2.6a)**. Where CS4363 and CS4363-F1 both accumulated small amounts of pyruvate, CS4363-F2 produced less (0.674 ± 0.077 mM for CS4363-F2 as compared to 2.628 ± 0.189 mM for CS4363-F1).

In addition to CS4363, a derivative lacking NADH oxidase and 2,3-butanediol dehydrogenase, AceN, was adapted as well **(Fig. 2.6c)**. AceN is only able to grow under aerobic conditions when respiration is active, i.e. in the presence of hemin or another heme source (33). Interestingly, the adapted derivate AceN-F could not grow aerobically with 2.5 μg/mL hemin after around 3 months of ALE **(Fig. 2.6d)**, i.e. AceN-F had lost the ability to respire. The color change observed when ferricyanide is reduced to ferrocyanide, occurred more quickly for AceN-F than its parent AceN **(Fig. 2.6d)**, and more ferrocyanide was able to accumulate; the AceN-F culture accumulated 46.874 ± 1.127 mM ferrocyanide, while the AceN culture accumulated 42.289 ± 1.242 mM

ferrocyanide. The final cell density (OD_{600}) for AceN-F was higher (1.413 ± 0.033) than for AceN **(Fig. 2.6e)**.

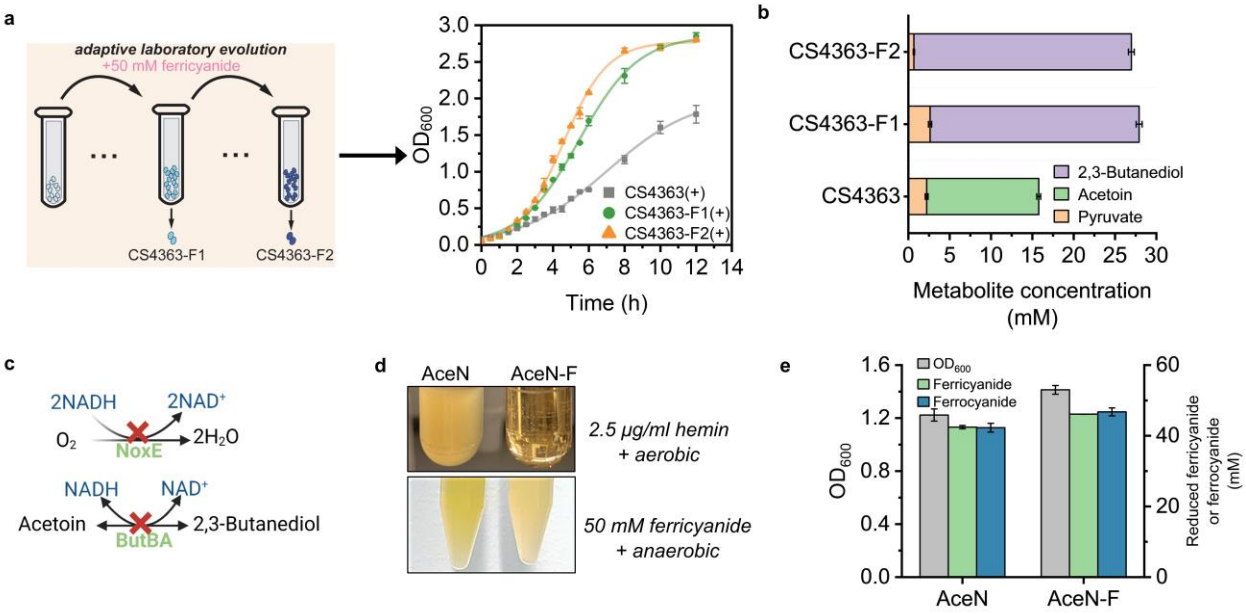

Fig. 2.6 The performance of wild-type strains and ALE strains. (a) Illustration of adaptive laboratory evolution under 50 mM ferricyanide (left). Growth performance of CS4363, CS4363-F1, and CS4363-F2 with 50 mM ferricyanide (right). (b) Metabolite compositions of CS4363, CS4363-F1, and CS4363-F2 with 50 mM ferricyanide at 12 h. (+) indicates the addition of 50 mM ferricyanide. (c) Two pathways for NAD^+ regeneration were blocked in AceN. (d) The observed difference between AceN and AceN-F under respiration and EET condition. (e) OD_{600}, ferricyanide reduction and ferrocyanide formation by strains AceN and AceN-F under 50 mM ferricyanide at 16 h.

2.4.5 Scrutinizing the genomes of the ferricyanide-adapted strains

To determine the underlying reason for (i) the faster growth of the adapted mutants derived from CS4363, and (ii) the lost ability of the adapted AceN mutant to respire, these mutants and their parent strains were sequenced. In CS4363-F1, the insertion sequence IS*905*, the smallest transposable element found in *L. lactis* (39), had integrated into the initial coding region of the gene *mlep* and into the region between gene *butB* and *rodA* **(Fig. 2.7a)**. Interestingly, the mapped reads corresponding to the region flanked by these two IS*905* elements were elevated 20-fold as compared to other genes in the genome, indicating the presence of many copies. The *butBA* operon, encoding 2,3-butanediol dehydrogenases, located to this region. For the mutant CS4363-F2, IS*905* had also inserted itself in the coding region of gene *menA* (the start codon ATG + 99 bp), leading

to premature termination and thus inactivation of *menA* **(Fig. 2.7b)**. In addition, a single-nucleotide variation (SNV) was found between genes *noxB* and *noxA*, encoding the NADH dehydrogenase (NoxAB), 73 bp upstream of the *noxB* start codon, resulting in an A to C nucleotide change **(Fig. 2.7b)**. By using the online promoter prediction tool BDGP (https://www.fruitfly.org/seq_tools/promoter.html), the promoter sequence of *noxB* was predicted **(Table S2.2)** and this SNV located to this promoter, probably altering the expression of *noxB*.

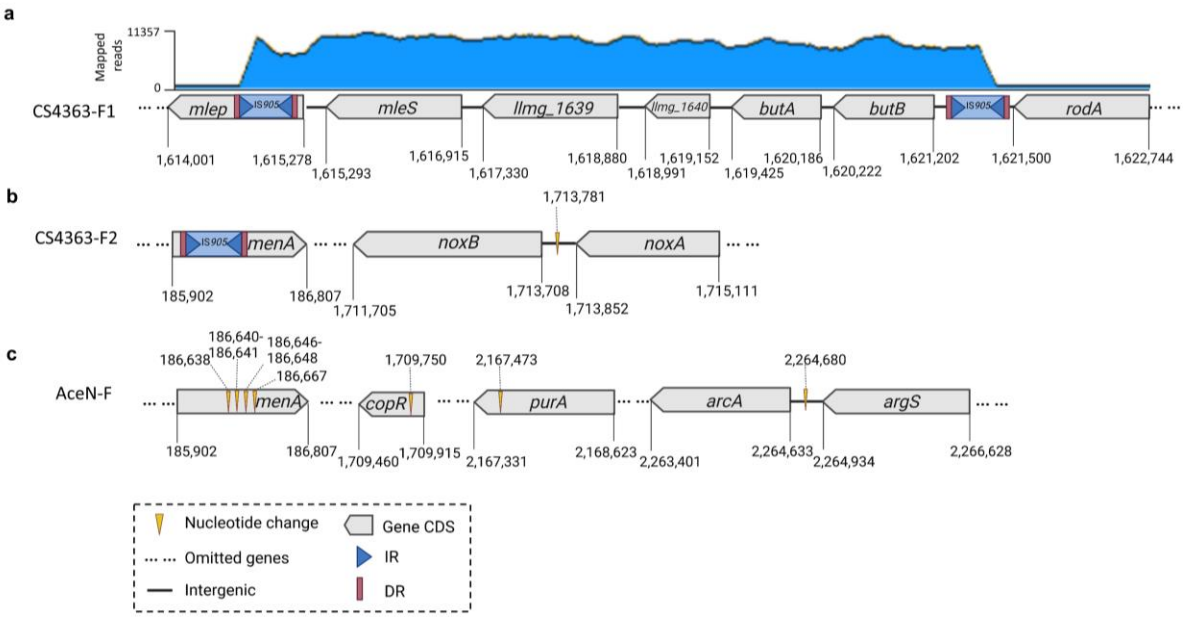

Fig. 2.7 Mutations identified in the ferricyanide-adapted mutants. (a) CS4363-F1, (b) CS4363-F2 and (c) AceN-F. Yellow triangle: nucleotide change; Dotted line: omitted genes; Bold line: intergenic; Pentagram: protein coding sequence (CDS) region of the gene; Blue triangle: short terminal inverted repeats (IR); Pink rectangle: directed repeats (DR). IS: insertion sequence. The number on the top of gene CDS: the location of the mutation in the gene. The number on the bottom of gene CDS: the location of the gene.

As shown in **Fig. 2.7c**, in mutant AceN-F, six SNVs were detected in the coding region of *menA*, in the middle of the gene, which most likely caused the inactivation of *menA*. Thus, both in CS4363-F2 and AceN-F, *menA* had been inactivated, leading to an enhanced capacity to respire with ferricyanide, something which was also observed for the engineered CS4363-MA mutant. As mentioned AceN normally depends on hemin-enabled oxygen respiration, since all other NAD^+ regenerating pathways have been eliminated. The loss of this ability concurred with the loss of a functional MenA activity. In addition to these SNVs, AceN-F contained three additional SNV's, one in *copR* encoding a copper-responsive repressor (C-A), one in *purA* encoding

adenylosuccinate synthase (C-A) and the final one in upstream of *arcA* encoding arginine deiminase (T-C). The SNV in gene *copR* resulted in an amino acid change from glutamic acid (GAA) to the stop codon (UAA), while the SNV in gene *purA* lead to the amino acid change from cysteine (UGC) to phenylalanine (UUC). The SNV in upstream of *arcA* was also found in the predicted promoter sequence **(Table S2.2)**.

2.5 Discussion

2.5.1 Ferricyanide has different effects on wild-type strain MG1363 and mutant CS4363

Ferricyanide was found to slightly inhibit the growth of the wild-type strain MG1363, and this most likely can be attributed to the toxicity of ferricyanide (31). We found that the metabolic flux of MG1363 was redirected in the presence of ferricyanide, and that this was due to EET to ferricyanide. These findings are in good agreement with previous research, although we found slightly different effects on fermentation product composition (21).

We also characterized the effect of ferricyanide on *L. lactis* CS4363, which is impaired in NAD^+ regeneration**.** We found that ferricyanide enabled excellent growth of CS4363, and the growth stimulating effect was found to increase with ferricyanide concentration. As CS4363 lacks LDH, PTA, and ADHE activities **(Fig. 2.1a)** (32), this strain generally requires aeration to grow and mainly forms acetoin and small amounts of pyruvate as its end products. Despite having genes encoding functional 2,3-butanediol dehydrogenases (*butBA*), these are usually not expressed sufficiently to allow for 2,3-butanediol to be formed. In the presence of ferricyanide, acetoin and pyruvate indeed were the main metabolic products formed by CS4363. The NADH generated by glycolysis could be re-oxidized to NAD^+ through EET and the effect of ferricyanide on growth of CS4363 correlated nicely with the NADH/NAD^+ ratio measured, which is similar to the performance of another respiration-dependent strain described in our previous research (40). The importance of rapid quenching for obtaining reliable values for intracellular metabolites has often been stressed (41). Here, we relied on a simple approach, where the culture was cooled down and centrifuged at 4°C, after which the cell pellets were frozen rapidly using liquid nitrogen. Although more rapid quenching is possible by using other approaches, we managed to clearly demonstrate the effect of ferricyanide respiration on the NADH/NAD^+ ratio.

We observed that the pH dropped along with cell growth, which at first may appear puzzling as CS4363 lacks a functional lactate dehydrogenase. However, when ferricyanide serves as the final

electron acceptor, two protons and two electrons formed are transferred from the quinone pool to the outside, and where the electrons are used to reduce ferricyanide to ferrocyanide, the protons will cause acidification of the fermentation medium. In general, growth of *L. lactis* is greatly hampered when the pH is below 5.0 (42). The wild-type strain MG1363 normally lowers the pH of the growth medium to around 4.3, but in our case, when CS4363 grew in the presence of ferricyanide, the culture attained a pH as low as 3.72, which has never been reported for *L. lactis*. This enhanced acid tolerance, might be attributed to the changes in cell morphology observed; in the presence of ferricyanide, the cells became enlarged, thereby reducing the surface area-to-volume ratio, which might help the cells to cope with a low extracellular pH, by reducing overall influx of protons (43). The cell wall of Gram-positive bacteria consists of peptidoglycan (PG) which is decorated with teichoic acids (TAs), polysaccharides (PSs), and proteins (44). PG provides strength and rigidity to the cell wall and maintains cell shape (45). The cell wall can serve as a reservoir of H^+ (46, 47), and since ferricyanide respiration generates protons, this may result in the breaking of bonds in the PG, thereby reducing the stiffness of the cell wall, enabling it to stretch and expand (48), ultimately resulting in the cell morphology we observe for CS4363 in the presence of ferricyanide. Further work is needed to verify this hypothesis.

2.5.2 ACNQ and NoxAB are essential for EET with ferricyanide as the final electron acceptor

In our case, inactivation of the *noxAB* genes in CS4363 resulted in poor growth with ferricyanide, similar to that observed for CS4363 grown without ferricyanide. This was somewhat expected, as NoxAB most is the most likely candidate for transferring electrons and protons from NADH to ACNQ. Due to its biphasic partition properties and ability to diffuse rapidly, ACNQ can serve as an electron shuttle inside and outside cells (37, 49, 50), and the reduced ACNQ can subsequently be reoxidized by ferricyanide in a non-enzymatic manner. The permeability of the cytoplasmic membrane to ferricyanide is low due to its large negative charge (51), and thus ferricyanide is reduced outside the cells.

Inactivation of *menA* in CS4363 surprisingly improved its growth rate, and this appeared to be due to accumulation of DHNA or ACNQ, which enhanced the capacity for EET to ferricyanide. It was possible to restore growth of a *menB* mutant of CS4363 by adding either DHNA, ACNQ, or the DMK analogue menadione to the medium, confirming the involvement of these quinone compounds in EET. However, MK-4 was not involved in EET of the *menB* mutant of CS4363.

Furthermore, it was demonstrated that both CS4363, and in particular its *menA* mutant could enable growth of *menB* mutant, when grown together on solid medium. Since only ACNQ, and not DHNA, could be detected in the culture medium of the *menB* mutant supplemented with DHNA, this substantiates that ACNQ indeed is the main involved quinone in EET.

2.5.3 The DMK analogue menadione can function in EET to ferricyanide

We found that the DMK analogue menadione also could restore the growth of a *menB* mutant of CS4363. This is compatible with menadione having a much lower E^0 than ferricyanide, low enough for it to serve as an electron carrier to ferricyanide. Since the DMK analogue menadione supported EET to ferricyanide, we decided to try and enhance the DMK pool by knocking out *ubiE*, which encodes an enzyme transforming DMK into MK. However, the resulting strain did not display an improved EET ability. This lack of stimulation could be due to menadione having a different structure from DMK (52), as menadione lacks the isoprenoid chain and is probably less hydrophobic enabling it to function like ACNQ (53, 54). Although menadione enabled the *menB* mutant to grow, this compound is far less efficient at facilitating EET. Yamazaki *et al.* mentioned that menadione was approximately 1000 times less efficient at stimulating growth of bifidobacteria than ACNQ (50).

2.5.4 Ferricyanide adaptation enhances EET capacity and proves the key role of gene *menA*

To help find the underlying cause for the observed enhanced EET ability, we conducted full genome sequencing. In the initial 300-generation ALE of CS4363, production of 2,3-butanediol increased drastically due to massive amplification on the chromosome of a gene fragment containing the *butBA* operon. Genome sequencing revealed that this was caused by insertion of two IS*905s*, which flanked the gene fragment. The two IS*905s* appeared to have generated a composite replicative transposon, which subsequently had replicated itself several times, inserting copies at new sites (55). Mutations in gene *menA* were found in both CS4363-F2 and AceN-F. The difference was that one was caused by insertion of IS*905* and another was caused by six SNVs closed to the C-terminal of *menA*. Combined with the previous results in this work, the inactivation of *menA* can enhance the EET ability. Here the mutations in *menA* after ALE in both strains were found to cause inactivation. The lack of *menA* resulted in the lack of MK, which explained why AceN-F had lost the ability to respire. Another mutation was found in *copR*, which encodes a CopY-type repressor can tightly regulate the copper homeostasis to preclude toxic effects (56).

MK can accentuate the toxic effect of copper, by facilitating copper reduction (56). The mutation in *copR* probably is not beneficial for EET, however, most likely does not confer any disadvantages to strains unable to generate MK. In CS4363-F2, the mutation in the promoter sequence of gene *noxB* may increase expression, which could be another reason for its improved EET ability. In AceN-F, the overexpression of adenylosuccinate synthase encoded by gene *purA* was recently shown to favor adenine nucleotide synthesis (57), which can promote the formation of ATP (58). The amino acid change in *purA* may increase the activity of the encoded enzyme and further improve the energy formation in AceN-F. Arginine deiminase (ADI) encoded by gene *arcA* is the first enzyme in the ADI pathway. The ADI pathway renders one molecule of ATP and consumes two H^+, which contributes to the internal pH homeostasis and opposes external acid stress (59). The SNV in the promoter sequence of *arcA* may promote the expression of ADI and thereby help cells to maintain internal pH homeostasis.

2.6 Conclusion

To the best of our knowledge, this is the first study describing the effect of EET on growth of *L. lactis* and the use of ALE to improve EET capacity. The main mechanism behind EET was elucidated and it was found that the capacity for EET could be enhanced by rendering *menA* inactive. ACNQ mediated EET appears to be the main type of EET in operation in *L. lactis*, however, other EET mechanisms seem to be functional, albeit at low level, and these need to be further explored (15, 60). For sustainable food applications, the toxic ferricyanide should be replaced with other harmless electron acceptors (with a similar redox potential and insensitive to dioxygen) or electrodes. In the future, there are many promising applications of EET, e.g. it could help avoid the oxidative stress frequently imposed on microorganisms during aerated culturing, and EET could serve as an alternative to costly aerated cultivation of microorganisms. Furthermore, EET can be used to redirect metabolic fluxes, by altering NADH/NAD^+, instead of using genetic engineering/mutagenesis to knock out NAD^+-regenerating pathways. The preliminary exploration carried out here can lay the foundation for future applications of the electro-fermentation technology. It is possible that harvesting of electricity and production of food ingredients can be accomplished simultaneously by using this promising technology.

2.7 References

1. Bourdichon F, Casaregola S, Farrokh C, Frisvad JC, Gerds ML, Hammes WP, Harnett J, Huys G, Laulund S,

Ouwehand A, Powell IB, Prajapati JB, Seto Y, Ter Schure E, Van Boven A, Vankerckhoven V, Zgoda A, Tuijtelaars S, Hansen EB. 2012. Food fermentations: Microorganisms with technological beneficial use. Int J Food Microbiol 154:87–97.

2. Hugenholtz J, Kleerebezem M, Starrenburg M, Delcour J, De Vos W, Hols P. 2000. *Lactococcus lactis* as a cell factory for high-level diacetyl production. Appl Environ Microbiol 66:4112–4114.

3. Pedersen MB, Gaudu P, Lechardeur D, Petit MA, Gruss A. 2012. Aerobic respiration metabolism in lactic acid bacteria and uses in biotechnology. Annu Rev Food Sci Technol 3:37–58.

4. Brooijmans RJW, Poolman B, Schuurman-Wolters G, de Vos WM, Hugenholtz J. 2007. Generation of a membrane potential by *Lactococcus lactis* through aerobic electron transport. J Bacteriol 189:5203–5209.

5. Koebmann B, Blank LM, Solem C, Petranovic D, Nielsen LK, Jensen PR. 2008. Increased biomass yield of *Lactococcus lactis* during energetically limited growth and respiratory conditions. Biotechnol Appl Biochem 50:25.

6. Rezaïki L, Cesselin B, Yamamoto Y, Vido K, Van West E, Gaudu P, Gruss A. 2004. Respiration metabolism reduces oxidative and acid stress to improve long-term survival of *Lactococcus lactis*. Mol Microbiol 53:1331–1342.

7. Johnson DR, Decker EA. 2015. The role of oxygen in lipid oxidation reactions: A review. Annu Rev Food Sci Technol 6:171–190.

8. Rodrigues F, Côrte-Real M, Leao C, Van Dijken JP, Pronk JT. 2001. Oxygen requirements of the food spoilage yeast *Zygosaccharomyces bailii* in synthetic and complex media. Appl Environ Microbiol 67:2123–2128.

9. Schröder U, Harnisch F, Angenent LT. 2015. Microbial electrochemistry and technology: Terminology and classification. Energy Environ Sci 8:513–519.

10. Shi L, Dong H, Reguera G, Beyenal H, Lu A, Liu J, Yu HQ, Fredrickson JK. 2016. Extracellular electron transfer mechanisms between microorganisms and minerals. Nat Rev Microbiol 14:651–662.

11. Logan BE. 2009. Exoelectrogenic bacteria that power microbial fuel cells. Nat Rev Microbiol 7:375–381.

12. Saunders SH, Newman DK. 2018. Extracellular electron transfer transcends microbe-mineral interactions. Cell Host Microbe 24:611–613.

13. Naradasu D, Miran W, Sakamoto M, Okamoto A. 2019. Isolation and characterization of human gut bacteria capable of extracellular electron transport by electrochemical techniques. Front Microbiol 10:1–9.

14. Wang W, Du Y, Yang S, Du X, Li M, Lin B, Zhou J, Lin L, Song Y, Li J, Zuo X, Yang C. 2019. Bacterial extracellular electron transfer occurs in mammalian gut. Anal Chem 91:12138–12141.

15. Light SH, Su L, Rivera-Lugo R, Cornejo JA, Louie A, Iavarone AT, Ajo-Franklin CM, Portnoy DA. 2018. A flavin-based extracellular electron transfer mechanism in diverse Gram-positive bacteria. Nature 562:140–157.

16. Pankratova G, Leech D, Gorton L, Hederstedt L. 2018. Extracellular electron transfer by the Gram-positive bacterium *Enterococcus faecalis*. Biochemistry 57:4597–4603.

17. Lam LN, Wong JJ, Matysik A, Paxman JJ, Chong KKL, Low PM, Chua ZS, Heras B, Marsili E, Kline KA. 2019. Sortase-assembled pili promote extracellular electron transfer and iron acquisition in *Enterococcus faecalis* biofilm. bioRxiv 601666.

18. Hederstedt L, Gorton L, Pankratovab G. 2020. Two routes for extracellular electron transfer in *Enterococcus faecalis*. J Bacteriol 202:1–9.

19. Tejedor-Sanz S, Stevens ET, Finnegan P, Nelson J, Knoessen A, Light SH, Ajo-Franklin CM, Marco ML. 2022. Extracellular electron transfer increases fermentation in lactic acid bacteria via a hybrid metabolism. Elife 11:e70684.

20. Freguia S, Masuda M, Tsujimura S, Kano K. 2009. *Lactococcus lactis* catalyses electricity generation at microbial fuel cell anodes via excretion of a soluble quinone. Bioelectrochemistry 76:14–18.

21. Yamazaki SI, Kaneko T, Taketomo N, Kano K, Ikeda T. 2002. Glucose metabolism of lactic acid bacteria changed by quinone-mediated extracellular electron transfer. Biosci Biotechnol Biochem 66:2100–2106.

22. Rhoads A, Beyenal H, Lewandowski Z. 2005. Microbial fuel cell using anaerobic respiration as an anodic reaction and biomineralized manganese as a cathodic reactant. Environ Sci Technol 39:4666–4671.

23. Lai B, Yu S, Bernhardt P V., Rabaey K, Virdis B, Krömer JO. 2016. Anoxic metabolism and biochemical production in *Pseudomonas putida* F1 driven by a bioelectrochemical system. Biotechnol Biofuels 9:1–13.

24. Holo H, Nes IF. 1989. High-frequency transformation, by electroporation, of *Lactococcus lactis* subsp. *cremoris* grown with glycine in osmotically stabilized media. Appl Environ Microbiol 55:3119–3123.

25. Solem C, Defoor E, Jensen PR, Martinussen J. 2008. Plasmid pCS1966, a new selection/counterselection tool for lactic acid bacterium strain construction based on the oroP gene, encoding an orotate transporter from *Lactococcus lactis*. Appl Environ Microbiol 74:4772–4775.

26. Widdel F. 2010. Theory and measurement of bacterial growth. A basic and practical aspects. Bremen: Grundpraktikum Mikrobiologie; University of Bremen.

27. Lan CQ, Oddone G, Mills DA, Block DE. 2006. Kinetics of *Lactococcus lactis* growth and metabolite formation under aerobic and anaerobic conditions in the presence or absence of hemin. Biotechnol Bioeng 95:1070–1080.

28. Zhou Y, Liu C, Zhou R, Lu A, Huang B, Liu L, Chen L, Luo B, Huang J, Tian Z. 2019. SEQdata-BEACON: A comprehensive database of sequencing performance and statistical tools for performance evaluation and yield simulation in BGISEQ-500. BioData Min 12:1–14.

29. Yan X, Jansen CU, Diao F, Qvortrup K, Tanner D, Ulstrup J, Xiao X. 2021. Surface-confined redox-active monolayers of a multifunctional anthraquinone derivative on nanoporous and single-crystal gold electrodes. Electrochem commun 124:106962.

30. Ucar D, Zhang Y, Angelidaki I. 2017. An overview of electron acceptors in microbial fuel cells. Front Microbiol 8:1–14.

31. Liu C, Sun T, Zhai Y, Dong S. 2009. Evaluation of ferricyanide effects on microorganisms with multi-methods. Talanta 78:613–617.

32. Solem C, Dehli T, Jensen PR. 2013. Rewiring *Lactococcus lactis* for ethanol production. Appl Environ Microbiol 79:2512–2518.

33. Liu J, Wang Z, Kandasamy V, Lee SY, Solem C, Jensen PR. 2017. Harnessing the respiration machinery for high-yield production of chemicals in metabolically engineered *Lactococcus lactis*. Metab Eng 44:22–29.

34. Domingo PL, Garcia B, Leal JM. 1990. Acid-base behaviour of the ferricyanide ion in perchloric acid media. Spectrophotometric and kinetic study. Can J Chem 68:228–235.

35. Husmann S, Zarbin AJG, Dryfe RAW. 2020. High-performance aqueous rechargeable potassium batteries prepared via interfacial synthesis of a Prussian blue-carbon nanotube composite. Electrochim Acta 349:136243.

36. Collins J, Zhang T, Huston S, Sun F, Percival Zhang YH, Fu J. 2016. A hidden transhydrogen activity of a FMN-bound diaphorase under anaerobic conditions. PLoS One 11:1–9.

37. Mevers E, Su L, Pishchany G, Baruch M, Cornejo J, Hobert E, Dimise E, Ajo-Franklin CM, Clardy J. 2019. An elusive electron shuttle from a facultative anaerobe. Elife 8:e48054.

38. Conley B, Gralnick J. 2019. Solving a shuttle mystery. Elife 8:e49831.

39. Vandecraen J, Chandler M, Aertsen A, Van Houdt R. 2017. The impact of insertion sequences on bacterial genome plasticity and adaptability. Crit Rev Microbiol 43:709–730.

40. Liu J, Chan SHJ, Brock-Nannestad T, Chen J, Lee SY, Solem C, Jensen PR. 2016. Combining metabolic engineering and biocompatible chemistry for high-yield production of homo-diacetyl and homo-(S,S)-2,3-butanediol. Metab Eng 36:57–67.

41. Bolten CJ, Kiefer P, Letisse F, Portais JC, Wittmann C. 2007. Sampling for metabolome analysis of microorganisms. Anal Chem 79:3843–3849.

42. Harvey RJ. 1965. Damage to *Streptococcus lactis* resulting from growth at low pH. J Bacteriol 90:1330–1336.

43. Neumann G, Veeranagouda Y, Karegoudar TB, Sahin Ö, Mäusezahl I, Kabelitz N, Kappelmeyer U, Heipieper HJ. 2005. Cells of *Pseudomonas putida* and *Enterobacter* sp. adapt to toxic organic compounds by increasing their size. Extremophiles 9:163–168.

44. Chapot-Chartier MP, Kulakauskas S. 2014. Cell wall structure and function in lactic acid bacteria. Microb Cell Fact 13:1–23.

45. Deghorain M, Fontaine L, David B, Mainardi JL, Courtin P, Daniel R, Errington J, Sorokin A, Bolotin A, Chapot-Chartier MP, Hallet B, Hols P. 2010. Functional and morphological adaptation to peptidoglycan precursor alteration in *Lactococcus lactis*. J Biol Chem 285:24003–24013.

46. Calamita HG, Ehringer WD, Koch AL, Doyle RJ. 2001. Evidence that the cell wall of *Bacillus subtilis* is protonated during respiration. Proc Natl Acad Sci U S A 98:15260–15263.

47. Kemper MA, Urrutia MM, Beveridge TJ, Koch AL, Doyle RJ. 1993. Proton motive force may regulate cell wall-associated enzymes of *Bacillus subtilis*. J Bacteriol 175:5690–5696.

48. Wheeler R, Turner RD, Bailey RG, Salamaga B, Mesnage S, Mohamad SAS, Hayhurst EJ, Horsburgh M, Hobbs JK, Foster SJ. 2015. Bacterial cell enlargement requires control of cell wall stiffness mediated by peptidoglycan hydrolases. mBio 6:1–10.

49. Newman DK, Kolter R. 2000. A role for excreted quinones in extracellular electron transfer. Nature 405:94–97.

50. Yamazaki SI, Kano K, Ikeda T, Isawa K, Kaneko T. 1998. Mechanistic study on the roles of a bifidogenetic growth stimulator based on physicochemical characterization. Biochim Biophys Acta - Gen Subj 1425:516–526.

51. Löw H, Crane FL, Partick EJ, Clark MG. 1985. α-Adrenergic stimulation of trans-sarcolemma electron efflux in perfused rat heart. Possible regulation of Ca^{2+}-channels by a sarcolemma redox system. Biochim Biophys Acta 844:142–148.

52. Rezaïki L, Lamberet G, Derré A, Gruss A, Gaudu P. 2008. *Lactococcus lactis* produces short-chain quinones that cross-feed Group B *Streptococcus* to activate respiration growth. Mol Microbiol 67:947–957.

53. Yashiki Y, Yamashoji S. 1996. Extracellular reduction of menadione and ferricyanide in yeast cell suspension. J Ferment Bioeng 82:319–321.

54. Koley D, Bard AJ. 2012. Inhibition of the MRP1-mediated transport of the menadione-glutathione conjugate (thiodione) in HeLa cells as studied by SECM. Proc Natl Acad Sci U S A 109:11522–11527.

55. Chandler MS. 1998. Insertion sequences and transposons BT - bacterial genomes: physical structure and

analysis, p. 30–37. *In* de Bruijn, FJ, Lupski, JR, Weinstock, GM (eds.), . Springer US, Boston, MA.

56. Abicht HK, Gonskikh Y, Gerber SD, Solioz M. 2013. Non-enzymic copper reduction by menaquinone enhances copper toxicity in *Lactococcus lactis* IL1403. Microbiology 159:1190–1197.

57. Dorau R, Chen J, Liu J, Ruhdal Jensen P, Solem C. 2021. Adaptive laboratory evolution as a means to generate *Lactococcus lactis* strains with improved thermotolerance and ability to autolyze. Appl Environ Microbiol 87:e0103521.

58. Kilstrup M, Hammer K, Jensen PR, Martinussen J. 2005. Nucleotide metabolism and its control in lactic acid bacteria. FEMS Microbiol Rev 29:555–590.

59. Díez L, Solopova A, Fernández-Pérez R, González M, Tenorio C, Kuipers OP, Ruiz-Larrea F. 2017. Transcriptome analysis shows activation of the arginine deiminase pathway in *Lactococcus lactis* as a response to ethanol stress. Int J Food Microbiol 257:41–48.

60. Masuda M, Freguia S, Wang YF, Tsujimura S, Kano K. 2010. Flavins contained in yeast extract are exploited for anodic electron transfer by *Lactococcus lactis*. Bioelectrochemistry 78:173–175.

2.8 Supplementary materials

Table S2.1 Primers used in this work.

Name	Sequence(5'-3')
2-up-F	AGAACTAGTGGATCCTGTTCAAGCGCTCATGATTG
2-up-R	AGCAAAACCTGAACCGCTTCGTCAGTTGACGAC
2-down-F	GTCAACTGACGAAGCGGTTCAGGTTTTGCTGCTC
2-down-R	CAAAAGCTGGGTACCCGCTTACTTCCATCATTGTCC
2-plas-F	TGATGGAAGTAAGCGGGTACCCAGCTTTTGTTCC
2-plas-R	ATGAGCGCTTGAACAGGATCCACTAGTTCTAGAGCGG
2-F	GAAGGCTGACAGAACTTGC
2-R	TGCAATATTCGTGCATGCTATG
3-up-F	AGAACTAGTGGATCCGTTACGAGATTGTTGCCATTG
3-up-R	CAAAATCAGGTTTGCGGATTTCTCCTTTAAGATGTGAGGG
3-down-F	TCTTAAAGGAGAAATCCGCAAACCTGATTTTGACC
3-down-R	CAAAAGCTGGGTACCAGACTGGCAAAGCTAATTCTTG
3-plas-F	TAGCTTTGCCAGTCTGGTACCCAGCTTTTGTTCC
3-plas-R	CAACAATCTCGTAACGGATCCACTAGTTCTAGAGCGG
3-F	GCACTTGTCAGCAACATTC
3-R	CAGTCAGTTCGTATGTGGTTAG
4-up-F	AGAACTAGTGGATCCGCATCACCACCAGTCAAAC

4-up-R	TCCAAGAGAAATGGCAAAATAGCTCTGCGGAGC
4-down-F	CCGCAGAGCTATTTTGCCATTTCTCTTGGA
4-down-R	CAAAAGCTGGGTACCGCAGATTGGCTCAATGGTC
4-plas-F	ATTGAGCCAATCTGCGGTACCCAGCTTTTGTTCC
4-plas-R	GACTGGTGGTGATGCGGATCCACTAGTTCTAGAGCGG
4-F	TACCAATTCGAGCAGCACC
4-R	GGCGTCAGTATTCATCAAGG
7-up-F	AGAACTAGTGGATCCCCTGACGTCGAGTCTGC
7-up-R	TCCAAGCGTTCAAAACTTACTGGTCACAAGGTCAGC
7-down-F	ACCTTGTGACCAGTAAGTTTTGAACGCTTGGATAGTG
7-down-R	CAAAAGCTGGGTACCGAACCTGCATGTAGTAATTCCTC
7-plas-F	ACTACATGCAGGTTCGGTACCCAGCTTTTGTTCC
7-plas-R	AGACTCGACGTCAGGGGATCCACTAGTTCTAGAGCGG
7-F	GAATGGGAAGTTTCGTAGCC
7-R	CAAGATACTTCTAGCTGAGTCACG

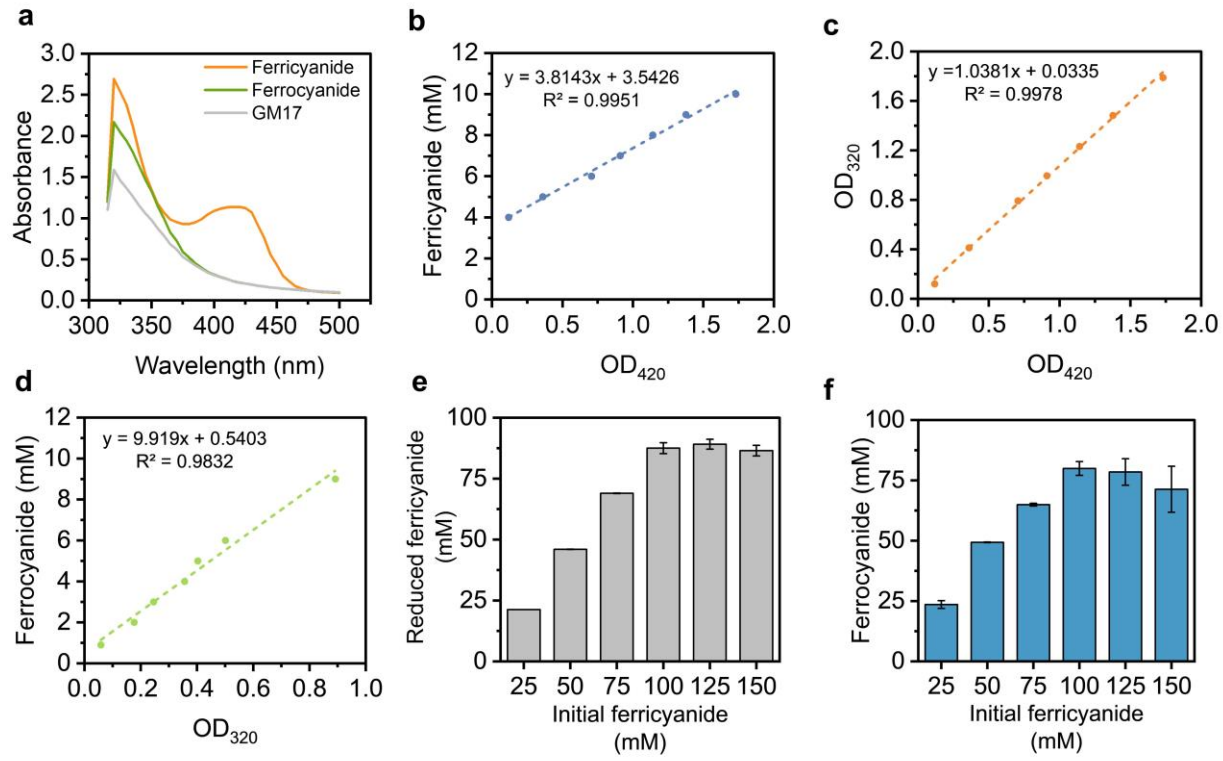

Fig. S2.1 Determination and quantification of ferricyanide and ferrocyanide. (a) UV-vis spectra of 8 mM ferricyanide, 8 mM ferrocyanide and GM17. (b) The calibration curve with the relationship between OD_{420} and ferricyanide

concentration. (c) The linear correlation between OD_{420} and OD_{320} of ferricyanide. (d) The calibration curve with the relationship between OD_{320} and ferrocyanide concentration. (e) Reduced ferricyanide under different concentration of ferricyanide at 16 h. (f) Ferrocyanide concentration under different concentration of ferricyanide at 16 h.

To avoid the interference of the medium GM17, the absorption of GM17 at 420 nm or 320 nm needs to be substracted when calculation. OD_{420} was used for the quantification of ferricyanide The equation based on the (b) is:

$$Ferricyanide\ (mM) = 3.8143 \times (OD_{420} - OD_{420}(GM17)) + 3.5426$$

Since ferricyanide also has absorbance at 320 nm, OD_{420} of ferricyanide can be converted into OD_{320} based on the equation from (c):

$$OD_{320}\ (ferricyanide) = 1.0381 \times (OD_{420} - OD_{420}(GM17)) + 0.0335$$

So the absorbance of ferrocyanide at 320 nm can be calculated by the following equation:

$$OD_{320}\ (ferrocyanide) = OD_{320} - OD_{320}(GM17) - OD_{320}\ (ferricyanide)$$

OD_{320} of ferrocyanide can be converted into concentration (mM) based on the equation from (d):

$$Ferrocyanide\ (mM) = 9.919 \times OD_{320}\ (ferrocyanide) + 0.5403$$

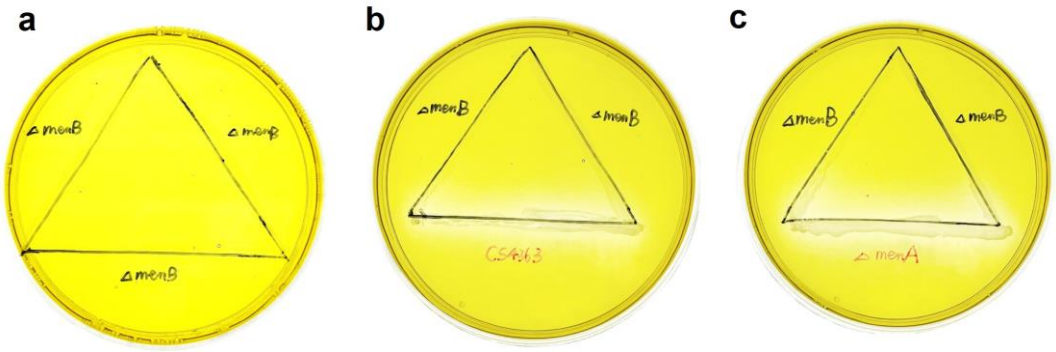

Fig. S2.2 Functional analysis of electron shuttle. (a) *menB* mutant was inoculated on the vertical lines and horizontal line. (b) CS4363 was inoculated on the horizontal line and *menB* mutant was inoculated on the vertical lines (x2). (c) *menA* mutant was inoculated on the horizontal line and *menB* mutant was inoculated on the vertical lines (x2). The solid medium was GM17 containing 50 mM ferricyanide. Reduction of ferricyanide (yellow) to ferrocyanide (colorless) was only observed by *menB* mutant where it was growing closed to *menA* mutant and CS4363.

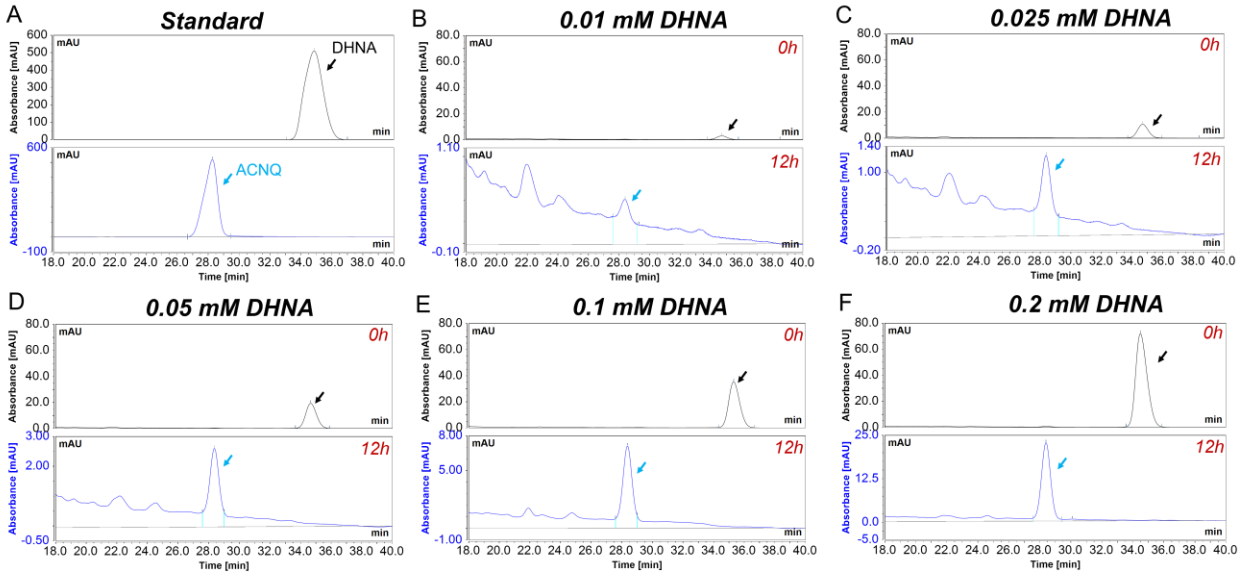

Fig. S2.3 (a) HPLC chromatogram of 2.3 mM DHNA standard (up) and 2.3 mM ACNQ standard (down). (b)-(f) HPLC chromatogram change at 0 h (up) and 12 h (down) with the addition of different concentrations of DHNA in CS4363-MB with 50 mM ferricaynide.

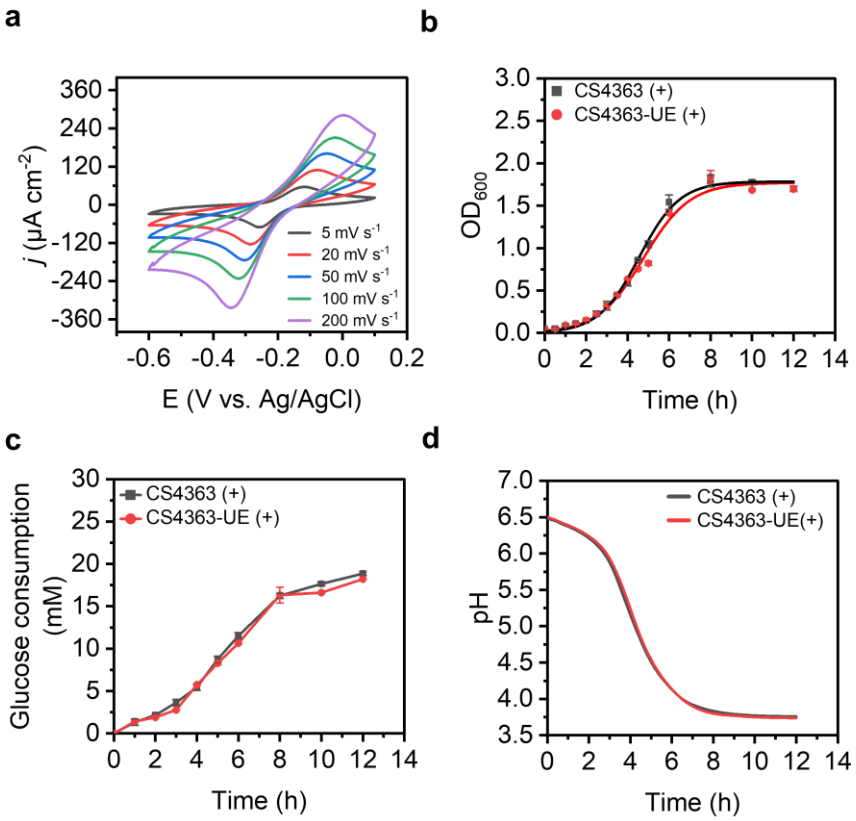

Fig. S2.4 (a) Cyclic Voltamograms (CVs) of 0.5 mM menadione at different scan rates. The growth curves (b), glucose consumption change with time (c) and pH change with time (d) of CS4363 and CS4363-UE with 150 mM ferricyanide. CS4363 and CS4363-UE were cultured in GM17 supplemented with 150 mM ferricyanide under relative anaerobic condition.

Table S2.2 Promoter prediction using online tool BDGP.

Promoter			Predicted	SNV	Gene
Sequence (5'-3')	Start	End	TSS[a]	position	
TAACAGTTTACAAATTGCTCTAAAAAGGATAT AATAGTGCCTGACGTTAT	81	31	41	73	*noxB*
TAGTGCTTGACAAAAAATATGCATAGATGTAT AATTTTCTTGTAAACGAT	90	40	50	47	*arcA*

[a]TSS: transcriptional start site.

CHAPTER 3. Systemic understanding of *L. lactis* with enhanced extracellular electron transfer ability using transcriptomics analysis and uncovering the key role of novel type-II NADH dehydrogenase in extracellular electron transfer

3.1 Abstract

Lactococcus lactis, a lactic acid bacterium used in food fermentations and commonly found in the human gut is known to possess a fermentative metabolism. *L. lactis*, however, has been demonstrated to transfer metabolically generated electrons to external electron acceptors, a process termed extracellular electron transfer (EET). Here, we investigate an *L. lactis* strain with an unusual high capacity for EET that was obtained in an adaptive laboratory evolution (ALE) experiment. First, we investigated how global gene expression had changed, and found that amino acid metabolism and nucleotide metabolism had been affected significantly. One of the most significantly upregulated genes encoded the NADH dehydrogenase NoxB. We determined that this could be attributed to a mutation in the promoter region of NoxB, which abolished carbon catabolite repression of this gene. A unique role of NoxB in EET could be attributed. Surprisingly, both NoxB and NoxA could support respiration to oxygen. NoxB, was shown to be a novel type-II NADH dehydrogenase that is widely distributed among gut microorganisms. This work expands our understanding of EET enhancement in Gram-positive electroactive microorganisms and the special significance of novel type-II NADH dehydrogenase in EET.

3.2 Introduction

Electroactive microorganisms (EAMs) are able to exchange electrons between themselves and extracellular electron acceptors such as naturally-occurring redox active compounds or electrodes, a process that is termed extracellular electron transfer (EET) (1). EET has many biotechnological applications, e.g. in bioremediation, for biorecovering/bioleeching and plays a central role in microbial electrochemical systems (2). EET has also been found to have important roles within plant and animal ecosystems, e.g. for enhancing bioavailability of iron, and has a great potential in food fermentations, where EET has been demonstrated to stimulate acidification (3).

Gram-negative mesophilic bacteria, especially the model organisms *Geobacter* and *Shewanella*, are well-studied EAMs, while knowledge of Gram-positive bacteria is more limited (4, 5). It has been mentioned that the thick and non-conductive cell wall has a negative impact on the electro-activity of Gram-positive bacteria (6). However, some Gram-positive bacteria do possess a capacity for EET, e.g. the pathogenic *Listeria monocytogenes* and certain lactic acid bacteria such as *Enterococcus faecalis*, *Lactococcus lactis*, and *Lactiplantibacillus plantarum* (7–12). A flavin-based EET (FLEET) mechanism was discovered in *L. monocytogenes*, involving a specialized

NADH dehydrogenase, Ndh2, that couples oxidation of NADH to the reduction of a quinone species, and where the electrons ultimately are transferred to external acceptors via two membrane proteins EetA and EetB and the flavoprotein PplA (7). Likewise, *E. faecalis* was reported to use FLEET to transfer electrons to ferric ions or ferricyanide, even with PplA inactivated, and for this a novel type II NADH dehydrogenase was involved (12). *E. faecalis* was also capable of transferring electrons to an osmium complex-modified redox polymer (OsRP) without the involvement of FLEET (12). The FLEET locus has also been found in *L. plantarum*, but FLEET activity requires an exogenous source of quinone, as *L. plantarum* lacks complete biosynthetic pathway for menaquinones. For *L. plantarum*, FLEET activity appeared to be beneficial for lactate formation rate, which was boosted significantly (8). The important food microorganism *L. lactis*, was also demonstrated to be capable of EET, and here the soluble redox mediator 2-amino-3-dicarboxy-1,4-naphthoquinone (ACNQ) is involved when ferricyanide is used as electron acceptor (9, 13). A lot of efforts have been invested in elucidating the mechanisms behind EET, and in finding the relevance of EET for microorganisms in different niches. However, how EET can be enhanced and harnessed for biotechnological applications has been less explored. Recently, we demonstrated that an *L. lactis* mutant CS4363 blocked in NAD^+ regeneration can grow with ferricyanide as the electron acceptor in the absence of oxygen. By adaptive laboratory evolution (ALE), an EET-enhanced mutant CS4363-F2 was obtained (9). CS4363-F2 displayed a remarkable performance in a bioelectrochemical system setup with an anode as the electron acceptor, reaching an unprecedented electron transfer rate (14). Whole genome sequencing revealed two alterations in the genome, which appeared to be the underlying reason for the enhanced capacity for EET; an insertion of a transposable element in the coding region of *menA*, thereby disrupting menaquinone biosynthesis, and a mutation in the *noxB* promoter region, a gene encoding a type II NADH dehydrogenase.

Here, to learn more about the observed behavior of CS4363-F2, we carry out a transcriptome analysis. We investigate the impact of the mutation upstream of *noxB*, and attempt to assign roles for the two NADH dehydrogenases harbored by *L. lactis*, NoxA and NoxB. Finally, a bioinformatics analysis is conducted, where we look into the structure of NoxB, and examine the distribution of this type of NADH dehydrogenase among microorganisms.

3.3 Materials and Methods

3.3.1 Bacterial strains and medium

All the constructed strains and plasmids are listed in **Table 3.1**. *E. coli* strains were aerobically grown at 30℃ in Luria-Bertani (LB) broth (Sigma-Aldrich, USA) supplemented with 0.2% glucose (Sigma-Aldrich, USA) for plasmid extraction. *L. lactis* was cultured at 30°C in M17 broth (Thermo Fisher Scientific, USA) supplemented with 1% glucose (GM17). When required, antibiotics were added to the following concentrations: erythromycin: 200 μg/mL for *E. coli* and 5 μg/mL for *L. lactis*; chloramphenicol: 5 μg/mL for both *E. coli* and *L. lactis*; tetracycline: 5 μg/ml for *L. lactis*. 5 μg/mL hemin (Sigma-Aldrich, USA) was added to activate respiration. Hemin was dissolved in 0.05 M NaOH to prepare a stock with a concentration of 500 μg/mL.

Table 3.1 Strains and plasmids used in the study.

Name	Genotype or description	Reference
***L. lactis* strains**		
MG1363	Wild-type *L. lactis* subsp. *cremoris*	(15)
CS4363	MG1363 *Δ^{3}ldh Δpta ΔadhE*	(16)
CS4363-F2	CS4363 mutant with enhanced EET ability	(9)
CS4363-NA	MG1363 *Δ^{3}ldh Δpta ΔadhE ΔnoxA*	This work
CS4363-NB	MG1363 *Δ^{3}ldh Δpta ΔadhE ΔnoxB*	This work
CS4363-NAB	MG1363 *Δ^{3}ldh Δpta ΔadhE ΔnoxA ΔnoxB*	(9)
CS4616	MG1363 *Δ^{3}ldh Δpta ΔadhE ΔbutBA ΔaldB ΔnoxE* pCS4564	(17)
CS4616-NA	MG1363 *Δ^{3}ldh Δpta ΔadhE ΔbutBA ΔaldB ΔnoxE ΔnoxA* pCS4564	This work
CS4616-NB	MG1363 *Δ^{3}ldh Δpta ΔadhE ΔbutBA ΔaldB ΔnoxE ΔnoxB* pCS4564	This work
CS4616-NAB	MG1363 *Δ^{3}ldh Δpta ΔadhE ΔbutBA ΔaldB ΔnoxE ΔnoxA ΔnoxB* pCS4564	This work
CS4616m	MG1363 *Δ^{3}ldh Δpta ΔadhE ΔbutBA ΔaldB ΔnoxE*	(17)
CS4616m-NA	MG1363 *Δ^{3}ldh Δpta ΔadhE ΔbutBA ΔaldB ΔnoxE ΔnoxA*	This work

CS4616m-NB	MG1363 *Δ*^{3}*ldh Δpta ΔadhE ΔbutBA ΔaldB ΔnoxE ΔnoxB*	This work
Plasmids		
pLB65	Derivative of pCI372 containing Orf1 integrase,	(18)
pLB85	Derivative of pBF12 containing *gusA* reporter gene, Em^{R}	(18)
pCS1966	*oroP*-based selection/counters election vector, Em^{R}	(19)
pCS4564	pG^{+}host8::SP-*ldhA* (*E. coli*), Tet^{R}, thermo-sensitive replicon	(17)
pLB85-P*wt*	pLB85 with wild-type *noxB* promoter	This work
pLB85-P*snv*	pLB85 with T-73G mutant *noxB* promoter	This work
pCS1966noxAB	Plasmid used for deleting *noxA* and *noxB*	(9)
pCS1966noxA	Plasmid used for deleting *noxA*	This work
pCS1966noxB	Plasmid used for deleting *noxB*	This work

3.3.2 Construction of promoter-*gusA* reporter plasmids and chromosomal single-copy transcriptional fusion strains

PCR primers used are shown in **Table S3.1**.The plasmid pLB85 was used for the construction of promoter-*gusA* reporter plasmids. The wild-type *noxB* promoter was amplified by colony PCR on CS4363, using primers A1-F/R and Phusion high-fidelity DNA polymerase (Thermo Fisher Scientific, USA). Likewise, the mutant *noxB* promoter was amplified using primers A1-F/R. Primers A1-plas-F/R were used for linearizing plasmid pLB85. The *noxB* promoter sequence and linearized plasmid were assembled by using the Gibson assembly HiFi master mix (Thermo Fisher Scientific, USA). The Gibson cloning reaction was further transformed into One shot™ top10 chemically competent *E. coli* (Thermo Fisher Scientific, USA). DreamTaq Hot Start DNA polymerase (Thermo Fisher Scientific, USA) was used for PCR verification of recombinant plasmids with primers pLB85-F/R. The PCR product was further sequenced by Macrogen (South Korea). The successfully constructed plasmids were named as pLB85-P*wt* and pLB85-P*snv*. The constructed plasmids were transformed into *L. lactis* MG1363 containing pLB65 encoding the TP901-1 integrase. Then the cells were plated on GM17 with selection for 5 μg/ml erythromycin resistance and with 200 μg/ml X-Gluc (Sigma-Aldrich, USA) (18).

3.3.3 Construction of knock-out plasmids and strains

The plasmid pCS1966 was used for knocking out genes in *L. lactis* (19) and derivatives of pCS1966 for deleting *noxA*, *noxB* and both were constructed as described below. When constructing knock-out plasmids: pCS1966noxA, pCS1966noxB and pCS1966noxAB, ~1000 bp regions upstream and downstream of the deleted genes were amplified using Phusion high-fidelity DNA polymerase (Thermo Fisher Scientific, USA). The primers used for amplifying upstream and downstream of the deleted genes: 4-up-F/R (*noxAB-upstream*), 8-up-F/R (*noxB-upstream*), 9-up-F/R (*noxA-upstream*), 4-down-F/R (*noxAB-downstream*), 8-down-F/R (*noxB-downstream*) and 9-down-F/R (*noxA downstream*). Phusion high-fidelity DNA polymerase was also used to linearize the plasmid pCS1966: primers 4-plas-F/R, 8-plas-F/R and 9-plas-F/R were used for corresponding genes. Upstream, downstream and linearized plasmid were assembled by using Gibson assembly HiFi master mix. The recombinant plasmids were verified by PCR and sequencing.

The successful recombinant plasmids were extracted by using GeneJET plasmid miniprep kit (Thermo Fisher Scientific, USA) and introduced into electro-competent *L. lactis* CS4363 or CS4616 prepared as previously described (20), where successful integration resulted in erythromycin resistance. For counter selection, 5-fluoroorotic acid (Thermo Fisher Scientific, USA) was used (19). Deletions were verified by colony PCR using primers 4-F/R (*noxA* and *noxB*), 8-F/R (*noxB*) and 9-F/R (*noxA*) with DreamTaq Hot Start DNA polymerase. PCR products were sequenced by Macrogen. To prevent plasmid loss, tetracycline was always present in medium used to cultivate CS4616. Strains with knocked-out *noxA*, *noxB* or combinations were named as CS4363-NAB (*ΔnoxA ΔnoxB*), CS4363-NA (*ΔnoxA*), CS4363-NB (*ΔnoxB*), CS4616-NAB (*ΔnoxA ΔnoxB*), CS4616-NA (*ΔnoxA*) and CS4616-NB (*ΔnoxB*).

3.3.4 Measurement of cell growth with ferricyanide as electron acceptor

To test the function of NoxA and NoxB in extracellular electron transfer to ferricyanide, the growth experiments of CS4363 and knock-out strains were conducted, following the detailed procedure described before (9). Cells were cultured in GM17 medium supplemented with 150 mM ferricyanide under relatively anaerobic conditions (i.e. static conditions).

3.3.5 Test the function of NoxA and NoxB in respiration

To get rid of plasmid pCS4564, knock-out strains CS4616-NAB, CS4616-NA and CS4616-NB were cultured in GM17 with 5 μg/mL hemin at 35℃. However, we found that it was difficult to lose the plasmid in CS4616-NAB, and we inferred that the lactate dehydrogenase plasmid was essential under these conditions (data not shown). For CS4616-NA and CS4616-NB the plasmid could readily be lost. The resulting strains were CS4616m-NA (MG1363 *Δ*^{3}*ldh Δpta ΔadhE ΔbutBA ΔaldB ΔnoxE ΔnoxA*) and CS4616m-NB (MG1363 *Δ*^{3}*ldh Δpta ΔadhE ΔbutBA ΔaldB ΔnoxE ΔnoxB)*. To test the ability of respiration, CS4616m, CS4616m-NA and CS4616m-NB were streaked on GM17 medium with 5 μg/mL hemin and GM17 medium with 5 μg/mL tetracycline. Digital photos were taken of plates placed on a lightbox.

3.3.6 Quantification of glucose

Quantification of glucose was carried out by high performance liquid chromatography (HPLC) using an Aminex HPX-87H column (Bio-Rad, Hercules, USA). 5 mM H_2SO_4 was used as mobile phase with 0.5 mL/min flow rate. The temperature of the column oven was set to 60℃. An RI detector was used for glucose quantification. The samples for HPLC analysis were filtered using 0.22 μM filters (Labsolute) immediately after sampling and were stored at −20℃ until analyzed.

3.3.7 Measurement of β-glucuronidase Activity

Strains were cultured at 30℃ in GM17 with 1 μg/ml erythromycin resistance. When OD_{600} reached around 0.6, 1 ml cells were by centrifugation at 4℃, 12,000 rpm for 2 minutes and resuspended in 1 ml of Z buffer (0.06 M Na_2HPO_4, 0.04 M NaH_2PO_4, 0.01 M KCl, 0.001 M $MgSO_4$, 0.05 M β-mercaptoethanol, pH 7). 12.5 μl 0.1% sodium dodecyl sulfate (SDS) and 25 μl chloroform were added, and then the suspension was vortexed vigorously followed by incubation at 30℃ for 5 min. 100 μL 4mg/ml *p*-nitrophenyl-β-D-glucuronide (PNPG) was added. When the color of the suspension became yellow, 800 μl Na_2CO_3 was added to stop the reaction and the time (min) needed for yellow color was recorded. Then the suspension was centrifuged at 12,000 rpm for 2 min. Absorbance at 420 nm of supernatant was measured. The promoter activity was calculated by the following formula and expressed in Miller units:

$$Promoter\ activity = \frac{OD_{420}}{OD_{600} \times time \times volume}$$

3.3.8 Bioinformatics analysis

The information about NoxA in *L. lactis* MG1363 was obtained from UniProt (https://www.uniprot.org/) under the accession number: A2RLY1. The information about novel type-II NADH dehydrogenase in different bacteria was also obtained from UniProt under the following accession numbers: A2RLY0 (*L. lactis* MG1363, NoxB), A0A1B4XSC7 (*Enterococcus faecalis*, Ndh3), and A0A5D5DS06 (*Listeria monocytogenes*, Ndh2). The 3D structures of NoxA and NoxB were predicted by AlphaFold in the structure part of UniProt. The comparisons of 3D structures were conducted by structure comparison of the Swiss-Model (https://swissmodel.expasy.org/). The comparison of *noxA* and *noxB* encoding amino acid sequences was conducted by CLUSTALW (https://www.genome.jp/tools-bin/clustalw). The transmembrane part was predicted by TMHMM (https://dtu.biolib.com/DeepTMHMM).

3.3.9 Transcriptomics analysis

RNA extraction from cells was carried out by BGI-Tech (HongKong). The transcriptomics analysis was accomplished using DNBSEQ based on the service of prokaryotic stranded RNA library at BGI-Tech. Datasets consisted of 12M clean reads per sample with a paired-end 100-bp read length. Afterward, the RNA-seq data was assembled and analyzed by comparing it with the translational region of annotated DNA sequence data of reference *L. lactis* MG1363 (Genbank accession number: NC009004) using RNA assembler in Geneious Prime (Auckland, New Zealand). DESeq2 was used for calculating and comparing expression levels of two sample conditions. The Kyoto Encyclopedia of Genes and Genomes (KEGG) pathway analysis was carried out by KOBAS-i (21). The RNA sequencing project has been deposited in the NCBI under the BioProject (https://www.ncbi.nlm.nih.gov/bioproject) accession PRJNA1022092.

3.4 Results and Discussion

3.4.1 Scrutinizing the transcriptome of *L. lactis* CS4363-F2, a strain with enhanced capacity for EET

CS4363-F2, an *L. lactis* strain with enhanced capacity for EET to ferricyanide, was obtained after a prolonged adaptive laboratory evolution in the presence of 50 mM ferricyanide (9). This strain depends on external electron acceptors, e.g. oxygen or ferricyanide, to grow, as it (and its parent CS4363), is blocked in remaining NAD^+ regenerative pathways. To determine the mechanism

behind the enhanced capacity for EET, a comparative transcriptomics analysis was performed for CS4363-F2 and CS4363, growing under EET conditions. This revealed a total of 416 differentially expressed genes; 215 were upregulated and 201 were downregulated in CS4363-F2 as compared to CS4363, and the top-10 differentially expressed genes **(Table S3.2)** are indicated in **Fig. 3.1a**. Most of the latter genes encoded putative proteins, making it difficult to associate mutations in them with the enhanced capacity for EET. There were, however, two exceptions, namely *noxB* (locus tag: llmg_1734), encoding a NADH dehydrogenase, and *mgtA*, encoding a magnesium-transporting ATPase (locus tag: llmg_1223), which were the most significantly upregulated and downregulated genes, respectively. NADH dehydrogenase is the first component of the EET pathway (9) and is reasonable to assume that upregulation of *noxB* could accelerate the transfer of electrons from NADH, and thereby enhance the capacity for EET. EET to ferricyanide results in protons being released without the weak conjugate base lactate, which could cause severe acid stress. We speculated that downregulation of *mgtA* resulted in increased acid stress tolerance due to EET since this gene was found to be downregulated in *L. lactis* under acid stress conditions previously (22).

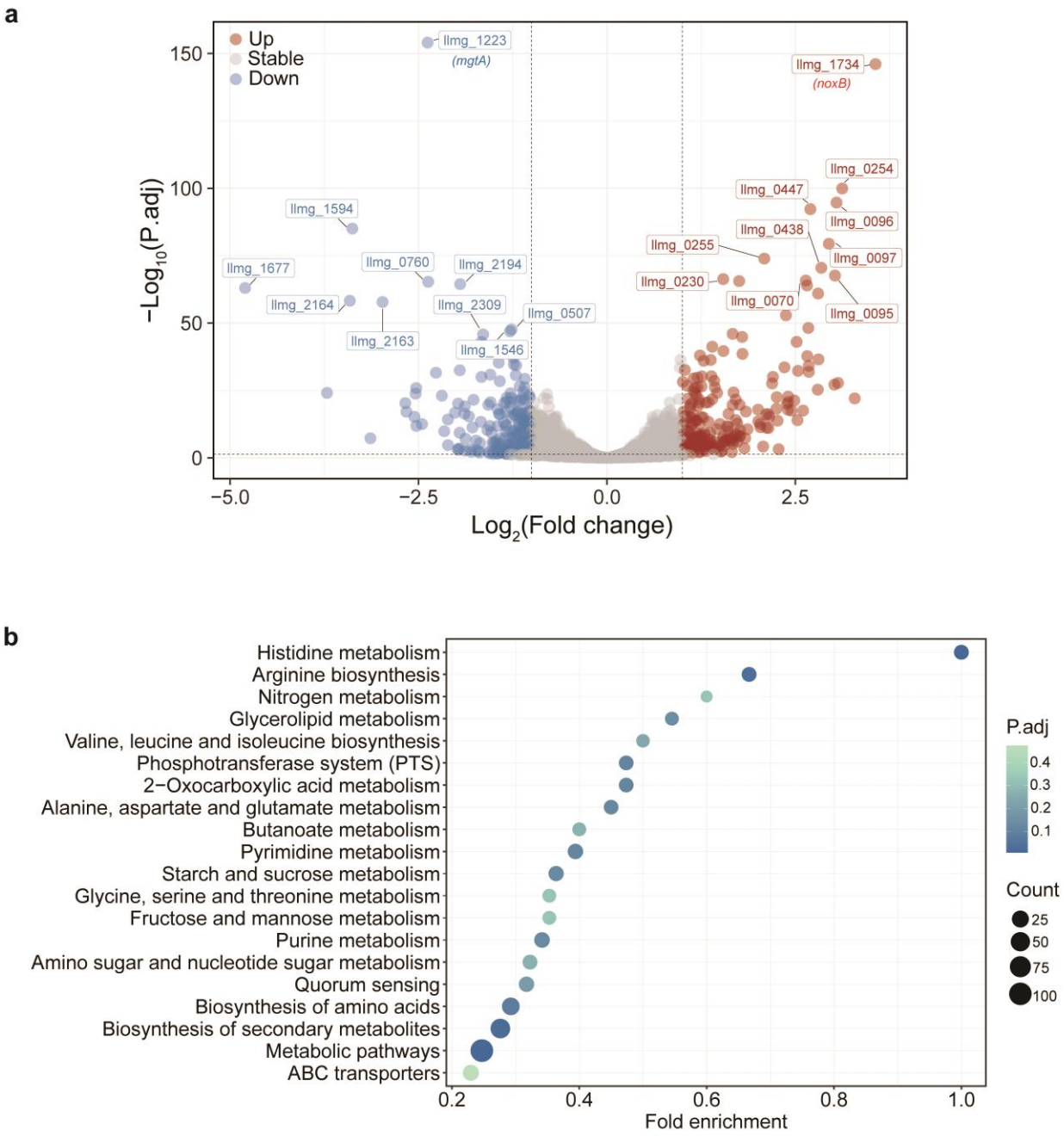

Fig. 3.1 Transcriptomic analysis of difference between CS4363 and ALE mutant CS4363-F2. (a) Volcanic map shows differentially expressed gens ($|Log_2(Fold\ change)| > 1$, P.adj < 0.05) between two strains. Red dots indicate upregulated genes, blue dots indicate downregulated genes and grey dots indicate stable genes. Top 10 upregulated or downregulated genes are labelled by gene locus tag. (b) The genes that are differentially expressed between two strains have been further classified according to gene functional annotations by using KEGG analysis. The size of circles represents the number of genes in relevant pathway. The color of circles (from blue to green) represents the adjusted p-value from higher to lower. The transcriptomics data for each strain was obtained based on biological triplicates.

Using KEGG (Kyoto Encyclopedia of Genes and Genomes) analysis, the differentially expressed genes were classified into different categories **(Fig. S3.1)**. Most of the differentially expressed genes ended up in the "Metabolism" category, highlighting the involvement of carbohydrate, amino acid and nucleotide metabolism. Sorted by adjusted P value < 0.5, the genes could be further subdivided into specific metabolic pathways **(Fig. 3.1b)**. An interesting finding was that the fold enrichment of histidine metabolism was 1, implying that the expression levels of all genes involved in histidine metabolism were changed. As shown in **Fig. 3.2**, genes involved in histidine metabolism, pyrimidine metabolism, valine metabolism, isoleucine metabolism and glutamate metabolism were upregulated, while genes involved in arginine metabolism and purine metabolism were downregulated.

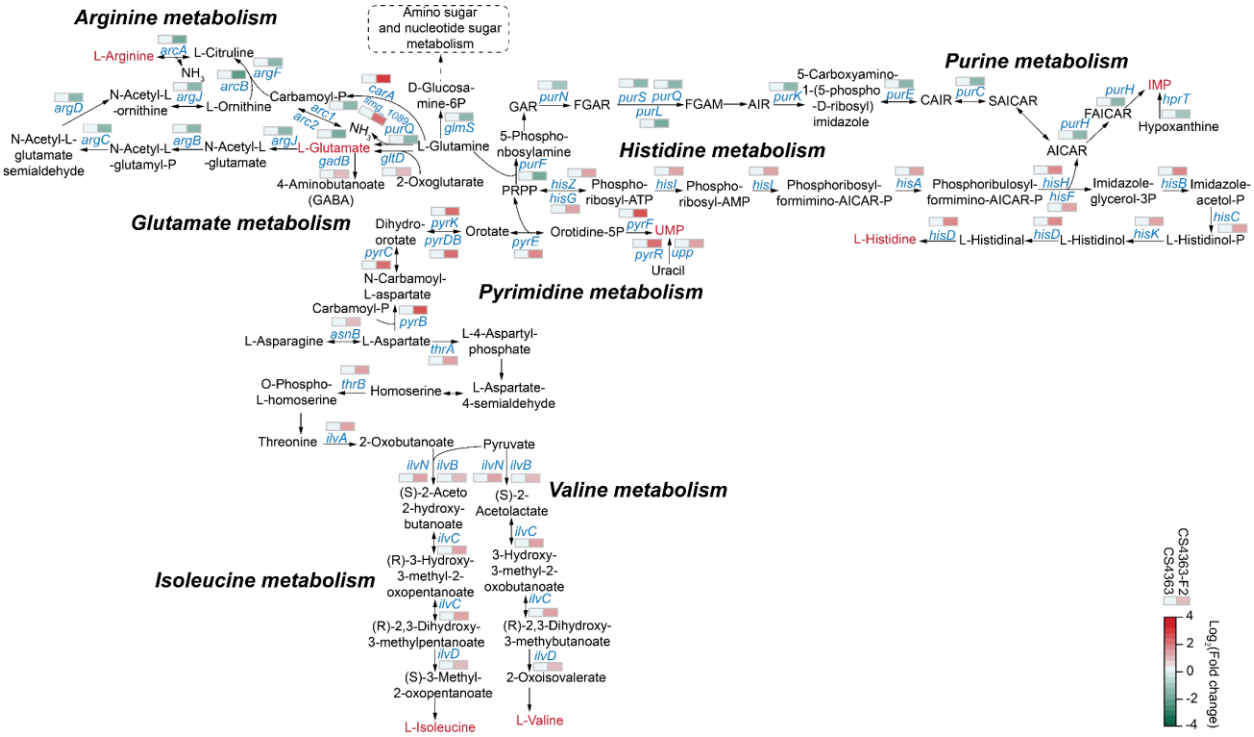

Fig. 3.2 The transcription levels of different genes involved in amino acid and nucleotide metabolism. Each gene is accompanied by Log_2(Fold change). The strains from left to right are: CS4363 and CS4363-F2.IMP: inosine monophosphate; UMP: uridine monophosphate; GAR: 5'-phosphoribosylglycinamide; FGAR: 5'-phosphoribosyl-N-formylglycinamide; FGAM: 2-(formamido)-N1-(5'-phosphoribosyl)acetamidine; AIR: aminoimidazole ribotide; CAIR: 1-(5-phospho-D-ribosyl)-5-amino-4-imidazolecarboxylate; SAICAR: 1-(5'-phosphoribosyl)-5-amino-4-(N-succinocarboxamide)-imidazole; AICAR: 1-(5'-phosphoribosyl)-5-amino-4-imidazolecarboxamide; FAICAR: 1-(5'-phosphoribosyl)-5-formamido-4-imidazolecarboxamide; PRPP: 5-phosphoribosyl diphosphate.

Previously it has been shown that the amino acid metabolism is important for internal pH homeostasis, energy generation and adaptation to stress in LAB (23). As mentioned above, EET to ferricyanide leads to strong acidification on the external face of the cell membrane, which might affect cytoplasmic pH (pH_i) (9), which could activate pH homeostasis mechanisms. In pH homeostasis, histidine has a special role, as it can serve as both a proton acceptor or a proton donor (24). Histidine metabolism was found to be upregulated in the EET-adapted mutant, indicating that measures to maintain intracellular pH had been activated in the EET-adapted strain. The arginine deiminase (ADI) pathway is another well-known pH homeostasis mechanism in *L. lactis* that generates NH_3 and ATP. NH_3 can neutralize protons and ATP can be used to promote extrusion of cytoplasmic protons by the F_0F_1-ATPase (25). The ADI pathway, however, was downregulated in the EET-adapted strain, indicating that other measures had been taken to ensure pH homeostasis. Surprisingly, another pH homeostasis mechanism, the glutamate decarboxylase (GAD) system, was upregulated. In *L. lactis*, this system, consists of glutamate decarboxylase (*gadB*) and an antiporter (*gadC*) (26, 27), where GadB catalyzes the decarboxylation of glutamate to 4-aminobutanoate (GABA), a reaction which consumes a proton. GABA can further be exported from the cell via GadC. In the EET-adapted strain *gadB* and *gadC* were upregulated to a similar extent, with a $\log_2$FC of 1.18 and 1.001, respectively. Why the GAD system, but not the ADI pathway was upregulated is an interesting finding that perhaps can be explained by the low abundance of free arginine in the rich M17 medium used, in combination with glucose repression of this particular pathway (28). None-the-less, this explanation should be substantiated. In *Lactobacillus* spp., the GAD system can provide metabolic energy by coupling electrogenic antiport and amino acid decarboxylation. Through three cycles of decarboxylation and antiport, a proton motive force can be created, which to some extent obviates the need for pumping out protons via the F_0F_1-ATPase, which helps save ATP that can be used for growth. It has been suggested that the proton motive force generated by the GAD system can drive the synthesis of ATP via the F_0F_1-ATPase (29, 30), however, in LAB, ATP synthesis by the F_0F_1-ATPase has not yet been convincingly demonstrated to take place (31).

Isoleucine and valine are branched-chain amino acids (BCAAs), which modulate the activity of the pleiotropic transcriptional repressor CodY in *L. lactis* (32). As a regulator globally controlling nitrogen metabolism, CodY can regulate genes involved in amino acid biosynthesis and nitrogen supply (33). CodY can also exert a feedback control on the expression of BCAA biosynthesis

genes, which is tightly regulated by CodY. When isoleucine is present in excess, it can exert a repressive effect on BCAA biosynthesis, which is due to CodY repression (33, 34). In CS4363-F2, the genes *ilvNBCD* involved in isoleucine and valine biosynthesis were upregulated. The reason for this could be the accelerated growth due to enhanced EET capacity; when *L. lactis* grows faster in a rich medium containing mostly peptides and little free amino acids, some amino acids may become limiting for growth, why it makes sense to upregulate their biosynthesis (9). For the EET-adapted strain, the BCAA apparently became limiting for growth.

L-glutamine is a core metabolite since it is a precursor for several metabolites. In the EET-adapted strain, the pathways from L-glutamine to carbamoyl-P (genes *carA* and *llmg_1089*) and L-glutamate (gene *gltD*) were upregulated. The upregulation of *gltD* ($log_2FC=1.10$) was directly related to the above-mentioned GAD system. The gene *pyrB* in the branching pathway from carbamoyl-P to pyrimidine was upregulated ($log_2FC=2.80$) and other downstream genes in pyrimidine metabolism were also upregulated. It has been shown previously that *pyrB* has a pivotal role in the utilization of L-aspartate (L-Asp) and its expression affects cell wall rigidity in a manner dependent on pyrimidine biosynthesis (35). The up-regulation of pyrimidine biosynthesis genes could lead to less L-Asp becoming available for peptidoglycan (PG) synthesis, which then reduces PG thickness and rigidity, which correlates well with our previous observations, where it was found that cell morphology changed when *L. lactis* growth was supported by EET to ferricyanide (9). Another interesting finding was that in CS4363-F2, the genes involved in purine metabolism were downregulated, resulting in less inosine monophosphate (IMP), a precursor of guanine nucleotides. It is plausible that lowering the IMP pool could increase the robustness of CS4363-F2 to various environmental stresses, as the opposite phenomenon, increased guanine nucleotide pools, were found to render *L. lactis* more sensitive to environmental stresses, e.g. acid stress, and heat stress (36).

3.4.2 The effect of the mutation in the *noxB* promoter

Genome sequencing revealed a single-nucleotide variation (SNV) T-73G in the *noxB* promoter in the EET-adapted strain CS4363-F2 (9). The transcriptomics analysis revealed that the expression of *noxB* had been significantly upregulated, and this could probably be attributed to the mutation, which, however, needed to be substantiated.

As shown in **Fig. 3.3a**, the mutation was found in the -35 region of the promoter. Interestingly, this mutation occurs in the *cre* site, which is involved in carbon catabolite repression, i.e. the CcpA binding site. CcpA is the main regulator of carbon catabolite repression in *L. lactis*. In the presence of glucose, CcpA, in complex with serine 46 phosphorylated Hpr, binds to the *cre* site and represses transcription (37). Previously it was found that the expression level of *noxB* was upregulated in *L. lactis* MG1363 *ΔccpA*, i.e. *noxB* is under catabolite repression (38). Thus, we speculated that the T-73G in the *cre* site mutation abolished repression *noxB*.

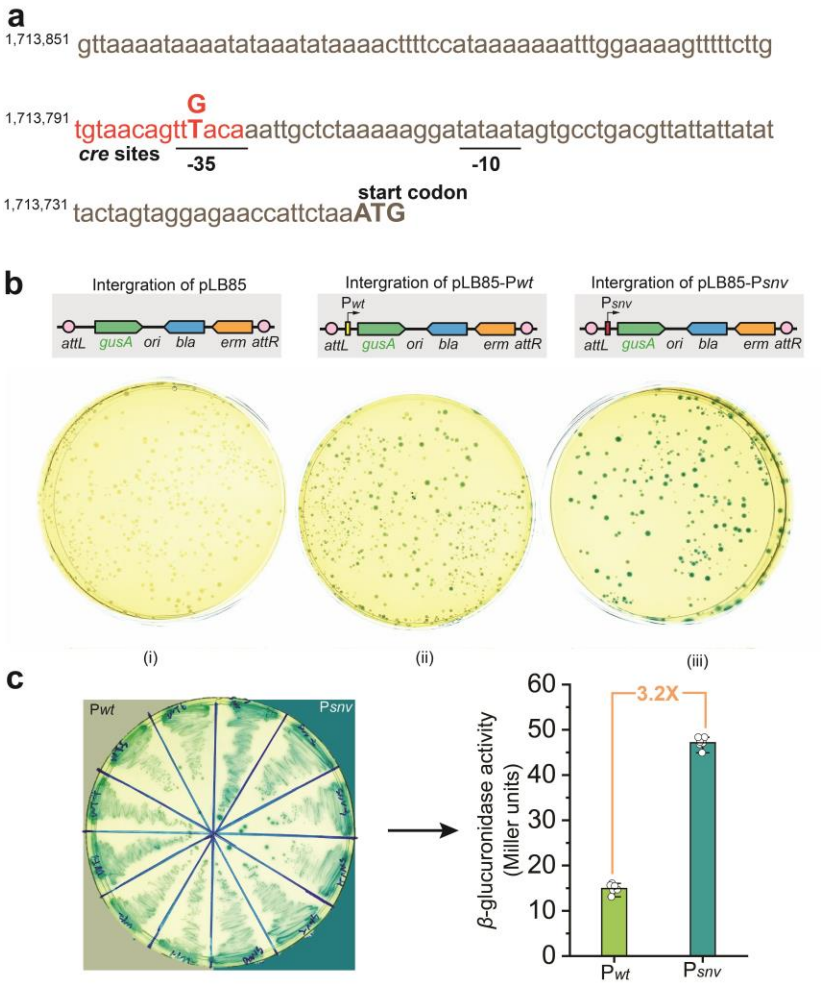

Fig. 3.3 The effect of SNV on *noxB* promoter activity. (a) The putative promoter of *noxB* in *L. lactis*. The *cre* site is indicated with red, the position in genome is indicated on the left of the top and the -10 and -35 elements are underlined. The mutation T-73G is indicated with red capital boldface letter. (b) Construction of chromosomal single-copy transcriptional fusion of *noxB* promoter in MG1363. (i) Integration of empty pLB85 into chromosome; (ii) integration of pLB85 with wild-type *noxB* promoter (P_{wt}) into chromosome; (iii) integration of pLB85 with T-73G mutant *noxB* promoter (P_{snv}) into chromosome. Schematic diagram of plasmid construction (up) and cells on GM17 medium with

erythromycin and X-Gluc (down). (c) Comparison of promoter activity of P_{wt} and P_{snv}. 12 single colonies of P_{wt} and P_{snv} picked from plates of (b) are restreaked (left). Promoter strength of P_{wt} (light green) and P_{snv} (dark green). Standard deviations are indicated by error bars.

To verify this hypothesis, transcriptional fusions between the *noxB* promoter and the reporter gene *gusA* (encoding β-glucuronidase) were constructed and chromosomally integrated into the phage TP901-1 *attB* site (18). As shown in **Fig. 3.3b**, indeed the mutation abolished repression of the *noxB* promoter; the mutated promoter gave a high expression of the *gusA* reporter gene, resulting in blue/green colonies on the agar plates containing the chromogenic substrate for the β-glucuronidase, X-gluc. Quantification of the promoter strength by measuring β-glucuronidase activity in liquid cultures revealed that the mutated promoter resulted in 3.2 times higher expression when compared to the wild-type *noxB* promoter **(Fig. 3.3c)**, which correlated nicely with the fold change in expression observed by RNA sequencing ($log_2FC=3.56$). This demonstrated that the enhanced expression of *noxB* could be attributed to the mutation in the promoter.

3.4.3 The special role of NoxB in EET of *L. lactis*

It is an interesting finding that the *noxB* promoter had mutated, leading to higher expression of NoxB, while the expression of *noxA* (encoding another NADH dehydrogenase) was unaffected in the EET-adapted mutant. This could indicate a special role for NoxB in EET, and that the two type-II NADH dehydrogenases (NoxA and NoxB) could have different functions. To test this hypothesis, we knocked out *noxA*, *noxB* or both genes in CS4363. The resulting mutants were named CS4363-NA, CS4363-NB and CS4363-NAB **(Fig. 3.4a)**. We previously have demonstrated that ferricyanide can support the growth of CS4363, a strain that cannot grow without an external electron acceptor, and that this is due to EET (9). Thus for CS4363 the EET ability is directly coupled to growth, which is convenient for isolating mutants with enhanced ability to do EET. As shown in **Fig. 3.4b**, compared with CS4363, the EET-supported growth of CS4363-NB and CS4363-NAB was not possible, whereas CS4363-NA was unaffected. The pH change and glucose consumption observed were directly linked to growth **(Fig. 3.4c)**. This shows the essential role of NoxB for EET, and that NoxA cannot support EET.

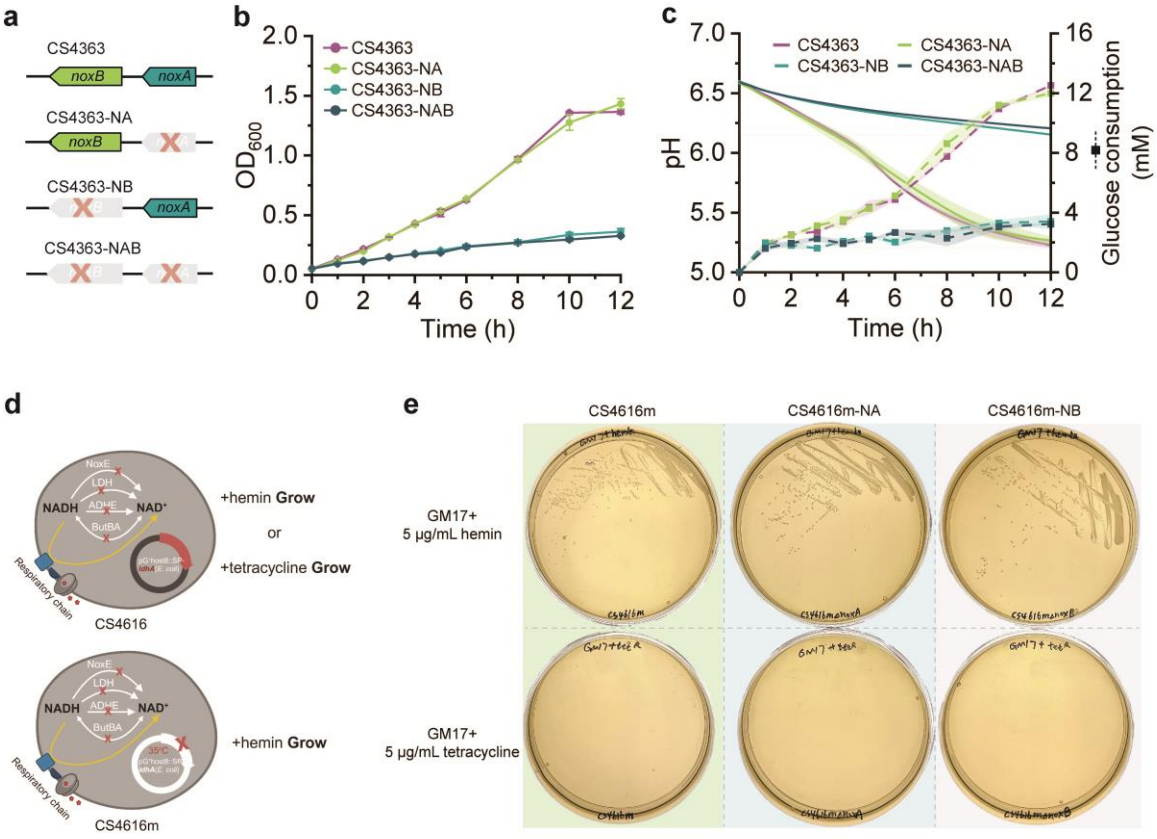

Fig. 3.4 Different function of NoxA and NoxB in *L. lactis*. (a) Schematic diagram of CS4363 knock-out strains. (b) Growth performance of CS4363 knock-out strains with 150 mM ferricyanide under relative anaerobic condition. (c) pH change and glucose consumption of CS4363 knock-out strains with 150 mM ferricyanide under relative anaerobic condition. (d) Schematic diagram of CS4616 and plasmid-cured strain CS4616m. NoxE: NADH oxidase; LDH: lactate dehydrogenase; ADHE: alcohol dehydrogenase; ButBA: 2, 3-butanediol dehydrogenase. (e) Plate validation of respiratory ability (up) and plasmid pCS4564 loss (down) in CS4616m-NA and CS4616m-NB under aerobic condition. CS4616m was used as positive control.

3.4.4 Respiration is supported by both NADH dehydrogenases NoxA and NoxB

In previous work on the respiratory chain of *L. lactis*, the presence of two genes encoding type II dehydrogenases has received little attention (39, 40), also it has not been made clear what their roles could be, although there have been speculations. Knocking out *noxA* and/or *noxB* and determining the consequence for respiration is a more direct approach. Considering that *L. lactis* harbors a NADH oxidase (NoxE) which can also re-oxidize NADH when oxygen is present, it was decided that CS4616 should be used. In CS4616 (17), all pathways for NAD^+ regeneration, except respiration, have been knocked-out, and this strain can only grow because of heterologous

expression of the *E. coli*-derived lactate dehydrogenase present on plasmid pCS4564, which has a temperature-sensitive replicon **(Fig. 3.4d)**. We knocked out *noxA*, *noxB* or both in CS4616, to construct CS4616-NA, CS4616-NB and CS4616-NAB. To eliminate pCS4616, the strains were cultured under aerobic conditions at 35 ℃ (non-permissive for pCS4616 replication) and 5 μg/mL hemin (to activate respiration). For CS4616-NAB, which is devoid of both NADH dehydrogenases, pCS4564 could not be lost, most likely because lactate formation was the only way for the cells to regenerate NAD^+. A similar phenomenon was observed in an *E. coli* mutant, only with plasmid carrying essential gene encoding translation initiation factor, can cells grow, making this *E. coli* totally dependent on the maintenance of the plasmid (41). However, the single knock-out strains could readily be obtained, demonstrating that either NADH dehydrogenase, NoxA or NoxB, could support respirative growth **(Fig. 3.4e)**.

3.4.5 Bioinformatics analysis of NoxB

To better understand the unique role of NoxB in EET, we aligned the amino acid sequences of NoxA and NoxB by CLUSTALW. As shown in **Fig. S3.2**, we found a high similarity between the two proteins for the first 414 amino acids, where the similarity reached 66%. Based on the primary structure of NADH dehydrogenase (42, 43), two conserved GXGXXG motifs within β-sheet-α-helix-β-sheet structures for binding flavin adenine dinucleotide and NADH were found in this region of NoxA and NoxB, showing that the two enzymes are group A type-II NADH dehydrogenases. The substrates of the NADH dehydrogenases are quinones, where 2-amino-3-carboxy-1,4-naphthoquinone has been shown to be particularly efficient for EET (9) while menaquinones participate in respiration (31). Differences in the quinone-binding site of NoxA and NoxB probably can explain the special role of NoxB in EET. However, due to the variability of quinone types and little information on the three-dimensional structures of quinone-containing proteins, it is difficult to identify quinone-binding sites only based on amino acid sequences (42). Furthermore, interestingly, we found that NoxB has an extra 248 AA in the C-terminal **(Fig. S3.2)**, which was predicted to contain transmembrane helices **(Fig. 3.5a)**. This is unusual because the common type-II NADH dehydrogenases lack transmembrane helices (42). No transmembrane helices have been identified in the C-terminal of NoxA, as predicted by TMHMM **(Fig. S3.3)**. So NoxB is a novel type-II NADH dehydrogenase and its transmembrane domain could be another reason for its special role in EET. It is worth mentioning that the type-II NADH dehydrogenase

NoxA is classified as a membrane protein and it belongs to the monotopic membrane proteins, which means that membrane anchoring is achieved via amphipathic helices positioned parallel to the membrane plane (44). NoxB also possesses this amphipathic helix **(Fig. 3.5a)**.

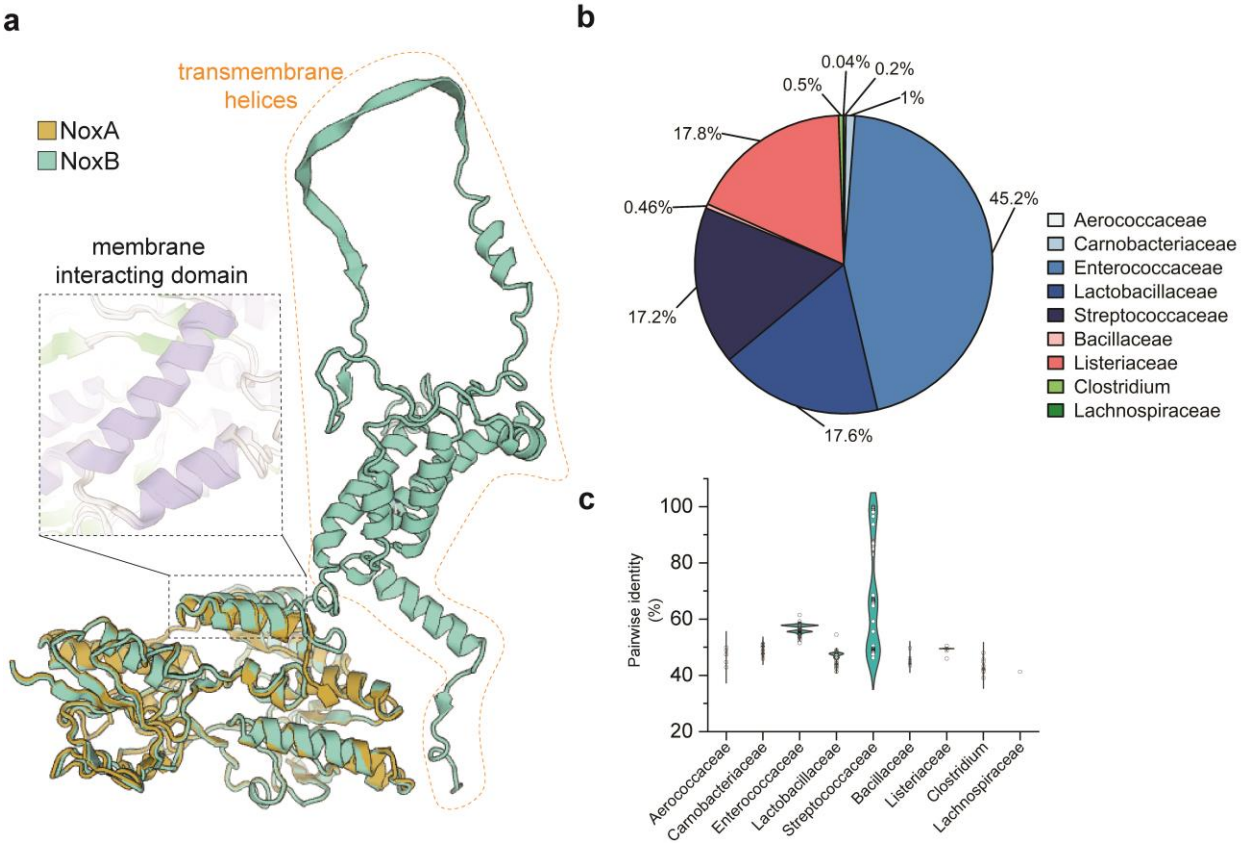

Fig. 3.5 Bioinformatics of NoxB. (a) Comparison of three-dimensional structures of NoxA and NoxB using Swiss-Model. (b) Pie chart showing the percentage of the order in *Bacilli* class and *Clostridia* class containing this novel type-II NADH dehydrogenase. tblastn was used for identifying database sequences in NCBI encoding proteins similar to NoxB (downloaded 10/12/2022). A match was considered positive with a Bit-score > 50 and E-value < 10^{-2}. 2158 strains were found to have sequences similar to NoxB and strains were sorted by order. The percentage of different orders was marked out. (c) Violin plot showing pairwise identity distribution of different order in *Bacilli* class and *Clostridia* class.

Type-II NADH dehydrogenases, similar to NoxB from *L. lactis*, have been identified in *Listeria monocytogenes* (Ndh2) (7) and *Enterococcus faecalis* (named as Ndh3) (12), which both are involved in EET. This attracted our interest and prompted us to make a three-dimensional structure comparison between the proteins using Swiss-Model. As shown in **Fig. S3.4**, the three-dimensional structure of NoxB and the other two type-II NADH dehydrogenases from different origins were similar. Another shared feature of these three microorganisms is that they often reside

in the animal gut. To investigate if the presence of NoxB-type NADH dehydrogenases could be linked to the presence in the gut environment, a homology search was conducted by tblastn and results were sorted by taxonomy. As shown in **Fig. 3.5b**, this novel type-II NADH dehydrogenase is very commonly found among gut microorganisms, both in commensals and pathogens. *Enterococcaceae* (45.2%), *Lactobacillaceae* (17.6%), *Listeriaceae* (17.8%) and *Streptococcaceae* (17.2%) are the most common families where it is found. This could indicate that the ability to do EET is beneficial in the gut environment (3). The pairwise identity was concentrated between 40% and 100%, and the pairwise identity range is the widest in *Streptococcaceae* **(Fig. 3.5c)**. The different pairwise identities of amino acid sequences of different orders could be the result of adaptive evolution to the environment.

3.5 Conclusion

In this study, an *L. lactis* mutant with an enhanced capacity for EET was studied systematically using a comparative transcriptomics approach. From a global perspective, it was found that expression of genes in the amino acid and nucleotide metabolism had been significantly altered. More specifically, it was found that a SNV in the *noxB* promoter region abolished catabolite repression. The special role of NoxB in EET was verified, and could be linked to its special structure. *L. lactis* harbors genes encoding two type II NADH dehydrogenases, NoxA and NoxB. We managed to verify that both NoxA and NoxB could support respiration (EET to oxygen), and that that only NoxB could support EET to ferricyanide. NoxB was found to be widely distributed among gut microorganisms. These findings have deepened our understanding of the mechanisms behind the enhanced EET capacity of *L. lactis*, and provide insights for future improvement of *L. lactis* exhibiting enhanced EET capacity.

3.6 References

1. Hernandez ME, Newman DK. 2001. Extracellular electron transfer. Cell Mol Life Sci 58:1562–1571.

2. Kato S. 2015. Biotechnological aspects of microbial extracellular electron transfer. Microbes Environ 30:133–139.

3. Stevens E, Marco ML. 2023. Bacterial extracellular electron transfer in plant and animal ecosystems. FEMS Microbiol Rev 47:fuad019.

4. Shi L, Richardson DJ, Wang Z, Kerisit SN, Rosso KM, Zachara JM, Fredrickson JK. 2009. The roles of outer membrane cytochromes of *Shewanella* and *Geobacter* in extracellular electron transfer. Environ Microbiol Rep 1:220–227.

5. Reguera G, McCarthy KD, Mehta T, Nicoll JS, Tuominen MT, Lovley DR. 2005. Extracellular electron transfer via microbial nanowires. Nature 435:1098–1101.

6. Paquete CM. 2020. Electroactivity across the cell wall of Gram-positive bacteria. Comput Struct Biotechnol J 18:3796–3802.

7. Light SH, Su L, Rivera-Lugo R, Cornejo JA, Louie A, Iavarone AT, Ajo-Franklin CM, Portnoy DA. 2018. A flavin-based extracellular electron transfer mechanism in diverse Gram-positive bacteria. 7725. Nature 562:140–144.

8. Tejedor-Sanz S, Stevens ET, Li S, Finnegan P, Nelson J, Knoesen A, Light SH, Ajo-Franklin CM, Marco ML. 2022. Extracellular electron transfer increases fermentation in lactic acid bacteria via a hybrid metabolism. eLife 11:e70684.

9. Gu L, Xiao X, Zhao G, Kempen P, Zhao S, Liu J, Lee SY, Solem C. 2023. Rewiring the respiratory pathway of *Lactococcus lactis* to enhance extracellular electron transfer. Microb Biotechnol 16:1277–1292.

10. Tolar JG, Li S, Ajo-Franklin CM. 2022. The differing roles of flavins and quinones in extracellular electron transfer in *Lactiplantibacillus plantarum*. Appl Environ Microbiol 0:e01313-22.

11. Pankratova G, Leech D, Gorton L, Hederstedt L. 2018. Extracellular electron transfer by the Gram-positive bacterium *Enterococcus faecalis*. Biochemistry 57:4597–4603.

12. Hederstedt L, Gorton L, Pankratova G. 2020. Two routes for extracellular electron transfer in *Enterococcus faecalis*. J Bacteriol 202:e00725-19.

13. Yamziki S, Kaneko T, Taketomo N, Kano K, Ikeda T. 2002. Glucose metabolism of lactic acid bacteria changed by quinone-mediated extracellular electron transfer. Biosci Biotechnol Biochem 66:2100–2106.

14. Gu L, Xiao X, Yup Lee S, Lai B, Solem C. 2023. Superior anodic electro-fermentation by enhancing capacity for extracellular electron transfer. Bioresour Technol 389:129813.

15. Gasson MJ. 1983. Plasmid complements of *Streptococcus lactis* NCDO 712 and other lactic streptococci after protoplast-induced curing. J Bacteriol 154:1–9.

16. Solem C, Dehli T, Jensen PR. 2013. Rewiring *Lactococcus lactis* for ethanol production. Appl Environ Microbiol 79:2512–2518.

17. Liu J, Chan SHJ, Brock-Nannestad T, Chen J, Lee SY, Solem C, Jensen PR. 2016. Combining metabolic engineering and biocompatible chemistry for high-yield production of homo-diacetyl and homo-(S,S)-2,3-butanediol. Metab Eng 36:57–67.

18. Lone B, Karin H. 1999. Use of the integration elements encoded by the temperate lactococcal bacteriophage TP901-1 to obtain chromosomal single-copy transcriptional fusions in *Lactococcus lactis*. Appl Environ Microbiol 65:752–758.

19. Solem C, Defoor E, Jensen PR, Martinussen J. 2008. Plasmid pCS1966, a new selection/counterselection tool for lactic acid bacterium strain construction based on the *oroP*gene, encoding an orotate transporter from *Lactococcus lactis*. Appl Environ Microbiol 74:4772–4775.

20. Holo H, Nes IF. 1989. High-frequency transformation, by electroporation, of *Lactococcus lactis* subsp. *cremoris* grown with glycine in osmotically stabilized media. Appl Environ Microbiol 55:3119–3123.

21. Bu D, Luo H, Huo P, Wang Z, Zhang S, He Z, Wu Y, Zhao L, Liu J, Guo J, Fang S, Cao W, Yi L, Zhao Y, Kong L. 2021. KOBAS-i: intelligent prioritization and exploratory visualization of biological functions for gene enrichment analysis. Nucleic Acids Res 49:W317–W325.

22. van der Meulen SB, de Jong A, Kok J. 2017. Early transcriptome response of *Lactococcus lactis* to environmental stresses reveals differentially expressed small regulatory RNAs and tRNAs. Front Microbiol 8:1704.

23. Fernández M, Zúñiga M. 2006. Amino acid catabolic pathways of lactic acid bacteria. Crit Rev Microbiol 32:155–183.

24. Kulis-Horn RK, Persicke M, Kalinowski J. 2014. Histidine biosynthesis, its regulation and biotechnological application in *Corynebacterium glutamicum*. Microb Biotechnol 7:5–25.

25. Sanders JW, Venema G, Kok J. 1999. Environmental stress responses in *Lactococcus lactis*. FEMS Microbiol Rev 23:483–501.

26. Nomura M, Nakajima I, Fujita Y, Kobayashi M, Kimoto H, Suzuki I, Aso H. 1999. *Lactococcus lactis* contains only one glutamate decarboxylase gene. Microbiology 145:1375–1380.

27. Yogeswara IBA, Maneerat S, Haltrich D. 2020. Glutamate decarboxylase from lactic acid bacteria—a key enzyme in GABA synthesis. Microorganisms 8:1923.

28. Poolman B, Driessen AJ, Konings WN. 1987. Regulation of arginine-ornithine exchange and the arginine deiminase pathway in *Streptococcus lactis*. J Bacteriol 169:5597–5604.

29. Higuchi T, Hayashi H, Abe K. 1997. Exchange of glutamate and gamma-aminobutyrate in a *Lactobacillus* strain. J Bacteriol 179:3362–3364.

30. Small PLC, Waterman SR. 1998. Acid stress, anaerobiosis and *gadCB*: lessons from *Lactococcus lactis* and *Escherichia coli*. Trends Microbiol 6:214–216.

31. Pedersen MB, Gaudu P, Lechardeur D, Petit M-A, Gruss A. 2012. Aerobic respiration metabolism in lactic acid bacteria and uses in biotechnology. Annu Rev Food Sci Technol 3:37–58.

32. Guédon E, Serror P, Ehrlich SD, Renault P, Delorme C. 2001. Pleiotropic transcriptional repressor CodY senses the intracellular pool of branched-chain amino acids in *Lactococcus lactis*. Mol Microbiol 40:1227–1239.

33. Guédon E, Sperandio B, Pons N, Ehrlich SD, Renault P. 2005. Overall control of nitrogen metabolism in *Lactococcus lactis* by CodY, and possible models for CodY regulation in Firmicutes. Microbiology 151:3895–3909.

34. Shivers RP, Sonenshein AL. 2004. Activation of the *Bacillus subtilis* global regulator CodY by direct interaction with branched-chain amino acids. Mol Microbiol 53:599–611.

35. Solopova A, Formosa-Dague C, Courtin P, Furlan S, Veiga P, Péchoux C, Armalyte J, Sadauskas M, Kok J, Hols P, Dufrêne YF, Kuipers OP, Chapot-Chartier M-P, Kulakauskas S. 2016. Regulation of cell wall plasticity by nucleotide metabolism in *Lactococcus lactis*. J Biol Chem 291:11323–11336.

36. Ryssel M, Hviid A-MM, Dawish MS, Haaber J, Hammer K, Martinussen J, Kilstrup M. 2014. Multi-stress resistance in *Lactococcus lactis* is actually escape from purine-induced stress sensitivity. Microbiology 160:2551–2559.

37. Seidel G, Diel M, Fuchsbauer N, Hillen W. 2005. Quantitative interdependence of coeffectors, CcpA and *cre* in carbon catabolite regulation of *Bacillus subtilis*. FEBS J 272:2566–2577.

38. Zomer AL, Buist G, Larsen R, Kok J, Kuipers OP. 2007. Time-Resolved determination of the CcpA regulon of *Lactococcus lactis* subsp. *cremoris* MG1363. J Bacteriol 189:1366–1381.

39. Lechardeur D, Cesselin B, Fernandez A, Lamberet G, Garrigues C, Pedersen M, Gaudu P, Gruss A. 2011. Using heme as an energy boost for lactic acid bacteria. Curr Opin Biotechnol 22:143–149.

40. Brooijmans RJW, Poolman B, Schuurman-Wolters GK, de Vos WM, Hugenholtz J. 2007. Generation of a membrane potential by *Lactococcus lactis* through aerobic electron transport. J Bacteriol 189:5203–5209.

41. Hägg P, de Pohl JW, Abdulkarim F, Isaksson LA. 2004. A host/plasmid system that is not dependent on antibiotics and antibiotic resistance genes for stable plasmid maintenance in *Escherichia coli*. J Biotechnol 111:17–30.

42. Melo AMP, Bandeiras TM, Teixeira M. 2004. New insights into type II NAD(P)H:quinone oxidoreductases. Microbiol Mol Biol Rev 68:603–616.

43. Marreiros BC, Sena FV, Sousa FM, Oliveira ASF, Soares CM, Batista AP, Pereira MM. 2017. Structural and functional insights into the catalytic mechanism of the type II NADH:quinone oxidoreductase family. Sci Rep 7:42303.

44. Allen KN, Entova S, Ray LC, Imperiali B. 2019. Monotopic membrane proteins join the fold. Trends Biochem Sci 44:7–20.

3.7 Supplementary materials

Table S3.1 Primers used in this work.

Name	Sequence(5'-3')
A1-F	GAAGGAATCCATATGGTTCAGGCTATGCGGTTG
A1-R	CAGGTCGACTCTAGAATAACGTCAGGCACTATTATATCC
A1-plas-F	AGTGCCTGACGTTATTCTAGAGTCGACCTGCAG
A1-plas-R	CCGCATAGCCTGAACCATATGGATTCCTTCTATGCATGAG
pLB85-F	CAAAGGTTGATGTTACTGCTG
pLB85-R	GACGTAACATAAGGGACTCCT
4-up-F	AGAACTAGTGGATCCGCATCACCACCAGTCAAAC
4-up-R	TCCAAGAGAAATGGCAAAATAGCTCTGCGGAGC
4-down-F	CCGCAGAGCTATTTTGCCATTTCTCTTGGA
4-down-R	CAAAAGCTGGGTACCGCAGATTGGCTCAATGGTC
4-plas-F	ATTGAGCCAATCTGCGGTACCCAGCTTTTGTTCC
4-plas-R	GACTGGTGGTGATGCGGATCCACTAGTTCTAGAGCGG
4-F	TACCAATTCGAGCAGCACC

4-R	GGCGTCAGTATTCATCAAGG
8-up-F	AGAACTAGTGGATCCGCATCACCACCAGTCAAAC
8-up-R	AATAGTGCCTGACGTAAAATAGCTCTGCGGAGC
8-down-F	CCGCAGAGCTATTTTACGTCAGGCACTATTATATCC
8-down-R	CAAAAGCTGGGTACCGTGTTAACGAATATGGCTTCAC
8-plas-F	CATATTCGTTAACACGGTACCCAGCTTTTGTTCC
8-plas-R	GACTGGTGGTGATGCGGATCCACTAGTTCTAGAGCGG
8-F	GCTTTCCCTGATTGAATGTAG
8-R	GCATCTATGTTGCAGGAGATG
9-up-F	AGAACTAGTGGATCCGAAGACGATGTCCACGTTC
9-up-R	TCCAAGAGAAATGGCTCCACAAAGGGGCAATTTAA
9-down-F	TTGCCCCTTTGTGGAGCCATTTCTCTTGGACTCC
9-down-R	CAAAAGCTGGGTACCGCAGATTGGCTCAATGGTC
9-plas-F	ATTGAGCCAATCTGCGGTACCCAGCTTTTGTTCC
9-plas-R	GTGGACATCGTCTTCGGATCCACTAGTTCTAGAGCGG
9-F	CCGATGACTACGATTTGTTTC
9-R	TGTCTTAATTGGCCATTCGATG

Table S3.2 Top-10 upregulated genes and top-10 downregulated genes.

NO.	Locus tag	Gene name	Function	Log_2FC	Adjusted P value	Change
Upregulated genes						
1	llmg_1734	*noxB*	NADH dehydrogenase	3.563238175	8.93E-147	Up
2	llmg_0254	*hadL*	Cryptic haloacid dehalogenase 1	3.121065906	1.23E-100	Up

3	llmg_0096	*llmg_0096*	Putative glyoxylase protein	3.046081101	2.11E-95	Up
4	llmg_0447	*nifJ*	NifJ protein	2.698454779	5.74E-93	Up
5	llmg_0097	*llmg_0097*	Putative flavoprotein oxygenase	2.944150261	3.79E-80	Up
6	llmg_0255	*dhaK*	Dihydroxyacetone kinase DhaK	2.087367228	1.24E-74	Up
7	llmg_0438	*ptcA*	PTS cellobiose transporter subunit IIA	2.844424482	3.21E-71	Up
8	llmg_0095	*llmg_0095*	Putative esterase	3.02544029	2.43E-68	Up
9	llmg_0230	*guaB*	Inosine-5'-monophosphate dehydrogenase	1.542427382	4.97E-67	Up
10	llmg_0070	*llmg_0070*	Putative permease	2.638566766	1.77E-66	Up
Downregulated genes						
1	llmg_1223	*mgtA*	Magnesium-transporting ATPase, P-type 1	-2.379504765	9.44E-155	Down
2	llmg_1594	*llmg_1594*	Gamma-glutamyl-diamino acid-endopeptidase	-3.378156345	8.73E-86	Down
3	llmg_0760	*llmg_0760*	Putative transglycosylase	-2.371642175	5.06E-66	Down
4	llmg_2194	*llmg_2194*	3D domain-containing protein	-1.947601921	3.59E-65	Down
5	llmg_1677	*llmg_1677*	Putative secreted protein	-4.80140021	9.63E-64	Down
6	llmg_2164	*llmg_2164*	Putative adhesin domain-containing protein	-3.411699062	5.43E-59	Down

7	llmg_2163	*llmg_2163*	Phage shock protein PspC N-terminal domain-containing protein	-2.977008238	1.58E-58	Down
8	llmg_0507	*llmg_0507*	Peptide ABC transporter substrate-binding protein	-1.265921735	2.37E-48	Down
9	llmg_1546	*ftsE*	Cell division ATP-binding protein FtsE	-1.286438817	1.23E-47	Down
10	llmg_2309	*arcC2*	Carbamate kinase	-1.642656191	1.71E-46	Down

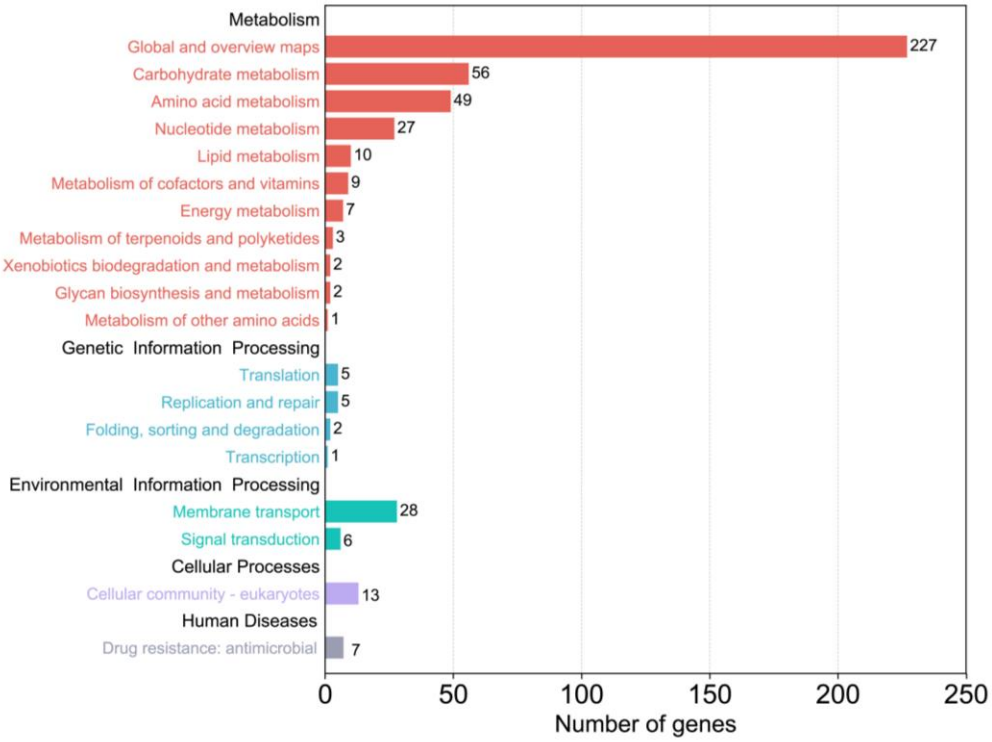

Fig. S3.1 KEGG pathway analysis of functions of differential genes using secondary classification. The number indicates genes involved in specific classifications.

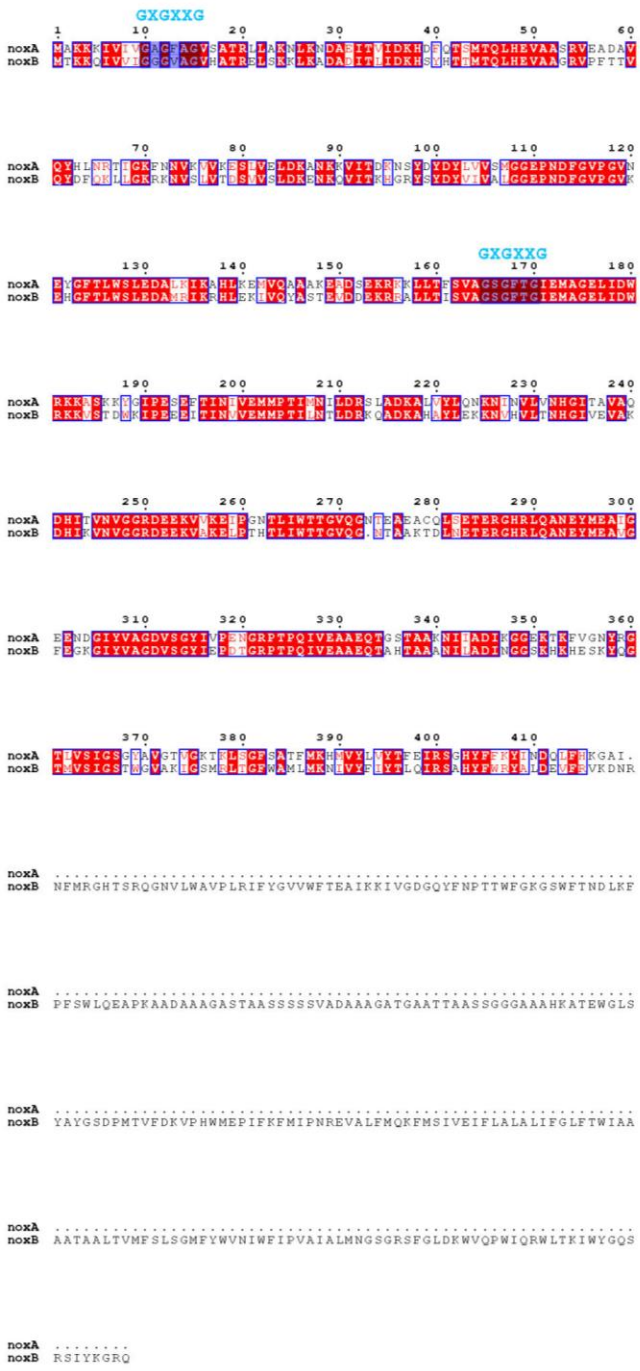

Fig. S3.2 Comparison of amino acid sequences of *noxA* and *noxB*. The red color indicates the same amino acids in *noxA* and *noxB.* Two highlight motifs (GXGXXG) are conserved dinucleotide binding domains: the first GXGXXG is flavin adenine dinucleotide binding site and the second GXGXXG is NADH binding site.

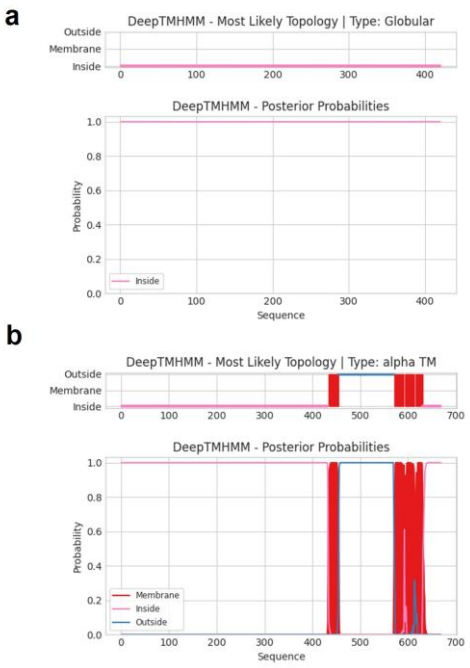

Fig. S3.3 Prediction of transmembrane helices in NoxA and NoxB by TMHMM. (a) Prediction of NoxA. (b) Prediction of NoxB.

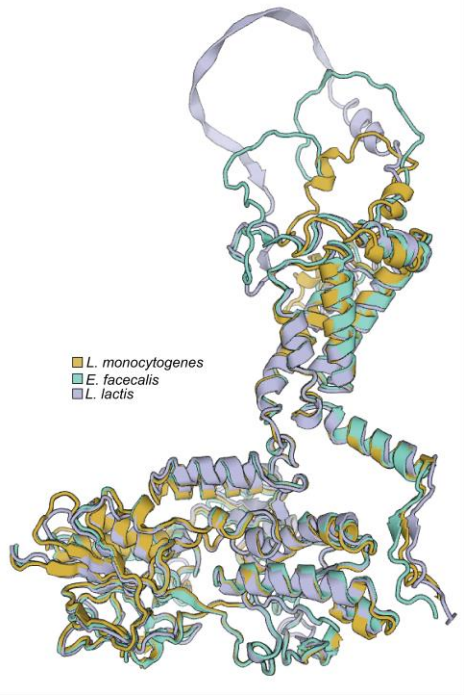

Fig. S3.4 Comparison of three-dimensional structures of novel type-II NADH dehydrogenases in different strains.

CHAPTER 4. Superior anodic electro-fermentation of *L. lactis* with enhanced extracellular electron transfer capacity

Published in Bioresource Technology, 2023, 389:129813. DOI: 10.1016/j.biortech.2023.129813.
Reprint with permission.

Bioresource Technology 389 (2023) 129813

Contents lists available at ScienceDirect

Bioresource Technology

journal homepage: www.elsevier.com/locate/biortech

Superior anodic electro-fermentation by enhancing capacity for extracellular electron transfer

Liuyan Gu [a], Xinxin Xiao [b], Sang Yup Lee [c], Bin Lai [d,*], Christian Solem [a,*]

[a] National Food Institute, Technical University of Denmark, Kongens Lyngby, 2800, Denmark
[b] Department of Chemistry and Bioscience, Aalborg University, 9220 Aalborg, Denmark
[c] Department of Chemical and Biomolecular Engineering, Korea Advanced Institute of Science and Technology (KAIST), Daejeon 34141, Republic of Korea
[d] BMBF junior research group Biophotovoltaics, Helmholtz Center for Environmental Research – UFZ, Leipzig 04318, Germany

4.1 Abstract

Anodic electro-fermentation (AEF), where an anode replaces the terminal electron acceptor, shows great promise. Recently a *Lactococcus lactis* strain blocked in NAD^+ regeneration was demonstrated to use ferricyanide as an alternative electron acceptor to support fast growth, but the need for high concentrations of this non-regenerated electron acceptor limits practical applications. To address this, growth of this *L. lactis* strain, and an adaptively evolved (ALE) mutant with enhanced ferricyanide respiration capacity were investigated using an anode as electron acceptor in a bioelectrochemical system (BES) setup. Both strains grew well, however, the ALE mutant was significantly faster. The ALE mutant almost exclusively generated 2,3-butanediol, whereas its parent strain mainly produced acetoin. The ALE mutant interacted efficiently with the anode, achieving a record high current density of 0.81±0.05 mA/cm^2. It is surprising that a Lactic Acid Bacterium, with fermentative metabolism, interacts so well with an anode, which demonstrates the potential of AEF.

4.2 Introduction

Aerated bioreactors are used to culture a wide range of important industrial microorganisms, including those used in food fermentations (1–4). However, the aeration process requires a high energy input and thus the running costs are high, often limiting the extent of scaling up of the bioreactors. The low solubility of oxygen in aqueous solutions makes it challenging to achieve a high volumetric gas-liquid coefficient (i.e. K_La) and dissolved oxygen (DO) level (5), which are important for cell growth and a high yield of the desired fermentation products (6). Common ways to improve DO level include costly measures e.g. high stirring speed, high gas flow rate (of even pure oxygen), high bioreactor pressure, etc. (7). Other challenges associated with aeration are foaming problems (8) and the strong oxidative stress imposed on the microorganisms (9–11). Nevertheless, oxygen still remains the most commonly used terminal electron acceptor, mainly due to lack of suitable alternatives and its relatively low cost.

The facultative anaerobic bacterium, *Lactococcus lactis*, is an important food microorganism and cell factory for producing food ingredients such as butter aroma, vitamins and nisin (12–14). In the culture industry, aerobic conditions are widely used to suppress lactate production, as lactate lowers pH and inhibits cell growth (15). In the presence of oxygen, NADH oxidase can oxidize NADH and change *L. lactis* from a homolactic bacterium to an efficient acetoin-producing

bacterium (16). Besides, some *L. lactis* strains are capable of respiring when either heme, hemin, or protoporphyrin IX is available, which has beneficial effects on growth and biomass yield, why culture manufacturers often harness respiration when culturing of *L. lactis* (17–19). However, as mentioned above aerated culturing is associated with some challenges, and furthermore the use of animal blood, as a source of heme, in microbial food cultures can be unwanted as well. Under anaerobic conditions, although the oxygen is avoided, the type of product is also limited because the regeneration of NAD^+ is mainly achieved by lactate dehydrogenases, and typically 90% of the metabolized sugar ends up as lactate (20). Therefore, by replacing oxygen with an alternative electron acceptor it may be possible to alter the fermentation product composition by affecting the redox balance, while at the same time avoiding some of the challenges associated with oxygen.

Recently, a mutant of *L. lactis* blocked in NAD^+ regeneration, CS4363, was demonstrated to grow in the absence of oxygen, when ferricyanide was used as electron acceptor, and extracellular electron transfer (EET) could be enhanced by adaptive laboratory evolution (ALE) (21). In that study, a high concentration of ferricyanide was used (50 mM), and ferricyanide was not regenerated. If the electron acceptor could be regenerated that it would be a great advantage, as this would allow lower concentrations to be used. Anodic electro-fermentation (AEF) could be the solution, where an anode accepts electrodes either directly from living cells or via mediators (22–24). The use of AEF to produce important chemicals has been systematically reviewed for other microorganisms previously (25), and has great potential. AEF enabled high-yield production of 2-keto-gluconate by the obligate aerobe *Pseudomonas putida* under anoxic condition in a bioelectrochemical system (BES) setup (26). AEF was able to boost the cellular energy supply and promote growth and production of L-lysine by *Corynebacterium glutamicum* (27). For another important industrial bacterium, *Bacillus subtilis*, AEF was shown to alter cofactor levels and enhance acetoin production under limited aeration conditions (28). A redox imbalance was also overcome in the production of 3-hydroxypropionic acid by *Klebsiella pneumonia* by using a BES (29).

This study aimed to investigate the performance of CS4363 and its adapted version in a BES where an anode functions as the electron sink. Hence, for the two strains, growth, product formation and the efficiency of interaction between strains and anode were characterized and compared under the electrochemical cultivation conditions with endogenous or exogenous mediator.

4.3 Material and Methods

4.3.1 Strains and cultivation conditions

In this study, mutant *L. lactis* CS4363 (*L. lactis* MG1363 *Δ*^{3}*ldh Δpta ΔadhE*) (30) and *L. lactis* CS4363-F2 (*L. lactis* CS4363 adapted on ferricyanide about 600 generations) (21) were used. Cells were cultivated in a customized defined medium (SALN) (29), modified from the SA medium designed by Jensen et al (31). The changes included: i) replacing the MOPS buffer with disodium-β-glycerophosphate buffer, since MOPS buffer was found to interfere with the quantification of acetoin; ii) adding six nucleosides (20 mg/L adenosine, 20 mg/L guanosine, 20 mg/L cytidine, 20 mg/L thymidine, 20 mg/L inosine, 20 mg/L uridine) and iii) adding 2 mg/L lipoic acid (cofactor for pyruvate dehydrogenase complex) in the final recipe. Glucose was used as the sole carbon source in all experiments. SALN medium was filtered using rapid-flow^{TM} sterile disposable bottle top filter (0.2 µm pore size, Thermo Scientific, USA).

To prepare pre-cultures, a single colony from M17 agar plates (Thermo Fisher Scientific, USA) with 1% glucose was inoculated into 25 ml SALN medium with 1% glucose in 250 mL shake flasks and incubated at 30^{o}C, 150 rpm for overnight. Then 1% overnight culture was transferred into fresh SALN medium with 1% glucose. The cells were harvested by centrifugation (7000 *g*, 5 min, 20°C) when the cell density reached OD_{600} = 0.2 (log phase), and then re-suspended in fresh SALN medium with 0.5% glucose for further fermentation experiments in bioreactors.

4.3.2 Cyclic voltammetry of different media

Cyclic voltammetry (CV) tests were recorded by using a potentiostat (Autolab PGSTAT12, EcoChemie, Netherlands) in a three-electrode setup with a Ag/AgCl/KCl_{sat} as the reference electrode, a platinum wire counter electrode, and a polished glassy carbon working electrodes (GCE, diameter: 0.4 cm) respectively. CVs of M17 and SALN medium with 1% glucose were recorded with a scan rate of 5 mV/s. Dissolved oxygen was removed by bubbling argon gas through the medium before and flushing the headspace with argon throughout the measurements. Detailed figure of this setup is provided **(Fig. S4.1)**.

4.3.3 Bioelectrochemical system setup

The construction and setup of the bioelectrochemical system (BES) were as previously described (26, 32). Briefly, pre-treated carbon cloth (projected surface area of 25 cm^2) was applied as the

working electrode, and stainless steel mesh was used as the counter electrode. The potential of the working electrode was poised at 0.5 V versus Ag/AgCl/KCl_{sat} using a potentiastat (VMP3, Bio-Logic, USA). Potassium ferricyanide (Sigma-Aldrich, USA) with a final concentration of 5 mM was added to the working chamber as electron transfer mediator. Anaerobic conditions throughout the experiments were assured by bubbling the culture medium with nitrogen (20 ml/min). The volume of medium in the BES reactor was 320 mL. The BES reactors were kept at 30°C using a circulator water batch, and the electrolytes in the working chamber were mixed at 400 rpm using magnetic stirring (25 × 25 × 9 mm cross-shape stir bar). All redox potentials in this manuscript were reported against the Ag/AgCl/KCl_{sat} reference electrode, unless specified.

4.3.4 Analytics and sampling

The concentrations of glucose and other exo-metabolites (acetoin, 2,3-butanediol, formate, lactate, pyruvate) were determined by high-performance liquid chromatography (HPLC) using an Agilent Hiplex H column (300 × 7.7 mm, PL1170-6830, Santa Clara, CA, USA). 3 mM H_2SO_4 was used as the mobile phase at a flow rate of 0.4 mL/min. The temperature of the column oven was set to 60°C. Glucose, acetoin and 2,3-butanediol were quantified using an RI detector, while pyruvate, lactate and formate were read out from the UV detector at the wavelength of 210 nm. For the detection of ferricyanide, the absorbance of the supernatant was measured at 420 nm (21, 26). For calibration, 7 concentrations of ferricyanide were used and then the formula was obtained:

$$Ferricyanide\ [mM] = 1.11 \times OD_{420}$$

The samples for the above analytics were collected and centrifuged at 17,000 g, 4°C for 10 mins to remove the cell pellets. The supernatant was stored at -20°C until analyzed.

4.3.5 Calculations

The optical cell density OD_{600} was converted into the cell dry weight (CDW) according to the following formula (33):

$$CDW\ [g/L] = 0.37 \times OD_{600}$$

The yield coefficients (Y) of quantified products were determined as the slope of plots of mmol product versus mmol glucose consumed **(Fig. S4.2)**.

The carbon balance (CB) was calculated according to the formula below:

$$CB\ (\%) = {\sum_i (m_i \times n_i)_t} \Big/ {\sum_i (m_i \times n_i)_{t_0}} \times 100$$

Where m_i is the absolute quantity [mmol] of specific product i at specific time t; n_i is the carbon atom number of this product i; t_0 is the initial 0 h of inoculation. Due to the low production rate, formed CO_2 was estimated based on the stoichiometric coefficients from the respective metabolic pathway **(Fig. 4.1)** (34). The biomass formula was assumed to be $CH_{1.82}O_{0.54}N_{0.198}$ (35).

The electron balance (EB) was calculated according to the formula below:

$$EB\ (\%) = {[\sum_i (m_i \times n_i \times \gamma)_t + e_{anode-t}]} \Big/ {[\sum_i (m_i \times n_i \times \gamma)_{t_0} + e_{anode-t_0}]} \times 100$$

Where $e_{anode\text{-}t}$ is the quantity [mmol] of electrons collected on the anode at specific time t; $e_{anode\text{-}t0}$ is the quantity [mmol] of electrons collected on the anode at initial 0 h. The degree of reduction (γ) of the respective chemical with the elemental composition $C_aH_bO_cN_d$ was calculated based on the formula (36):

$$\gamma = \frac{a \times 4 + b \times 1 + c \times (-2) + d \times (-3)}{a}$$

The total turnover number (TTN) of ferricyanide was calculated based on the formula (37):

$$TTN = {e_{anode-t}} \Big/ {(m_{mediator} \times z_{mediator})}$$

Where $m_{mediator}$ is the absolute quantity of mediator ferricyanide in the system; $z_{mediator}$ is the number of electrons that can be transferred by mediator in one turnover, for ferricyanide, it is equal to 1.

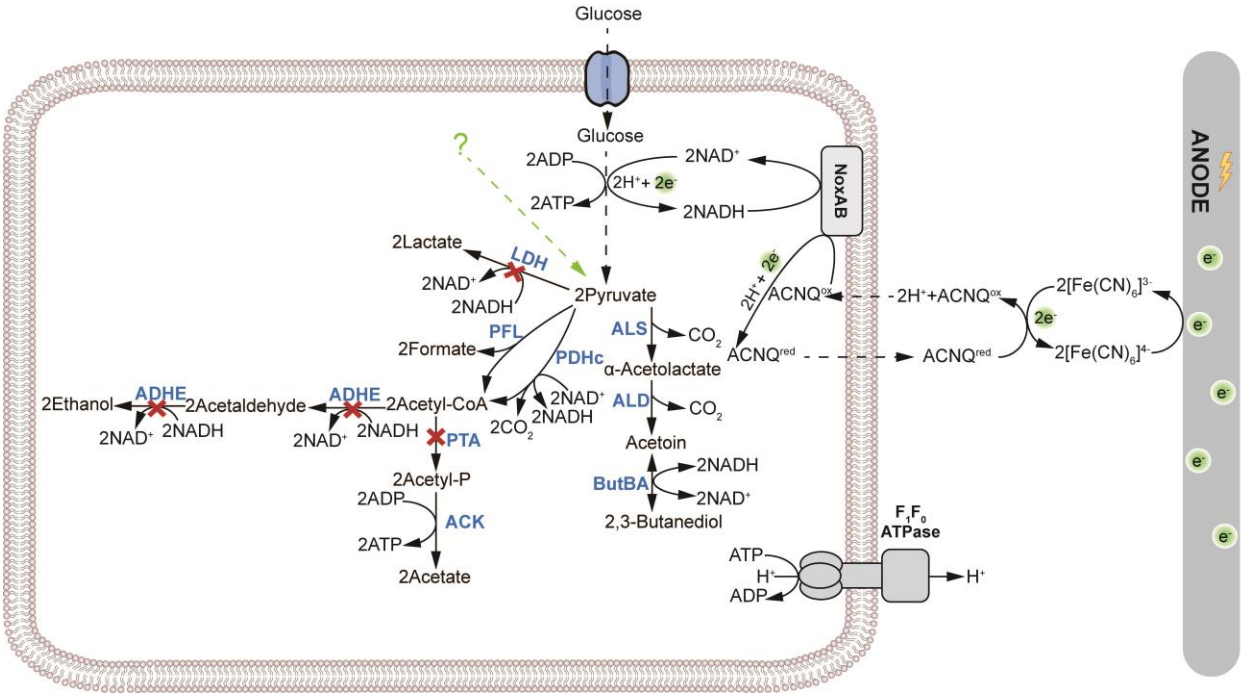

Fig. 4.1 Metabolism of *L. lactis* in anode compartment of the BES reactor. LDH: lactate dehydrogenases; ALS: α-acetolactate synthase; ALD: α-acetolactate decarboxylase; ButBA: 2, 3-butanediol dehydrogenase; PDHc: pyruvate dehydrogenase complex; PFL: pyruvate-formate lyase; ADHE: acetaldehyde dehydrogenase and alcohol dehydrogenase; PTA: phosphate acetyltransferase; ACK: acetate kinase. The red crosses indicate inactivated pathways in *L. lactis* CS4363 and CS436-F2. The light green question mark indicates possible pathway for pyruvate formation in *L. lactis* CS4363 and CS436-F2.

4.4 Results and Discussion

4.4.1 SALN is a compatible medium for BES of *L. lactis*

M17 medium with glucose is widely used for culturing *L. lactis* (38). However, an unknown oxidation event, at 0.36 V, occurred during a cyclic voltammetry testing of the blank medium **(Fig. S4.1)**. An unknown component in the GM17 medium was irreversibly oxidized at an onset potential of ca. +0.04 V. This was not observed in previous experiments, and it may be due to batch to batch variation in M17 broth. This made GM17 medium incompatible with the planned electrochemical testing.

Due to this, the GM17 medium was exchanged with the chemically defined SALN medium (39). Riboflavin has been shown to serve as a redox shuttle with a redox peak around -0.4 V vs. Ag/AgCl, and was left out as previously suggested (40). The redox background noise observed for M17 was not seen for the SALN medium **(Fig. S4.1)**.

4.4.2 Hampered glucose metabolism in the BES without the exogenous mediator

L. lactis CS4363 is partly blocked in NAD^+ regeneration, and is unable to grow under strictly anaerobic conditions without alternative electron acceptors. *L. lactis* CS4363 has been shown to be able to use the endogenous mediator 2-amino-3-carboxy-1,4-naphthoquinone (ACNQ) to transfer electrons to electron acceptors (21). Considering that *L. lactis* is an electroactive bacterium, the anode here was used as the final electron acceptor for *L. lactis* CS4363 in the BES.

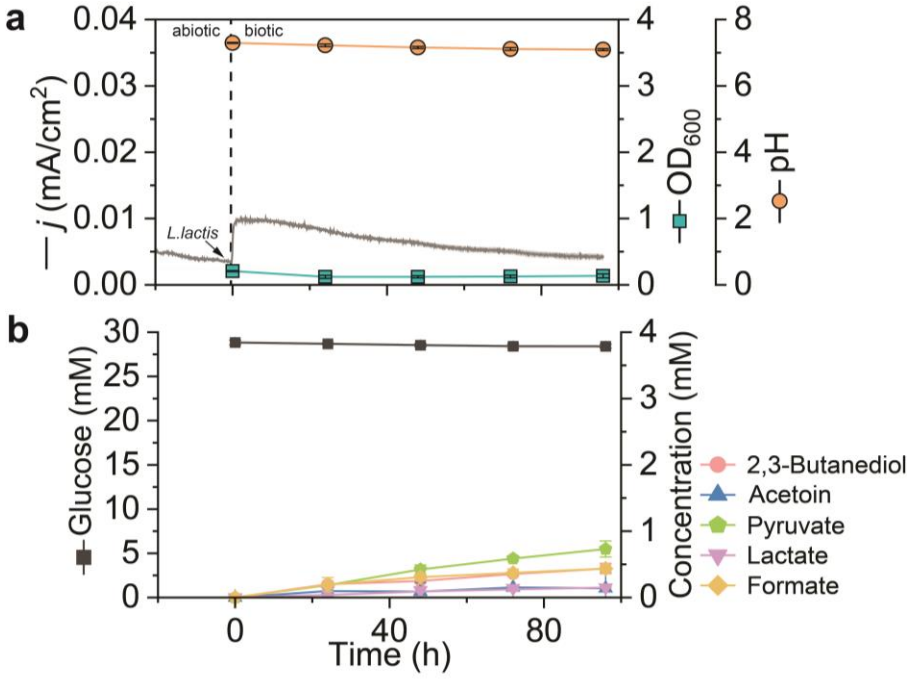

Fig. 4.2 Electrochemical activity and anoxic glucose metabolism of *L. lactis* CS4363 driven by BES. Working electrode potential was set up at 0.5 V versus Ag/AgCl. (a) Current density (*j*), pH and OD_{600}. (b) Glucose consumption and metabolic products. The presented data are the mean and standard deviations from biological replicates (N=3).

First it was tested whether CS4363 could grow in the BES without any mediators added. As shown in **Fig. 4.2a**, the max current density attained was quite low (0.0010±0.0003 mA/cm^2) and only little glucose was consumed (0.43±0.12 mM) over 90 h after inoculation. A slight drop in pH (0.20±0.02) was observed, which indicated that *L. lactis* CS4363 can transfer electrons and protons out of the cells by using an endogenous mediator, similar to the observation in the previous research when using ferricyanide (21). However, the quantity of electrons transferred to the anode was only 0.723±0.013 mmol, which was not sufficient to support the growth of CS4363. Pyruvate (0.73±0.12 mM), 2,3-butanediol (0.44±0.08 mM) and formate (0.44±0.06 mM) were main

products, and small amounts of lactate and acetoin could also be detected **(Fig. 4.2b)**. Although the genes encoding the three known lactate dehydrogenases (*ldh, ldhX, ldhB*) had been knocked out in CS4363 (30), a residual lactate dehydrogenase activity giving rise to lactate was apparently present. This could be due to some unannotated gene coding for an enzyme with lactate dehydrogenase activity, which has not been reported previously. In *L. lactis*, the pyruvate dehydrogenase complex (PDHc) is usually not active under anaerobic conditions (41), whereas the pyruvate-formate lyase (PFL) is functional and responsible for decarboxylation of pyruvate to acetyl-CoA (42). CS4363, however, normally does not accumulate formate, due to lack of phosphotransacetylase (PTA) and alcohol dehydrogenase (ADHE) activities (21), and thus it was unexpected that formate could be formed as there is no apparent sink for the acetyl-CoA generated.

4.4.3 Ferricyanide could facilitate transfer of electrons from CS4363 to an anode and thereby support its growth

In BES, electron transfer from microorganisms to the electrode is a major bottleneck (43). Since the observed interaction of CS4363 with the anode was very limited without an added mediator, 5 mM ferricyanide was added to the growth medium. A ferricyanide concentration that was 10 times lower than that used in the previous study (21) was chosen, since ferricyanide can be regenerated at the anode (26, 28, 37). To prevent accumulation of toxic HCN at low pH (44), pH was maintained >= 6 by manually adding KOH when necessary.

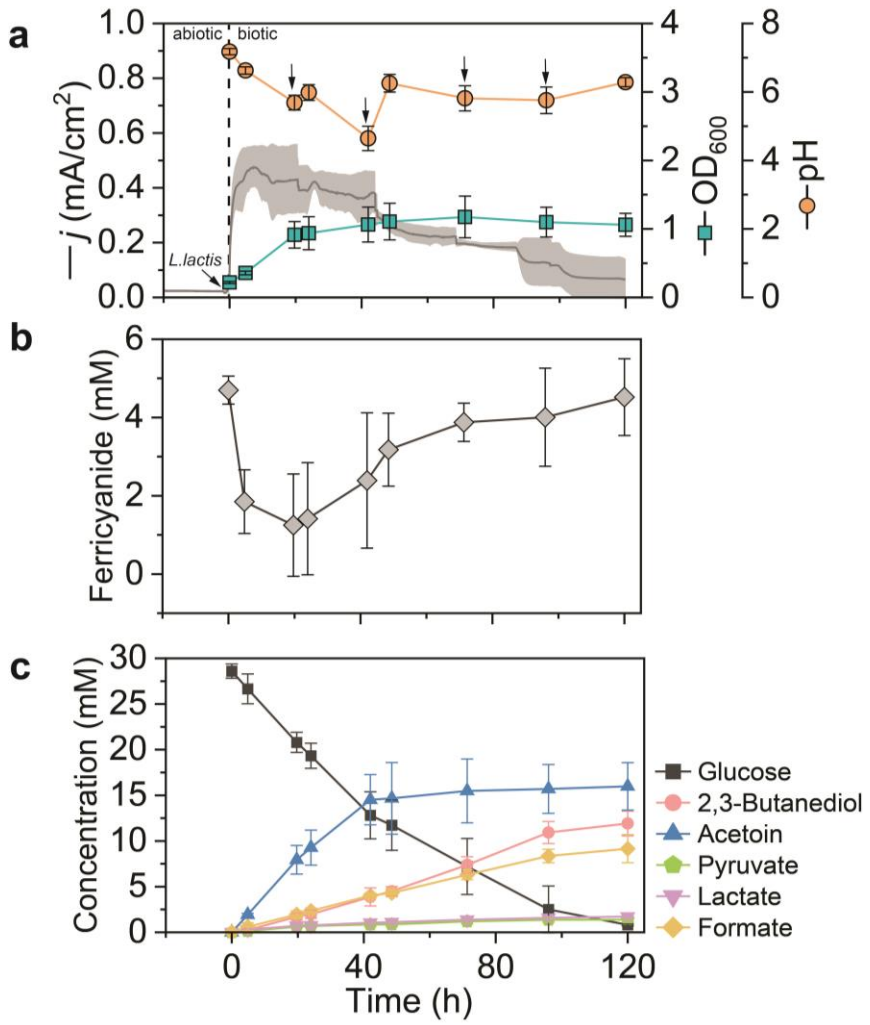

Fig. 4.3 Electrochemical activity and anoxic glucose metabolism of *L. lactis* CS4363 driven by BES with 5 mM ferricyanide as mediator. Working electrode potential was set up at 0.5 V versus Ag/AgCl. (a) Current density (*j*), pH and OD_{600}. (b) The concentration of potassium ferricyanide varies with time. (c) Glucose consumption and metabolic products. The arrows in (a) indicate the addition of 1M KOH for adjustment of pH. The presented data are the mean and standard deviations from biological replicates (N=3).

The presence of 5 mM ferricyanide had a great impact, and the current density increased to a maximum of 0.47±0.08 mA/cm^2 **(Fig. 4.3a)** and the electron formation rate was 6.979±1.096 mmol/g_{CDW}/h **(Table 4.1)**. However, when KOH was added to maintain pH, a decrease in current was observed, possibly due to an excessive inward movement of K^+ that affected the transport of the endogenous mediator ACNQ, which further affected electron transfer from ACNQ to ferricyanide. Further work is needed to verify this hypothesis. Under these conditions, the final cell density (OD_{600}) of CS4363 reached 1.06±0.17 in 120 h. After inoculation, the ferricyanide

concentration dropped quickly to below 2 mM, due to its reduction by CS4363. After growth and current density had slowed down, ferricyanide gradually was fully re-oxidized by the anode **(Fig. 4.3b)**. Using the formula proposed by Gemünde et al. (37), for calculating the total turnover number (TTN) of ferricyanide in AEF, a TTN of 18.88±0.59 was determined for CS4363, which demonstrates the reversibility of the ferricyanide redox reaction during the cultivation period. CB and EB of CS4363 exceeded 100% slightly **(Table 4.1)**. There could be two possible explanations for this: 1) the inoculated cells contained some intracellular glucose from the seed culture medium, while the measured initial glucose was only extracellular; 2) the carbon in the product came from other pathways, e.g. amino acid catabolism, which can also result in pyruvate which can be transformed into downstream metabolites (45).

Table 4.1 Key progress parameters of glucose metabolism of CS4363 and CS4363-F2

Strain	CS4363	CS4363-F2
Glucose consumed time in BES	120 h	24 h
CB (%)	112.32±2.20	104.09±2.08
EB (%)	114.48±2.75	105.73±2.36
μ_{max} (h^{-1})	0.068±0.010	0.316±0.038
$C_{x,max}$ (g_{CDW}/L)	0.44±0.11	0.59±0.08
Yields($mol_{product}/mol_{glucose}$)		
$Y_{2,3\text{-butanediol}}$	0.352±0.022	0.801±0.020
$Y_{acetoin}$	0.503±0.048	0.040±0.010
$Y_{pyruvate}$	0.041±0.003	0.012±0.003
$Y_{formate}$	0.263±0.014	0.118±0.017
$Y_{lactate}$	0.047±0.002	0.060±0.005
$Y_{electrons}$	3.234±0.076	2.083±0.070
Rates($mmol/g_{CDW}/h$)		
$r_{glucose}$	2.246±0.460	9.603±2.228

$r_{2,3\text{-butanediol}}$	0.457±0.069	5.714±0.970
$r_{acetoin}$	2.024±0.322	0.501±0.156
$r_{pyruvate}$	0.149±0.028	0.528±0.070
$r_{formate}$	0.421±0.125	0.776±0.300
$r_{lactate}$	0.155±0.041	0.784±0.168
$r_{electrons}$	6.979±1.096	11.471±1.711

The detailed calculation of yield by linear fitting and rates of glucose consumption and other products formation were determined **(Fig. S4.2, Fig. S4.3, Fig. S4.4)**.

The 0.5% glucose initially present was fully depleted in 120 h and the glucose consumption rate was 2.246±0.460 mmol/g_{CDW}/h **(Table 4.1)**, giving rise to a mixture of mainly acetoin, 2,3-butanediol, and formate. Small amounts of lactate and pyruvate were formed as well. Acetoin was the dominant metabolic product, which is consistent with the previous findings where ferricyanide was used as the final electron acceptor (21), and the yield for acetoin was 0.503±0.048 $mol_{product}/mol_{glucose}$ **(Fig. 4.3c)**. The final concentration of acetoin and 2,3-butanediol reached 15.98±2.60 mM and 11.91±1.35 mM, respectively. The product distribution in the presence of ferricyanide was different from when it was absent, e.g. pyruvate no longer accumulated in significant amounts, and was converted to downstream metabolites. Overall, the NADH generated in glycolysis could be re-oxidized by an anode in the presence of ferricyanide as electron mediator, thereby establishing the redox balance necessary to sustain metabolism, which is a basic requirement for living cells (46). CS4363 was found to donated more electrons in the BES setup (666.87±16.25 mM) as compared to CS4363 was grown under non-BES condition (345.66±13.19 mM) (21), which could also been seen from the glucose consumption. However, the growth rate in BES was 0.068±0.010 h^{-1} **(Table 4.1)**, i.e. significantly lower than non-BES condition (μ_{max}=0.419 ± 0.006 h^{-1}) (21). The faster growth under non-BES conditions can be explained by differences in medium and cultivation conditions since non-BES experiments were carried out in rich M17 medium with higher nutritional content and the growth condition was not completely anaerobic. Besides, it seems that electron transfer to the electrode limits growth in the current BES setup. There could be two explanations for this. Either ferricyanide was regenerated too slowly by

the anode, or perhaps the reduced ferricyanide concentration hampered electron transfer between the cell and ferricyanide. The latter phenomenon appears to be the case as next results demonstrate.

4.4.4 Enhancing capacity for ferricyanide respiration enhances performance in the BES

In the previous research, CS4363 was adaptively evolved to enhance its capacity for EET with ferricyanide, and one of the mutants obtained was CS4363-F2. CS4363-F2 was further characterized by using the same BES setup. In the absence of ferricyanide, CS4363-F2 grew poorly and only metabolized little glucose **(Fig. 4.4a)**, although glucose consumption increased approximately by a factor 3 to 1.61±0.35 mM and the pH drop was more significant (0.48±0.15) than for CS4363. Another difference between the two strains was that the dominant fermentation product was 2,3-butanediol (1.35±0.31 mM) rather than pyruvate **(Fig. 4.4b)**, findings that are partly consistent with previous results (21).

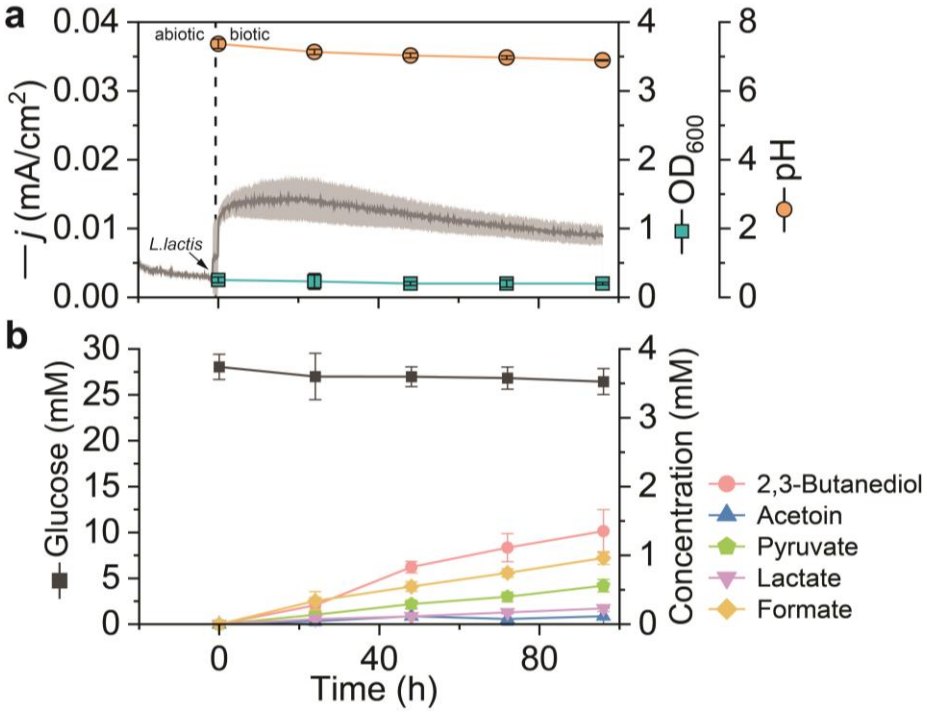

Fig. 4.4 Electrochemical activity and anoxic glucose metabolism of mutant *L. lactis* CS4363-F2 driven by BES. Working electrode potential was set up at 0.5 V versus Ag/AgCl. (a) Current density (*j*), pH and OD_{600}. (b) Glucose consumption and metabolic products. The presented data are the mean and standard deviations from biological replicates (N=3).

In the presence of 5 mM ferricyanide the situation, however, changed radically. As shown in **Fig. 4.5a**, the current density increased to 0.81±0.05 mA/cm^2 (equivalent to 20.25 mA), which was about twice that observed for CS4363, and record high when compared to current densities reported by others **(Table S4.1)**. Besides, CS4363-F2 also displayed enhanced electron formation rate (11.471±1.711 mmol/g_{CDW}/h) in comparison to CS4363, which demonstrated that this mutant had enhanced electron transfer ability.

The time needed for CS4363-F2 to reach the stationary phase was shortened to 24 h, half of the time needed for CS4363. The final OD_{600} reached 1.45±0.33 **(Fig. 4.5a)** and the growth rate increased to 0.316±0.038 h^{-1} **(Table 4.1)**. The maximum CDW also increased to 0.59±0.08 g_{CDW}/L, while the maximum CDW of CS4363 was 0.44±0.11 g_{CDW}/L. CS4363-F2, almost immediately, depleted ferricyanide within 3 hours after inoculation, which illustrates the superior ability of CS4363-F2 to respire with ferricyanide **(Fig. 4.5b)**. Thus, enhancing the capacity for EET with ferricyanide, greatly enhances ability for anodic electro-fermentation. After the cessation of growth after 24 h, the concentration of ferricyanide gradually increased to the initial 5 mM and was fully regenerated at 120 h **(Fig. 4.5b)**.

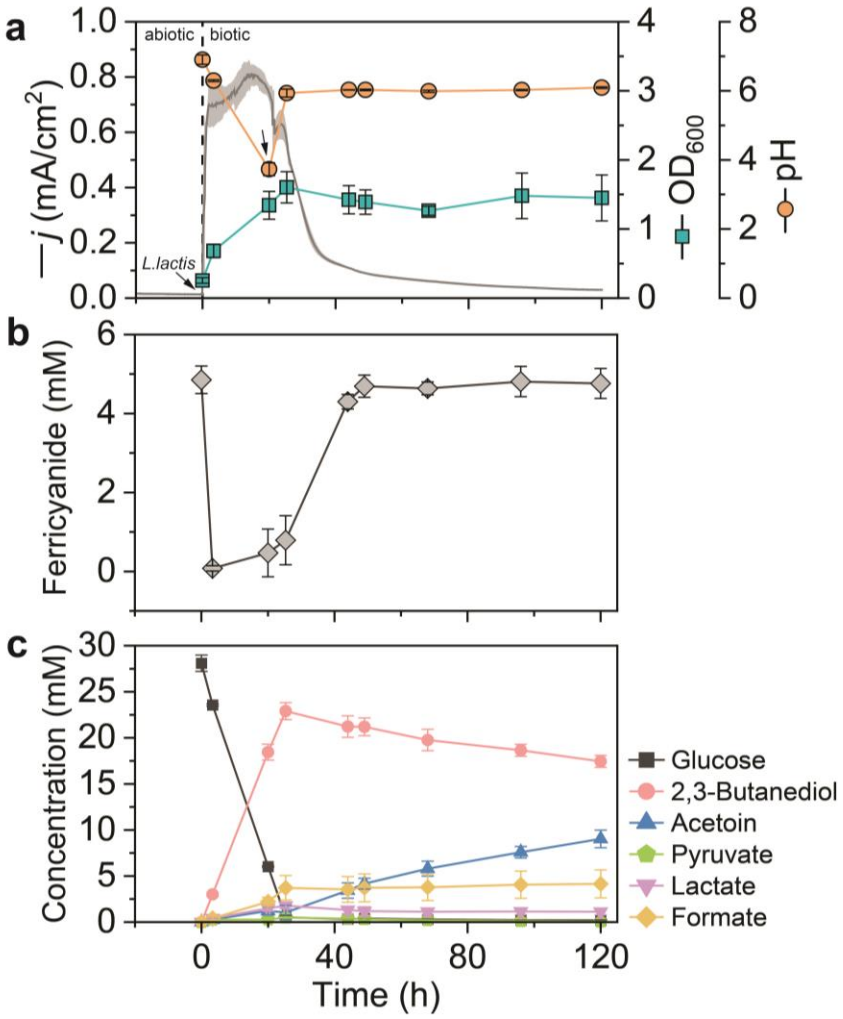

Fig. 4.5 Electrochemical activity and anoxic glucose metabolism of mutant L. lactis CS4363-F2 driven by BES with 5 mM ferricyanide as mediator. Working electrode potential was set up at 0.5 V versus Ag/AgCl. (a) Current density (j), pH and OD_{600}. (b) The concentration of potassium ferricyanide varies with time. (c) Glucose consumption and metabolic products. The arrow in (a) indicates the addition of 1M KOH for adjustment of pH. The presented data are the mean and standard deviations from biological replicates (N=3).

For CS4363-F2, the time needed to deplete glucose was less than 24 h, as compared to 120 h for CS4363. The glucose consumption rate was increased to 9.603±2.228 mmol/g_{CDW}/h. In contrast to what was observed for CS4363, CS4363-F2 mostly converted glucose into 2,3-butanediol (22.90±0.92 mM) and only small amounts of acetoin were generated, 1.04±0.78 mM at 24 h **(Fig. 4.5c)**. The amount of 2,3-butanediol generated was similar to that under non-BES condition (21), while biomass only required half. In CS4363-F2, the *butBA* operon, encoding the 2,3-butanediol dehydrogenase, has been massively amplified (21), and this had an impact on the yield of 2,3-

butanediol which reached 0.801±0.020 $mol_{product}/mol_{glucose}$, which was around twice as much as formed by CS4363 (0.352±0.022 $mol_{product}/mol_{glucose}$). In addition, 2,3-butanediol was formed 12.5 times faster by CS4363-F2 (5.714±0.970 $mmol/g_{CDW}/h$) than by CS4363 (0.457±0.069 $mmol/g_{CDW}/h$). For acetoin, the yield for CS4363 reached 0.503±0.048 $mol_{product}/mol_{glucose}$, whereas the yield for CS4363-F2 only was 0.040±0.010 $mol_{product}/mol_{glucose}$ **(Table 4.1)**.

After 24 h, growth ceased due to glucose depletion. An interesting finding was that after cells had entered the stationary phase, 2,3-butanediol was gradually reduced into acetoin. Thus the anode facilitated biotransformation by non-growing cells, where the 2,3-butanediol dehydrogenase functioned in the reverse orientation, generating acetoin and NADH, where the latter was oxidized back to NAD^+ by EET to ferricyanide, thereby funneling additional electrons to the anode.

4.5 Conclusion

This is the first study describing the potential of anode-assisted electro-fermentation of growing *L. lactis*. In an anodic BES setup, growth profile and product composition of NAD^+ regeneration-blocked *L. lactis* strains vary with electron mediator ferricyanide presence or not. The ALE strain CS4363-F2 displays remarkable performance in a BES setup, achieving record high current densities not previously observed, indicating it is possible to enhance the capacity for AEF by adapting the microorganism to respire better with ferricyanide. CS4363-F2 is also proved to be an efficient cell factory for producing the bulk chemical 2,3-butanediol in BES setup.

4.6 References

1. Kirsop BH. 1974. Oxygen in brewery fermentation. J Inst Brew 80:252–259.

2. Pedersen MB, Gaudu P, Lechardeur D, Petit M-A, Gruss A. 2012. Aerobic respiration metabolism in lactic acid bacteria and uses in biotechnology. Annu Rev Food Sci Technol 3:37–58.

3. Koebmann B, Blank LM, Solem C, Petranovic D, Nielsen LK, Jensen PR. 2008. Increased biomass yield of *Lactococcus lactis* during energetically limited growth and respiratory conditions. Biotechnol Appl Biochem 50:25–33.

4. Suttikul S, Charalampopoulos D, Chatzifragkou A. 2023. Biotechnological production of optically pure 2,3-butanediol by *Bacillus subtilis* based on dissolved oxygen control strategy. Fermentation 9:15.

5. Doran PM. 1995. 9 - Mass Transfer, p. 190–217. *In* Doran, PM (ed.), Bioprocess Engineering Principles. Academic Press, London.

6. Lv PJ, Qiang S, Liu L, Hu CY, Meng YH. 2020. Dissolved-oxygen feedback control fermentation for enhancing β-carotene in engineered *Yarrowia lipolytica*. Sci Rep 10:17114.

7. Garcia-Ochoa F, Gomez E. 2009. Bioreactor scale-up and oxygen transfer rate in microbial processes: An overview. Biotechnol Adv 27:153–176.

8. Delvigne F, Lecomte J. 2010. Foam formation and control in bioreactors, p. 1–13. *In* Encyclopedia of Industrial Biotechnology. John Wiley & Sons, Ltd.

9. Gibson BR, Lawrence SJ, Boulton CA, Box WG, Graham NS, Linforth RST, Smart KA. 2008. The oxidative stress response of a lager brewing yeast strain during industrial propagation and fermentation. FEMS Yeast Res 8:574–585.

10. Cesselin B, Derré-Bobillot A, Fernandez A, Lamberet G, Lechardeur D, Yamamoto Y, Pedersen MB, Garrigues C, Gruss A, Gaudu P. 2011. Responses of lactic acid bacteria to oxidative stress, p. 111–127. *In* Tsakalidou, E, Papadimitriou, K (eds.), Stress Responses of Lactic Acid Bacteria. Springer US, Boston, MA.

11. Li Q, Bai Z, O'Donnell A, Harvey LM, Hoskisson PA, McNeil B. 2011. Oxidative stress in fungal fermentation processes: the roles of alternative respiration. Biotechnol Lett 33:457–467.

12. Zhao G, Liu J, Zhao J, Dorau R, Jensen PR, Solem C. 2021. Efficient production of nisin A from low-value dairy side streams using a nonengineered dairy *Lactococcus lactis* strain with low lactate dehydrogenase activity. J Agric Food Chem 69:2826–2835.

13. Liu J-M, Chen L, Dorau R, Lillevang SK, Jensen PR, Solem C. 2020. From waste to taste—efficient production of the butter aroma compound acetoin from low-value dairy side streams using a natural (nonengineered) *Lactococcus lactis* dairy isolate. J Agric Food Chem 68:5891–5899.

14. Sybesma W, Burgess C, Starrenburg M, Sinderen D van, Hugenholtz J. 2004. Multivitamin production in *Lactococcus lactis* using metabolic engineering. Metab Eng 6:109–115.

15. Sano A, Takatera M, Kawai M, Ichinose R, Yamasaki-Yashiki S, Katakura Y. 2020. Suppression of lactate production by aerobic fed-batch cultures of *Lactococcus lactis*. J Biosci Bioeng 130:402–408.

16. Lopez de Felipe F, Kleerebezem M, de Vos WM, Hugenholtz J. 1998. Cofactor engineering: a novel approach to metabolic engineering in *Lactococcus lactis* by controlled expression of NADH oxidase. J Bacteriol 180:3804–3808.

17. Rezaïki L, Cesselin B, Yamamoto Y, Vido K, Van West E, Gaudu P, Gruss A. 2004. Respiration metabolism reduces oxidative and acid stress to improve long-term survival of *Lactococcus lactis*. Mol Microbiol 53:1331–1342.

18. Duwat P, Sourice S, Cesselin B, Lamberet G, Vido K, Gaudu P, Le Loir Y, Violet F, Loubière P, Gruss A. 2001. Respiration capacity of the fermenting bacterium *Lactococcus lactis* and its positive effects on growth and survival. J Bacteriol 183:4509–4516.

19. Lechardeur D, Cesselin B, Fernandez A, Lamberet G, Garrigues C, Pedersen M, Gaudu P, Gruss A. 2011. Using heme as an energy boost for lactic acid bacteria. Curr Opin Biotechnol 22:143–149.

20. Nordkvist M, Jensen NBS, Villadsen J. 2003. Glucose metabolism in *Lactococcus lactis* MG1363 under different aeration conditions: requirement of acetate to sustain growth under microaerobic conditions. Appl Environ Microbiol 69:3462–3468.

21. Gu L, Xiao X, Zhao G, Kempen P, Zhao S, Liu J, Lee SY, Solem C. 2023. Rewiring the respiratory pathway of *Lactococcus lactis* to enhance extracellular electron transfer. Microb Biotechnol 16:1277–1292.

22. Virdis B, D. Hoelzle R, Marchetti A, Boto ST, Rosenbaum MA, Blasco-Gómez R, Puig S, Freguia S, Villano M. 2022. Electro-fermentation: Sustainable bioproductions steered by electricity. Biotechnol Adv 59:107950.

23. Moscoviz R, Toledo-Alarcón J, Trably E, Bernet N. 2016. Electro-fermentation: How to drive fermentation using electrochemical systems. Trends Biotechnol 34:856–865.

24. Vassilev I, Averesch NJH, Ledezma P, Kokko M. 2021. Anodic electro-fermentation: Empowering anaerobic production processes via anodic respiration. Biotechnol Adv 48:107728.

25. Gong Z, Yu H, Zhang J, Li F, Song H. 2020. Microbial electro-fermentation for synthesis of chemicals and biofuels driven by bi-directional extracellular electron transfer. Synth Syst Biotechnol 5:304–313.

26. Lai B, Yu S, Bernhardt PV, Rabaey K, Virdis B, Krömer JO. 2016. Anoxic metabolism and biochemical production in *Pseudomonas putida* F1 driven by a bioelectrochemical system. Biotechnol Biofuels 9:39.

27. Vassilev I, Gießelmann G, Schwechheimer SK, Wittmann C, Virdis B, Krömer JO. 2018. Anodic electro-fermentation: Anaerobic production of L-Lysine by recombinant *Corynebacterium glutamicum*. Biotechnol Bioeng 115:1499–1508.

28. Sun Y, Kokko M, Vassilev I. 2023. Anode-assisted electro-fermentation with *Bacillus subtilis* under oxygen-limited conditions. Biotechnol Biofuels Bioprod 16:6.

29. Kim C, Kim MY, Michie I, Jeon B-H, Premier GC, Park S, Kim JR. 2017. Anodic electro-fermentation of 3-hydroxypropionic acid from glycerol by recombinant *Klebsiella pneumoniae* L17 in a bioelectrochemical system. Biotechnol Biofuels 10:199.

30. Solem C, Dehli T, Jensen PR. 2013. Rewiring *Lactococcus lactis* for ethanol production. Appl Environ Microbiol 79:2512–2518.

31. Jensen PR, Hammer K. 1993. Minimal requirements for exponential growth of *Lactococcus lactis*. Appl Environ Microbiol 59:4363–4366.

32. Lai B, Nguyen AV, Krömer JO. 2019. Characterizing the anoxic phenotype of *Pseudomonas putida* using a bioelectrochemical system. Methods Protoc 2:26.

33. Lan CQ, Oddone G, Mills DA, Block DE. 2006. Kinetics of *Lactococcus lactis* growth and metabolite formation under aerobic and anaerobic conditions in the presence or absence of hemin. Biotechnol Bioeng 95:1070–1080.

34. Yu S, Lai B, Plan MR, Hodson MP, Lestari EA, Song H, Krömer JO. 2018. Improved performance of *Pseudomonas putida* in a bioelectrochemical system through overexpression of periplasmic glucose dehydrogenase. Biotechnol Bioeng 115:145–155.

35. Novák L, Loubiere P. 2000. The metabolic network of *Lactococcus lactis*: distribution of 14C-labeled substrates between catabolic and anabolic pathways. J Bacteriol 182:1136–1143.

36. Stephanopoulos G, Aristidou AA, Nielsen J. 1998. Metabolic Engineering: principles and methodologies. Elsevier.

37. Gemünde A, Gail J, Holtmann D. 2023. Anodic respiration of *Vibrio natriegens* in a bioelectrochemical system. ChemSusChem 1–8.

38. Terzaghi BE, Sandine WE. 1975. Improved medium for lactic streptococci and their bacteriophages. Appl Environ Microbiol 29:807–813.

39. Solem C, Koebmann B, Yang F, Jensen PR. 2007. The las enzymes control pyruvate metabolism in *Lactococcus lactis* during growth on maltose. J Bacteriol 189:6727–6730.

40. Masuda M, Freguia S, Wang Y-F, Tsujimura S, Kano K. 2010. Flavins contained in yeast extract are exploited for anodic electron transfer by *Lactococcus lactis*. Bioelectrochemistry 78:173–175.

41. Snoep JL, de Graef MR, Westphal AH, de Kok A, Joost Teixeira de Mattos M, Neijssel OM. 1993. Differences in sensitivity to NADH of purified pyruvate dehydrogenase complexes of *Enterococcus faecalis*, *Lactococcus lactis*, *Azotobacter vinelandii* and *Escherichia coli*: Implications for their activity in vivo. FEMS Microbiol Lett 114:279–283.

42. Cocaign-Bousquet M, Even S, Lindley ND, Loubière P. 2002. Anaerobic sugar catabolism in *Lactococcus lactis*: genetic regulation and enzyme control over pathway flux. Appl Microbiol Biotechnol 60:24–32.

43. Vielstich W, Lamm A, A. Gasteiger H. 2003. Handbook of fuel cells: fundamentals, technology, applications, 4 volume set. John Wiley & Sons.

44. Husmann S, Zarbin AJG, Dryfe RAW. 2020. High-performance aqueous rechargeable potassium batteries prepared via interfacial synthesis of a Prussian blue-carbon nanotube composite. Electrochimica Acta 349:136243.

45. Le Bars D, Yvon M. 2008. Formation of diacetyl and acetoin by *Lactococcus lactis* via aspartate catabolism. J Appl Microbiol 104:171–177.

46. Chen X, Li S, Liu L. 2014. Engineering redox balance through cofactor systems. Trends Biotechnol 32:337–343.

4.7 Supplementary materials

Table S4.1 Comparison of current density of different organisms in anode-assisted electro-fermentation

Organism	Current density/Current	Condition	Publish time
Pseudomonas putida KT2440/644D-*gcd*	0.12 mA/cm^2	anaerobic	2018
Pseudomonas putida F1	0.066 mA	anaerobic	2016
Bacillus subtilis 168 trpC xyl$^+$	0.17 mA/cm^2	limited aeration	2023
Corynebacterium glutamicum lysC	89.5 μA/cm^2	anaerobic	2018
Klebsiella pneumoniae (L17K)	~3.6 mA	anaerobic	2017
Lactiplantibacillus plantarum NCIMB8826	225 μA/cm^2	anaerobic	2022
Escherichia coli cymAmtr$^{0.18}$	~100 μA/cm^2	anaerobic	2016
Ralstonia eutropha H16	~6 μA/cm^2	anaerobic	2014
Vibrio natriegens DSM 759	196 μA/cm^2	anaerobic	2023
L. lactis CS4363	**0.47 mA/cm^2**	anaerobic	this study
L. lactis CS4363-F2	**0.81 mA/cm^2**	anaerobic	this study

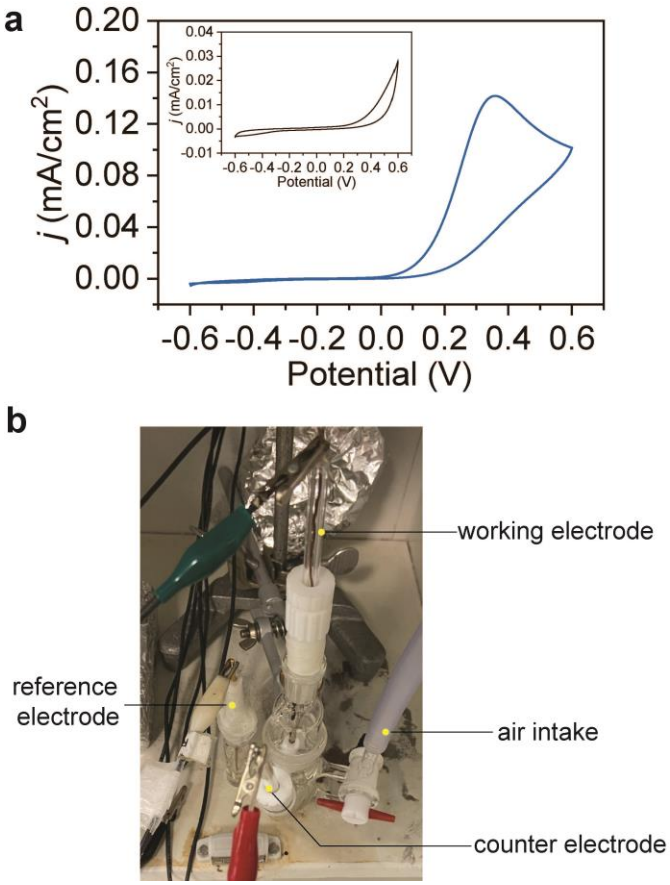

Fig. S4.1 Cyclic voltammograms of different medium. (a) M17 medium and SALN medium with 1% glucose (left top). (b) The picture of three-electrode electrochemical cell. The scan range was from -0.6 V to 0.6 V with a scan rate of 5 mV/s. The testing volume of medium was 15 ml.

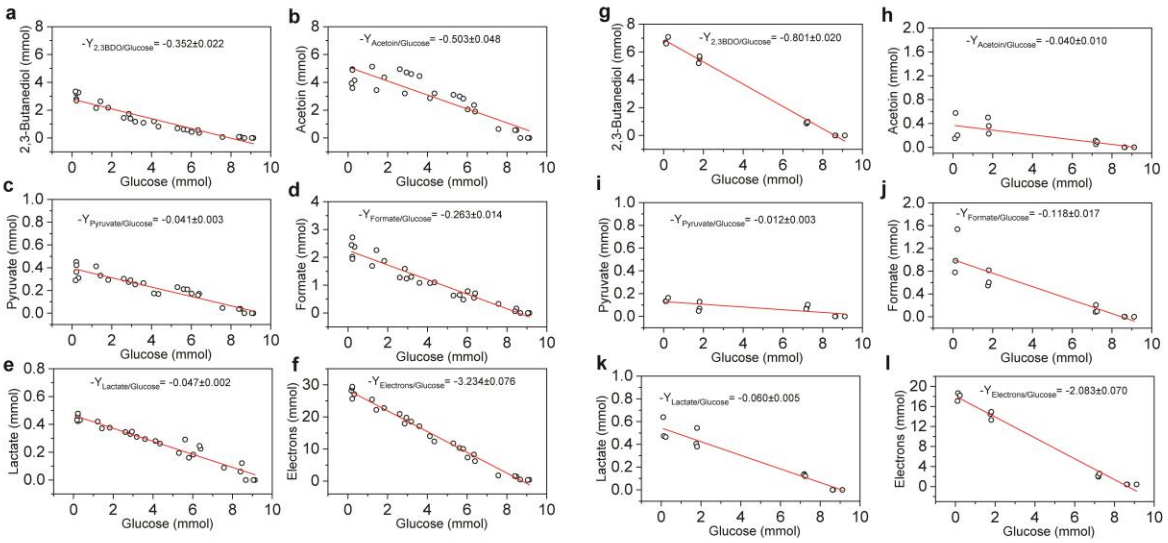

Fig. S4.2 Regression analysis for the determination of different product/glucose yield coefficients for *L. lactis* CS4363 and ALE mutant *L. lactis* CS4363-F2 in BES. The slope of fitted line is the yield coefficient for *L. lactis* CS4363: (a) 2, 3-Butanediol. (b) Acetoin. (c) Pyruvate. (d) Formate. (e) Lactate. (f) Electrons. Three biologic replicates with a total of 27 samples were used for analysis of *L. lactis* CS4363. R^2: 2, 3-butanediol, 0.912; acetoin, 0.816; pyruvate, 0.898; formate, 0.936; lactate, 0.941; electrons, 0.986. The slope of fitted line is the yield coefficient for ALE mutant *L. lactis* CS4363-F2: (g) 2, 3-Butanediol. (h) Acetoin. (i) Pyruvate. (j) Formate. (k) Lactate. (l) Electrons. Three biologic replicates with a total of 12 samples were used for analysis of ALE mutant *L. lactis* CS4363-F2. R^2: 2, 3-butanediol, 0.994; acetoin, 0.598; pyruvate, 0.616; formate, 0.822; lactate, 0.938; electrons, 0.989. Origin 2022 was used for analysis.

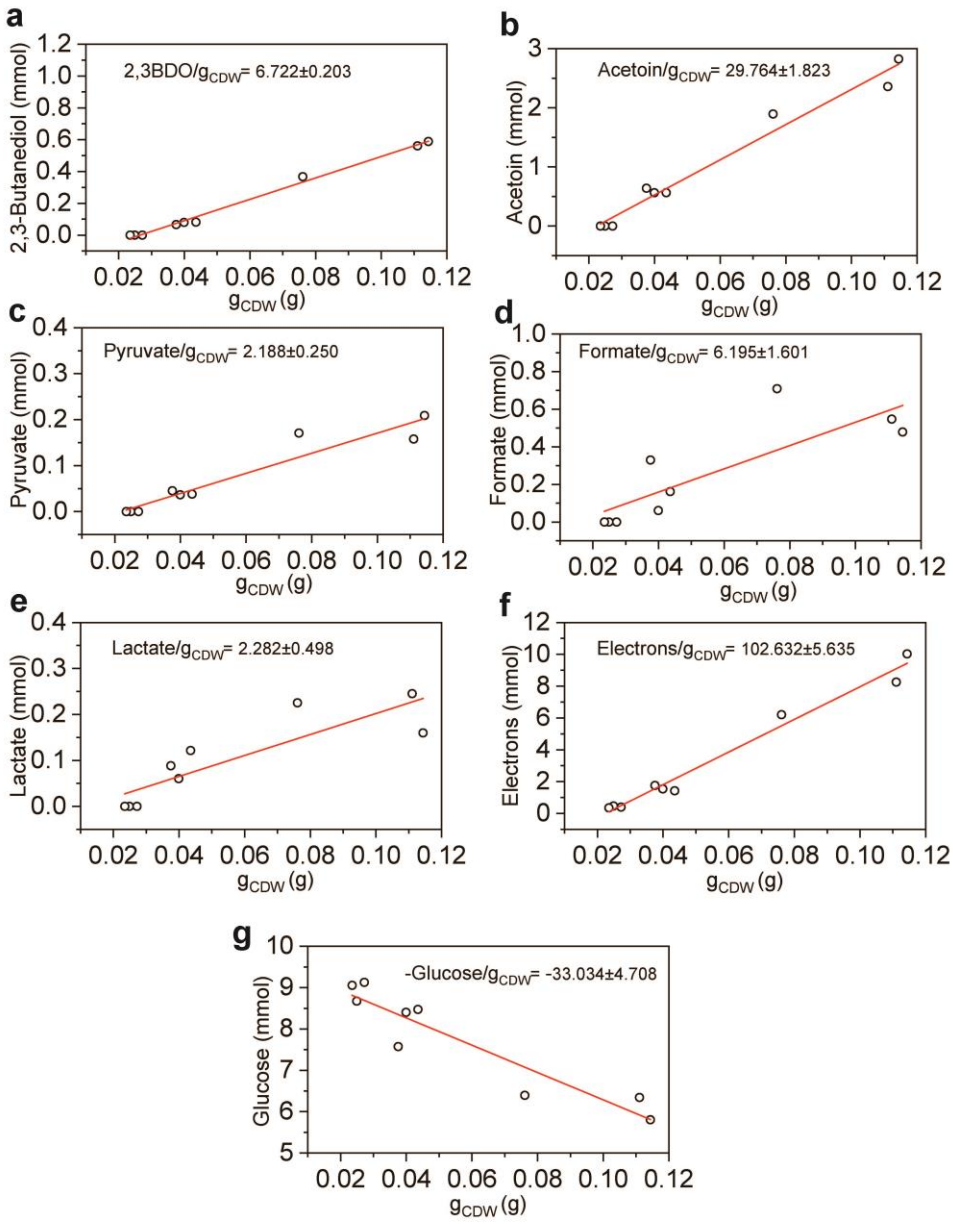

Fig. S4.3 Regression analysis for the determination of different metabolite/biomass coefficients during exponential growth phase for *L. lactis* CS4363 in BES. The rate (mmol/g_{CDW}/h) is obtained by multiplying the slope of the fitted line and the growth rate μ_{max}. (a) 2, 3-Butanediol. (b) Acetoin. (c) Pyruvate. (d) Formate. (e) Lactate. (f) Electrons. (g) Glucose. Origin 2022 was used for analysis. Three biologic replicates with a total of 9 samples were used for analysis. R^2: 2, 3-butanediol, 0.994; acetoin, 0.974; pyruvate, 0.916; formate, 0.681; lactate, 0.750; electrons, 0.979; glucose, 0.876.

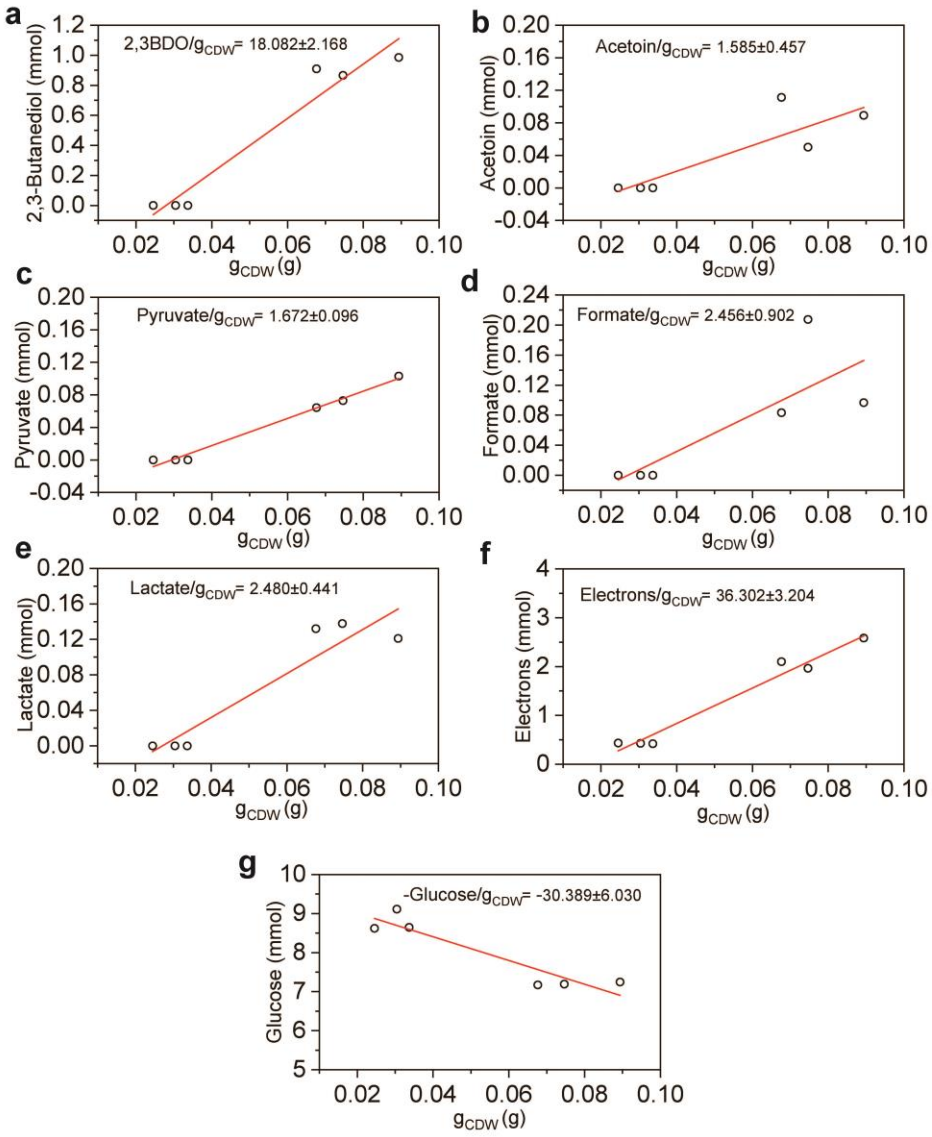

Fig. S4.4 Regression analysis for the determination of different metabolite/biomass coefficients during exponential growth phase for ALE mutant *L. lactis* CS4363-F2 in BES. The rate (mmol/g_{CDW}/h) is obtained by multiplying the slope of the fitted line and the growth rate μ_{max}. (a) 2, 3-Butanediol. (b) Acetoin. (c) Pyruvate. (d) Formate. (e) Lactate. (f) Electrons. (g) Glucose. Origin 2022 was used for analysis. Three biologic replicates with a total of 6 samples were used for analysis. R^2: 2, 3-butanediol, 0.946; acetoin, 0.750; pyruvate, 0.987; formate, 0.649; lactate, 0.888; electrons, 0.970; glucose, 0.863.

CHAPTER 5. Conclusions and Future directions

In the present study, we have focused on the two aspects of EET of *L. lactis*: fundamentals and applications. A *L. lactis* mutant CS4363 blocked in NAD^+ regeneration, which cannot grow without oxygen, was the research object in this study. We figured out the following questions:

1) Can the extracellular electron acceptor ferricyanide replace oxygen to support the growth of CS4363 and its impact?

In this study, ferricyanide was proven to support the growth of CS4363 for the first time because NADH produced by glycolysis can be re-oxidized by EET with acetoin as the main fermentation product. The growth-stimulating effect increased and the pH dropped with ferricyanide concentration, which was directly related to the ratio of intracellular NADH/NAD^+. With ferricyanide, CS4363 showed strong acid tolerance as it can grow at a pH as low as 3.72. Besides, the cell morphology became more rod-shaped.

2) What is the EET pathway in *L. lactis*?

The NADH dehydrogenase and quinone derivate ACNQ were verified to be important in the EET pathway. The 2 mol NADH produced by glycolysis firstly re-oxidized to 2 mol NAD^+ by NADH dehydrogenase, then released 2 mol electrons and 2 mol protons were transferred to ACNQ, an electron mediator. Due to its biphasic partition properties and ability to diffuse rapidly, ACNQ can shuttle inside and outside cells. The reduced ACNQ can subsequently be re-oxidized by 2 mol ferricyanide in a non-enzymatic manner. 2 mol electrons were transferred to ferrocyanide and 2 mol protons were released in the outside of cells. Besides, we found the DMK analog menadione can also serve as an electron carrier to restore the EET ability of the ACNQ-blocked mutant.

3) How to enhance EET capacity and the underlying mechanism in metabolism of enhanced EET capacity?

Adaptive laboratory evolution can be successfully applied for the enhancement of EET ability (related to cell growth), obtaining a fast-growing isolate CS4363-F2. Two mutations were found on genome of CS4363-F2, one was the insertion of the transposable element IS*905* in the coding region of menaquinone biosynthesis gene *menA* and another was the SNV (T-73G) in the promoter region of one NADH dehydrogenase encoded by *noxB*. The knock-out of *menA* improved the EET

ability, proving that the insertion of IS*905* can inactive *menA* and result in the accumulation of electron mediator ACNQ. The SNV (T-73G) was found in -35 region of *noxB* promoter and also in the regulator CcpA binding motifs *cre* sites. This mutation can alleviate the repression of CcpA on the promoter and increase the expression of *noxB*, which was later demonstrated to encode a novel type-II NADH dehydrogenase in EET and widely distributed in gut microbiota. In CS4363-F2, at the transcriptional level, amino acid and nucleotide metabolism changed significantly. The histidine metabolism, pyrimidine metabolism, valine metabolism, isoleucine metabolism and glutamate metabolism were upregulated, while arginine metabolism and purine metabolism were downregulated. These metabolic changes were mainly related to acid stress caused by pH decrease and changes in cell morphology.

4) How do CS4363 and its adapted version perform in anodic electro-fermentation using a non-consumable anode as an electron acceptor?

CS4363 and its adapted version CS4363-F2 cannot grow in BES setup if only reply on endogenous electron mediator ACNQ to transfer electrons to the anode. Electron transfer from cells to the electrode was a major bottleneck and the addition of small amount of ferricyanide can alleviate this problem. Unlike above where we used ferricyanide as the electron acceptor, here it acted as mediator and it can be regenerated at the anode. Both strains grew efficiently, however, the ALE strain CS4363-F2 grew significantly faster. Where CS4363 mainly produced acetoin, CS4363-F2 almost exclusively produced 2,3-butanediol (0.801±0.020 $mol_{product}/mol_{glucose}$). CS4363-F2 interacted efficiently with the anode, resulting in an unusually high electron formation rate (11.471±1.711 mmol/gCDW/h) and the maximum current density was 0.809±0.051 mA/cm^2. The time needed for consuming glucose was reduced from 120 h for CS4363 to 24 h for CS4363-F2.

Based on current results, future work can be conducted in the following aspects:

1) Testing non-GMO strain for EET

Here, we used a GMO *L. lactis* CS4363 blocked in NAD^+ regeneration for the research. However, GMOs are usually unaccepted by the food industry. Therefore, to achieve the same performance as CS4363, we can use slowly metabolized sugar in wild-type for lower LDH activity or inactive LDH by mutagenesis for EET research.

2) Combining protein engineering and metabolic engineering to enhance EET

If *L. lactis* is used as a cell factory for the production of important chemicals rather than used in the food industry, genetic engineering can be conducted for *L. lactis*. Protein engineering, e.g. rational protein design and directed evolution, can be used to enhance the activity of NoxB. The concentration of mediator ACNQ can be increased by metabolic engineering methods.

3) Reducing the cost of medium for AEF

In AEF, we used chemically defined medium SALN which was complicated. We can further minimize the medium composition. Meanwhile, we can use dairy waste, e.g. mother liquor, to test whether EET can still work. Considering that lactose is rich in mother liquor, plasmid pLP71, encoding genes for lactose utilization can be transferred into CS4363.

Appendix A. The list of differentially expressed genes after EET enhancement

gene_name	log_2FC	adj.P.Val	old_locus_tag	UniProtKB AC	Change
NAD(P)/FAD-dependent oxidoreductase CDS	3.563238175	8.93E-147	llmg_1734	A2RLY0	UP
haloacid dehalogenase type II CDS	3.121065906	1.23E-100	llmg_0254	A2RHX2	UP
ring-cleaving dioxygenase CDS	3.046081101	2.11E-95	llmg_0096	A2RHG7	UP
nifJ CDS	2.698454779	5.74E-93	llmg_0447	A2RIF6	UP
flavin reductase family protein CDS	2.944150261	3.79E-80	llmg_0097	A2RHG8	UP
dhaQ CDS	2.087367228	1.24E-74	llmg_0255	A2RHX3	UP
PTS lactose/cellobiose transporter subunit IIA CDS	2.844424482	3.21E-71	llmg_0438	A2RIE7	UP
alpha/beta hydrolase CDS	3.02544029	2.43E-68	llmg_0095	A2RHG6	UP
guaB CDS	1.542427382	4.97E-67	llmg_0230	A2RHU9	UP
MFS transporter CDS	2.638566766	1.77E-66	llmg_0070	A2RHE0	UP
trpS CDS	1.753925195	2.69E-66	llmg_0079	A2RHE9	UP
YkgJ family cysteine cluster protein CDS	2.654004219	1.16E-64	llmg_2449	A2RNW9	UP
PTS sugar transporter subunit IIB CDS	2.801808821	1.10E-61	llmg_0437	A2RIE6	UP
fibronectin-binding SSURE repeat-containing protein CDS	2.375409047	1.30E-53	llmg_1723	A2RLW9	UP
TetR/AcrR family transcriptional regulator CDS	2.671831524	6.58E-49	llmg_2517	A2RP34	UP
leucine-rich repeat domain-containing protein CDS	1.667671249	1.03E-46	llmg_0877	A2RJL9	UP
HU family DNA-binding protein CDS	1.793563811	1.39E-45	llmg_1661	A2RLR5	UP
MurR/RpiR family transcriptional regulator CDS	2.516661921	9.42E-44	llmg_0439	A2RIE8	UP
D-alanyl-D-alanine carboxypeptidase family protein CDS	1.397504683	5.76E-42	llmg_1578	A2RLI5	UP
trpB CDS	1.544992531	2.39E-40	llmg_1041	A2RK24	UP
U32 family peptidase CDS	1.798178592	2.66E-39	llmg_2243	A2RNC0	UP
phosphoglycerate mutase family protein CDS	1.234849537	1.10E-38	llmg_1579	A2RLI6	UP
cadA CDS	2.657573857	1.84E-38	llmg_0100	A2RHH1	UP
(Fe-S)-binding protein CDS	2.806712276	3.07E-37	llmg_1915	A2RMF4	UP
leuS CDS	1.376559079	4.84E-37	llmg_1741	A2RLY6	UP
valine--tRNA ligase CDS	1.28384835	1.03E-36	llmg_2455	A2RNX5	UP
hypothetical protein CDS	2.676787085	7.32E-35	llmg_0094	A2RHG5	UP
thiE CDS	2.355005596	2.61E-34	llmg_1218	A2RKJ7	UP
N-acetylmannosamine-6-phosphate 2-epimerase CDS	1.034156712	2.44E-33	llmg_1317	A2RKU2	UP

lactate utilization protein C CDS	2.535343704	5.28E-33	llmg_1917	A2RMF6	UP
LutB/LldF family L-lactate oxidation iron-sulfurprotein CDS	2.679001215	1.25E-32	llmg_1916	A2RMF5	UP
ATP-dependent RecD-like DNA helicase CDS	1.38594453	5.37E-31	llmg_1922	A2RMG1	UP
ileS CDS	1.260403571	5.99E-31	llmg_2053	A2RMT4	UP
thiD CDS	2.202647567	9.24E-31	llmg_1217	A2RKJ6	UP
class I SAM-dependent methyltransferase CDS	1.200720047	1.64E-30	llmg_2562	A2RP78	UP
IS3 family transposase CDS	1.151245949	3.34E-30	llmg_0122	A2RHJ3	UP
upp CDS	1.422848692	2.62E-29	llmg_2176	P50926	UP
ahpF CDS	1.007395675	6.58E-29	llmg_0357	A2RI69	UP
carbamoyl phosphate synthase small subunit CDS	3.065615087	1.63E-28	llmg_0894	Q9L4N5	UP
thiM CDS	2.191073299	2.50E-28	llmg_1216	A2RKJ5	UP
cell surface protein CDS	3.01727097	6.85E-28	llmg_0009	A2RH82	UP
hypothetical protein CDS	1.064748012	1.77E-27	llmg_1580	A2RLI7	UP
nuclear transport factor 2 family protein CDS	1.25510337	3.20E-27	llmg_0300	A2RI14	UP
PTS mannose/fructose/sorbose transporter subunitIIC CDS	1.202659772	6.59E-27	llmg_0728	A2RJ81	UP
glucose PTS transporter subunit IIA CDS	1.432654496	7.07E-27	llmg_1426	A2RL42	UP
IS3 family transposase CDS	1.169144375	1.41E-26	llmg_2174	A2RHJ3	UP
aspartate carbamoyltransferase catalytic subunit CDS	2.797107899	5.07E-26	llmg_0893	Q9L4N6	UP
nrdD CDS	1.146947622	9.30E-26	llmg_0281	A2RHZ6	UP
ParM/StbA family protein CDS	1.679484409	5.49E-25	llmg_1140	A2RKC4	UP
hypothetical protein CDS	1.461654812	8.01E-25	llmg_2423	A2RNU3	UP
nrdG CDS	1.165177405	9.57E-25	llmg_0282	A2RHZ7	UP
PTS system mannose/fructose/sorbose family transporter subunit IID CDS	1.187151079	6.28E-24	llmg_0727	A2RJ80	UP
pyrF CDS	2.40438586	1.91E-23	llmg_1107	P50924	UP
aminoacyl-tRNA deacylase CDS	2.253312687	3.18E-23	llmg_0333	A2RI46	UP
helix-turn-helix domain-containing protein CDS	3.287182385	8.88E-23	llmg_1507	A2RLB8	UP
polyprenyl synthetase family protein CDS	1.069442726	1.17E-22	llmg_1110	A2RK94	UP
thrB CDS	1.216994181	1.77E-22	llmg_1331	A2RKV6	UP
site-specific integrase CDS	1.396155679	1.77E-22	llmg_2268	A2RNE5	UP
hypothetical protein CDS	1.708915409	2.45E-22	llmg_0078	A2RHE8	UP
uracil-xanthine permease family protein CDS	2.485803196	5.30E-22	llmg_0891	A2RJN3	UP

phage repressor protein/antirepressor Ant CDS	2.403174292	1.85E-21	llmg_2134	A2RN14	UP
amino acid ABC transporter ATP-binding protein CDS	1.348398742	2.35E-21	llmg_1943	A2RMH9	UP
PTS sugar transporter subunit IIB CDS	1.312058549	3.34E-21	llmg_0729	A2RJ82	UP
NUDIX domain-containing protein CDS	1.225720244	3.44E-21	llmg_0872	A2RJL4	UP
MerR family transcriptional regulator CDS	1.129081181	4.82E-21	llmg_0301	A2RI15	UP
pyrR CDS	2.387502526	1.11E-20	llmg_0890	Q9L4N8	UP
hypothetical protein CDS	1.760907839	2.16E-20	llmg_2016	A2RMQ0	UP
pnuC CDS	1.103213064	2.50E-20	llmg_1664	A2RLR8	UP
NUDIX hydrolase CDS	1.667141665	2.63E-20	llmg_2510	A2RP27	UP
DeoR/GlpR family DNA-binding transcription regulator CDS	1.207822859	5.02E-20	llmg_1570	A2RLH7	UP
tyrS CDS	1.102932534	2.74E-19	llmg_0401	A2RIB1	UP
glycoside-pentoside-hexuronide (GPH):cation symporter CDS	2.24906033	6.26E-19	llmg_2237	A2RNB6	UP
ugpC CDS	2.005439752	1.34E-18	llmg_0446	A2RIF5	UP
hypothetical protein CDS	2.402339816	1.46E-18	llmg_1108	A2RK92	UP
alpha-amylase family glycosyl hydrolase CDS	2.602362707	2.90E-18	llmg_0743	A2RJ95	UP
alpha-glucosidase CDS	2.448824468	3.22E-18	llmg_0741	A2RJ93	UP
pgmB CDS	1.843641818	6.76E-18	llmg_0456	A2RIG5	UP
rpoC CDS	1.018314761	7.07E-18	llmg_1981	A2RML8	UP
nucleotide sugar dehydrogenase CDS	1.61280783	4.87E-17	llmg_1616	A2RLM1	UP
carB CDS	2.139684062	6.56E-17	llmg_1089	O32771	UP
dihydroorotate dehydrogenase CDS	2.11358206	6.74E-17	llmg_1106	P54322	UP
carbon starvation protein A CDS	1.145028417	8.50E-17	llmg_0430	A2RID9	UP
6-phospho-beta-glucosidase CDS	1.041937649	2.65E-16	llmg_0441	A2RIF0	UP
Rgg/GadR/MutR family transcriptional regulator CDS	1.02373175	3.74E-16	llmg_0069	A2RHD9	UP
Gx transporter family protein CDS	1.097416115	5.94E-16	llmg_1111	A2RK95	UP
nucleoside 2-deoxyribosyltransferase CDS	1.250710615	6.41E-16	llmg_0478	A2RII7	UP
dihydroorotase CDS	2.153830597	6.89E-16	llmg_1508	A2RLB9	UP
oligopeptide ABC transporter substrate-binding protein CDS	1.278554376	1.13E-15	llmg_2024	A2RMQ8	UP
NusG domain II-containing protein CDS	1.118212144	1.19E-15	llmg_1112	A2RK96	UP
extracellular solute-binding protein CDS	1.709556715	9.73E-15	llmg_1011	A2RJZ8	UP
sugar O-acetyltransferase CDS	2.528243451	1.04E-14	llmg_0742	A2RJ94	UP
trpA CDS	1.188372379	1.27E-14	llmg_1042	A2RK25	UP

thiT CDS	2.263530946	1.65E-14	llmg_0334	A2RI47	UP
glutamate decarboxylase CDS	1.181669691	2.18E-14	llmg_1179	O30418	UP
glycosyltransferase CDS	1.166357444	2.29E-14	llmg_1617	A2RLM2	UP
dihydroorotate dehydrogenase electron transfer subunit CDS	2.007425745	2.92E-14	llmg_1105	P56968	UP
lactonase family protein CDS	1.346384116	4.38E-14	llmg_2431	O86281	UP
MFS transporter CDS	1.026019752	1.63E-13	llmg_0523	A2RIN2	UP
MurR/RpiR family transcriptional regulator CDS	1.728806667	1.72E-13	llmg_0522	A2RIN1	UP
NUDIX hydrolase CDS	1.131184768	2.18E-13	llmg_0873	A2RJL5	UP
pfkB CDS	1.226449036	2.40E-13	llmg_1569	A2RLH6	UP
glycoside hydrolase family 65 protein CDS	2.032747595	2.85E-13	llmg_0455	A2RIG4	UP
hypothetical protein CDS	1.498824609	2.90E-13	llmg_1139	A2RKC3	UP
glycoside hydrolase family 13 protein CDS	1.014712706	4.78E-13	llmg_1869	A2RMB2	UP
TIGR00730 family Rossman fold protein CDS	1.12653616	4.86E-13	llmg_0479	A2RII8	UP
bifunctional phosphoribosyl-AMP cyclohydrolase/phosphoribosyl-ATP diphosphatase HisIE CDS	1.593654908	1.68E-12	llmg_1289	A2RKR6	UP
tetracycline resistance MFS efflux pump CDS	1.603424042	3.85E-12	llmg_0320	A2RI33	UP
peptide ABC transporter substrate-binding protein CDS	2.036522952	4.25E-12	llmg_0362	A2RI74	UP
bacterial Ig-like domain-containing protein CDS	2.116741257	6.49E-12	llmg_1506	A2RLB7	UP
alpha-glucosidase CDS	2.142050733	8.77E-12	llmg_0744	A2RJ96	UP
hypothetical protein CDS	1.458946965	2.39E-11	llmg_0101	A2RHH2	UP
sugar ABC transporter permease CDS	1.865389096	2.48E-11	llmg_0737	A2RJ89	UP
aminoglycoside 3'-phosphotransferase CDS	1.767143191	5.36E-11	llmg_1293	A2RKS0	UP
alpha-amylase family glycosyl hydrolase CDS	1.067721865	6.18E-11	llmg_0158	A2RHM9	UP
amino acid permease CDS	1.075279837	8.26E-11	llmg_0386	A2RI97	UP
DUF3440 domain-containing protein CDS	1.612582214	1.25E-10	llmg_1052	A2RK35	UP
hypothetical protein CDS	1.10193351	1.44E-10	llmg_0985	A2RJX2	UP
ParB/RepB/Spo0J family partition protein CDS	1.371202486	4.71E-10	llmg_1054	A2RK37	UP
glycosyltransferase family 2 protein CDS	1.29775056	6.18E-10	llmg_1620	A2RLM5	UP
phage antirepressor Ant CDS	1.20730951	9.85E-10	llmg_0797	A2RJE6	UP
manA CDS	1.014695997	1.58E-09	llmg_1789	A2RM34	UP
pyrE CDS	1.724812225	1.64E-09	llmg_1509	A2RLC0	UP
metal ABC transporter substrate-binding protein CDS	1.702340073	2.53E-09	llmg_1138	A2RKC2	UP

ilvC CDS	1.295377984	2.69E-09	llmg_1277	A2RKQ6	UP
dut CDS	1.107216549	3.03E-09	llmg_2114	A2RMZ4	UP
ilvA CDS	1.259906593	4.00E-09	llmg_1276	A2RKQ5	UP
aspartate kinase CDS	1.222578378	4.42E-09	llmg_1820	A2RM64	UP
ABC transporter permease CDS	1.23411691	6.59E-09	llmg_2025	A2RMQ9	UP
hypothetical protein CDS	1.766316775	7.28E-09	llmg_2133	A2RN13	UP
glycoside hydrolase family 65 protein CDS	1.543864266	7.76E-09	llmg_0745	A2RJ97	UP
hypothetical protein CDS	1.243221576	1.13E-08	llmg_2124	A2RN04	UP
glpK CDS	1.760998387	1.21E-08	llmg_1099	A2RK83	UP
hypothetical protein CDS	1.075544266	1.94E-08	llmg_2132	A2RN12	UP
gadC CDS	1.001027343	1.96E-08	llmg_1178	O30417	UP
extracellular solute-binding protein CDS	1.669502737	2.01E-08	llmg_0739	A2RJ91	UP
serB CDS	1.192532097	2.03E-08	llmg_0567	A2RIS4	UP
helix-turn-helix domain-containing protein CDS	1.180223221	2.07E-08	llmg_0008	A2RH81	UP
hisB CDS	1.834156206	5.07E-08	llmg_1294	A2RKS1	UP
AAA family ATPase CDS	1.649566079	7.53E-08	llmg_0805	A2RJF3	UP
type IV secretory system conjugative DNA transfer family protein CDS	1.132483077	8.53E-08	llmg_1383	A2RL04	UP
glycosyltransferase family 2 protein CDS	1.53957974	8.54E-08	llmg_1621	A2RLM6	UP
ssb CDS	1.598090256	1.39E-07	llmg_2126	A2RN06	UP
FMN-dependent NADH-azoreductase CDS	1.009064013	1.66E-07	llmg_0123	A2RHJ4	UP
murQ CDS	1.039876244	1.69E-07	llmg_1427	A2RL43	UP
Rad52/Rad22 family DNA repair protein CDS	1.372530009	1.82E-07	llmg_2128	A2RN08	UP
dhaL CDS	1.136428058	1.83E-07	llmg_0257	A2RHX4	UP
hypothetical protein CDS	1.35266863	2.37E-07	llmg_2544	A2RP60	UP
XcbB/CpsF family capsular polysaccharide biosynthesis protein CDS	1.141068775	2.86E-07	llmg_1618	A2RLM3	UP
hisF CDS	1.576844032	4.66E-07	llmg_1290	A2RKR7	UP
hisH CDS	1.681477979	4.92E-07	llmg_1292	A2RKR9	UP
hypothetical protein CDS	1.643670437	5.22E-07	llmg_0470	A2RIH9	UP
glycoside hydrolase family 1 protein CDS	1.224675531	7.84E-07	llmg_1738	A2RLY4	UP
anti-sigma factor CDS	1.263275209	8.10E-07	llmg_2447	A2RNW7	UP
glycerol-3-phosphate dehydrogenase/oxidase CDS	1.565214804	8.36E-07	llmg_1098	A2RK82	UP

hisD CDS	1.728185381	9.91E-07	llmg_1295	A2RKS2	UP
hypothetical protein CDS	1.55040556	1.06E-06	llmg_0806	A2RJF4	UP
amino acid permease CDS	1.432623681	1.18E-06	llmg_0118	A2RHI9	UP
hypothetical protein CDS	1.144882014	1.30E-06	llmg_2286	A2RNG3	UP
MFS transporter CDS	1.235719822	3.29E-06	llmg_0860	A2RJK3	UP
helix-turn-helix transcriptional regulator CDS	1.298265999	3.81E-06	llmg_0147	A2RHL8	UP
hypothetical protein CDS	1.095621569	3.94E-06	llmg_0442	A2RIF1	UP
sugar ABC transporter permease CDS	1.365264451	4.25E-06	llmg_0738	A2RJ90	UP
ABC transporter ATP-binding protein/permease CDS	1.126835451	4.80E-06	llmg_0329	A2RI42	UP
LysR family transcriptional regulator CDS	1.138899679	5.10E-06	llmg_0947	A2RJT5	UP
DUF1642 domain-containing protein CDS	1.343542676	6.86E-06	llmg_0815	A2RJG2	UP
phage replisome organiser protein CDS	1.152321514	7.13E-06	llmg_2125	A2RN05	UP
radical SAM protein CDS	1.670733931	7.38E-06	llmg_2436	A2RNV6	UP
ilvD CDS	1.190584061	8.20E-06	llmg_1280	A2RKQ9	UP
hisA CDS	1.401934586	9.31E-06	llmg_1291	A2RKR8	UP
acetyltransferase CDS	1.145118583	1.14E-05	llmg_1615	A2RLM0	UP
histidinol-phosphatase HisJ family protein CDS	1.238456987	1.37E-05	llmg_1288	A2RKR5	UP
DUF1642 domain-containing protein CDS	1.065994518	1.47E-05	llmg_2115	A2RMZ5	UP
hypothetical protein CDS	1.313983113	1.61E-05	llmg_2118	A2RMZ8	UP
ilvN CDS	1.250818648	2.59E-05	llmg_1278	A2RKQ7	UP
carbohydrate ABC transporter permease CDS	1.555946043	2.93E-05	llmg_1010	A2RJZ7	UP
ATP phosphoribosyltransferase regulatory subunit CDS	1.487709404	3.00E-05	llmg_1297	A2RKS4	UP
metal ABC transporter permease CDS	1.100848377	3.15E-05	llmg_1137	A2RKC1	UP
oligopeptide ABC transporter substrate-binding protein CDS	1.255776271	3.87E-05	llmg_0701	A2RJ53	UP
uxuA CDS	1.172341166	4.08E-05	llmg_0859	A2RJK2	UP
ABC transporter permease CDS	1.177209389	4.63E-05	llmg_2026	A2RMR0	UP
hypothetical protein CDS	1.104317596	4.81E-05	llmg_2119	A2RMZ9	UP
hypothetical protein CDS	1.352835811	5.66E-05	llmg_2129	A2RN09	UP
hypothetical protein CDS	1.09564379	6.03E-05	llmg_1619	A2RLM4	UP
PTS transporter subunit EIIC CDS	2.072227247	6.05E-05	llmg_0454	A2RIG3	UP
acetolactate synthase large subunit CDS	1.030844386	6.73E-05	llmg_1279	A2RKQ8	UP
glutamate synthase subunit beta CDS	1.09993376	7.93E-05	llmg_1184	A2RKG7	UP

hypothetical protein CDS	1.385621947	8.14E-05	llmg_0811	A2RJF8	UP
pepO CDS	1.124810256	9.87E-05	llmg_0702	A2RJ54	UP
hisC CDS	1.390629444	0.000107124	llmg_1298	A2RKS5	UP
hypothetical protein CDS	1.055223276	0.000129992	llmg_2251	A2RNC8	UP
sugar O-acetyltransferase CDS	1.062571324	0.000177521	llmg_1182	A2RKG5	UP
hypothetical protein CDS	1.449294342	0.000179476	llmg_2435	A2RNV5	UP
hisG CDS	1.474452352	0.000194768	llmg_1296	A2RKS3	UP
VOC family protein CDS	1.028556586	0.000227062	llmg_1037	A2RK20	UP
tyrosine-type recombinase/integrase CDS	1.241561462	0.000237425	llmg_0618	A2RIX2	UP
hypothetical protein CDS	1.389557301	0.000274725	llmg_0468	A2RIH7	UP
asnB CDS	1.038248609	0.000279219	llmg_0372	A2RI83	UP
hypothetical protein CDS	1.823357845	0.000304481	llmg_0796	A2RJE5	UP
hypothetical protein CDS	1.14977544	0.000347711	llmg_2116	A2RMZ6	UP
ATP-binding protein CDS	1.07906508	0.000433483	llmg_0808	A2RJF6	UP
PTS glucose transporter subunit IIA CDS	2.27835757	0.000634182	llmg_0453	A2RIG2	UP
PTS-dependent dihydroxyacetone kinase phosphotransferase subunit DhaM CDS	1.019632453	0.00073249	llmg_0258	A2RHX5	UP
hypothetical protein CDS	1.284360157	0.000739138	llmg_0328	A2RI41	UP
host-nuclease inhibitor Gam family protein CDS	1.427206515	0.000781299	llmg_0804	A2RJF2	UP
oppC CDS	1.054239916	0.001152854	llmg_0700	A2RJ52	UP
hypothetical protein CDS	1.524206575	0.002303878	llmg_0819	A2RJG6	UP
bifunctional 4-hydroxy-2-oxoglutarate aldolase/2-dehydro-3-deoxy-phosphogluconate aldolase CDS	1.31285818	0.003083906	llmg_0864	A2RJK6	UP
MFS transporter CDS	1.243064342	0.00382939	llmg_2066	A2RMU7	UP
ROK family protein CDS	1.10490309	0.004735153	llmg_1241	A2RKM0	UP
helix-turn-helix transcriptional regulator CDS	1.514345544	0.005002318	llmg_2135	A2RN15	UP
MFS transporter CDS	1.656461576	0.007353494	llmg_2439	A2RNV8	UP
phage portal protein CDS	1.222512794	0.009493243	llmg_2098	A2RMX9	UP
L-lactate dehydrogenase CDS	1.056729399	0.010501114	llmg_0392	P0CI34	UP
hypothetical protein CDS	1.139344968	0.014229628	llmg_1614	A2RLL9	UP
PTS sugar transporter subunit IIB CDS	1.019857512	0.049770589	llmg_0866	A2RJK8	UP
mgtA CDS	-2.379504765	9.44E-155	llmg_1223	A2RKK2	DOWN
C40 family peptidase CDS	-3.378156345	8.73E-86	llmg_1594	A2RLK0	DOWN

transglycosylase CDS	-2.371642175	5.06E-66	llmg_0760	A2RJB2	DOWN
3D domain-containing protein CDS	-1.947601921	3.59E-65	llmg_2194	A2RN73	DOWN
hypothetical protein CDS	-4.80140021	9.63E-64	llmg_1677	A2RLT0	DOWN
DUF4097 domain-containing protein CDS	-3.411699062	5.43E-59	llmg_2164	A2RN44	DOWN
PspC domain-containing protein CDS	-2.977008238	1.58E-58	llmg_2163	A2RN43	DOWN
peptide ABC transporter substrate-binding protein CDS	-1.265921735	2.37E-48	llmg_0507	A2RIL6	DOWN
ftsE CDS	-1.286438817	1.23E-47	llmg_1546	A2RLF4	DOWN
arcC CDS	-1.642656191	1.71E-46	llmg_2309	A2RNI3	DOWN
amino acid permease CDS	-1.665530839	9.99E-44	llmg_2011	A2RMP5	DOWN
NADPH-dependent F420 reductase CDS	-1.242306768	8.12E-38	llmg_0880	A2RJM2	DOWN
FMN-dependent NADH-azoreductase CDS	-1.436052723	5.02E-36	llmg_0397	A2RIA7	DOWN
amino acid ABC transporter substrate-binding protein CDS	-1.23554097	2.20E-35	llmg_2330	A2RNK3	DOWN
ftsX CDS	-1.203841511	4.85E-35	llmg_1545	A2RLF3	DOWN
toxic anion resistance protein CDS	-1.952458467	3.33E-33	llmg_1116	A2RKA0	DOWN
argF CDS	-2.268811833	2.63E-32	llmg_2312	Q9K575	DOWN
pflB CDS	-1.547786877	1.43E-31	llmg_0629	O32799	DOWN
mraY CDS	-1.209375378	2.13E-31	llmg_1678	A2RLT1	DOWN
HD domain-containing protein CDS	-1.665163603	1.01E-30	llmg_1920	A2RMF9	DOWN
CHAP domain-containing protein CDS	-1.089172023	5.04E-30	llmg_2507	P22865	DOWN
LPXTG cell wall anchor domain-containing protein CDS	-1.42155361	3.57E-29	llmg_1127	A2RKB1	DOWN
SPFH domain-containing protein CDS	-1.157079812	2.78E-27	llmg_1103	A2RK87	DOWN
C39 family peptidase CDS	-1.090984197	7.34E-27	llmg_0482	A2RIJ1	DOWN
hypothetical protein CDS	-2.531001006	1.28E-26	llmg_0458	A2RIG7	DOWN
response regulator transcription factor CDS	-1.107251081	2.86E-25	llmg_1929	A2RMG8	DOWN
hypothetical protein CDS	-3.714407589	7.79E-25	llmg_0169	A2RHN9	DOWN
dltA CDS	-1.27901832	1.14E-24	llmg_1219	A2RKJ8	DOWN
5-bromo-4-chloroindolyl phosphate hydrolysis family protein CDS	-2.538613734	1.42E-24	llmg_1115	A2RK99	DOWN
metal-dependent transcriptional regulator CDS	-1.030304401	7.35E-24	llmg_1224	A2RKK3	DOWN
cell wall-active antibiotics response protein LiaF CDS	-2.189930033	8.43E-24	llmg_1650	A2RLQ4	DOWN
yidC CDS	-1.023396095	3.90E-23	llmg_0540	A2RIP8	DOWN
heavy metal-binding domain-containing protein CDS	-1.330520846	4.98E-23	llmg_1596	A2RLK2	DOWN

arcC CDS	-1.271611012	5.10E-23	llmg_2310	A2RNI4	DOWN
ASCH domain-containing protein CDS	-1.131538509	5.85E-23	llmg_1597	A2RLK3	DOWN
CvpA family protein CDS	-1.093209946	2.06E-22	llmg_0777	A2RJC7	DOWN
response regulator transcription factor CDS	-1.769859243	2.99E-22	llmg_0747	A2RJ99	DOWN
hypothetical protein CDS	-1.182497906	6.33E-22	llmg_0229	A2RHU8	DOWN
rsmH CDS	-1.15128438	6.61E-22	llmg_1681	A2RLT4	DOWN
hypothetical protein CDS	-1.335215787	1.48E-21	llmg_1269	A2RKP8	DOWN
PadR family transcriptional regulator CDS	-1.544521248	2.28E-21	llmg_0323	A2RI36	DOWN
LysR family transcriptional regulator CDS	-1.280866172	2.57E-21	llmg_1674	A2RLS7	DOWN
Spx-like protein CDS	-2.675123345	4.89E-21	llmg_1155	A2RKD9	DOWN
amino acid ABC transporter substrate-binding protein CDS	-1.364494394	5.04E-21	llmg_1593	A2RLJ9	DOWN
glyoxalase CDS	-1.974807939	6.92E-21	llmg_0552	A2RIQ9	DOWN
glmS CDS	-1.57312558	2.21E-20	llmg_1516	A2RLC5	DOWN
arcA CDS	-1.886595178	7.47E-20	llmg_2313	Q9K576	DOWN
basic amino acid/polyamine antiporter CDS	-1.280176914	2.34E-19	llmg_2311	A2RNI5	DOWN
tgt CDS	-1.059032141	3.09E-19	llmg_0164	A2RHN5	DOWN
MucBP domain-containing protein CDS	-1.45090308	8.34E-19	llmg_2465	A2RNY4	DOWN
mvk CDS	-1.034351767	2.46E-18	llmg_0425	A2RID4	DOWN
secG CDS	-1.020815985	4.99E-18	llmg_1587	A2RLJ4	DOWN
LysR family transcriptional regulator CDS	-1.174755177	6.24E-18	llmg_0390	A2RIA1	DOWN
M20 peptidase aminoacylase family protein CDS	-2.660653286	7.97E-18	llmg_1571	A2RLH8	DOWN
tRNA (cytidine(34)-2'-O)-methyltransferase CDS	-1.345999994	9.28E-18	llmg_1343	A2RKW7	DOWN
diacylglycerol kinase family lipid kinase CDS	-1.193994786	1.05E-17	llmg_1919	A2RMF8	DOWN
hypothetical protein CDS	-1.192665922	1.78E-17	llmg_2051	A2RMT2	DOWN
DegV family EDD domain-containing protein CDS	-2.016423149	1.85E-17	llmg_1301	A2RKS8	DOWN
acyl carrier protein CDS	-1.078249218	2.16E-17	llmg_1786	A2RM31	DOWN
ATP-binding protein CDS	-1.129881192	3.89E-17	llmg_1518	A2RLC7	DOWN
bacterial Ig-like domain-containing protein CDS	-1.891271384	3.91E-17	llmg_1152	A2RKD6	DOWN
hypothetical protein CDS	-1.432254001	4.77E-17	llmg_1663	A2RLR7	DOWN
xerS CDS	-1.419222501	7.04E-17	llmg_1268	A2RKP7	DOWN
class I SAM-dependent methyltransferase CDS	-1.228205482	1.17E-16	llmg_1026	A2RK11	DOWN
GNAT family N-acetyltransferase CDS	-1.211805549	1.56E-16	llmg_1076	A2RK60	DOWN

DUF1295 domain-containing protein CDS	-1.831496473	3.96E-16	llmg_1299	A2RKS6	DOWN
DUF3272 family protein CDS	-1.06458089	5.39E-16	llmg_0581	A2RIT5	DOWN
hypothetical protein CDS	-2.553867788	5.94E-16	llmg_0090	A2RHG1	DOWN
RNA-binding S4 domain-containing protein CDS	-1.268513478	6.77E-16	llmg_0015	A2RH87	DOWN
C39 family peptidase CDS	-1.055906254	2.57E-15	llmg_0481	A2RIJ0	DOWN
topA CDS	-1.160393162	4.94E-15	llmg_1272	A2RKQ1	DOWN
hypothetical protein CDS	-2.109393982	5.77E-15	llmg_0639	A2RIZ3	DOWN
carboxymuconolactone decarboxylase family protein CDS	-1.115818654	5.97E-15	llmg_0970	A2RJV7	DOWN
DUF2255 family protein CDS	-1.113361387	9.29E-15	llmg_0969	A2RJV6	DOWN
hypothetical protein CDS	-1.120226311	1.04E-14	llmg_2009	A2RMP3	DOWN
hypothetical protein CDS	-1.049662339	1.10E-14	llmg_1498	A2RLA9	DOWN
NAD(P)-dependent oxidoreductase CDS	-1.08864195	1.88E-14	llmg_1759	A2RM04	DOWN
metallophosphoesterase CDS	-1.673726193	4.30E-14	llmg_0903	A2RJP4	DOWN
AzlC family ABC transporter permease CDS	-1.368154941	8.67E-14	llmg_0881	A2RJM3	DOWN
plsY CDS	-1.166784346	1.93E-13	llmg_1540	A2RLE8	DOWN
mutM CDS	-1.002263346	1.98E-13	llmg_0373	A2RI84	DOWN
spx CDS	-1.098897579	2.87E-13	llmg_0640	P60376	DOWN
ABC transporter permease CDS	-2.453376245	3.06E-13	llmg_1676	A2RLS9	DOWN
DUF2127 domain-containing protein CDS	-1.064075718	3.26E-13	llmg_1519	A2RLC8	DOWN
acetolactate decarboxylase CDS	-1.341462702	6.14E-13	llmg_1464	A2RL77	DOWN
DUF6287 domain-containing protein CDS	-2.528861432	1.40E-12	llmg_2554	A2RP70	DOWN
PH domain-containing protein CDS	-1.553605479	1.47E-12	llmg_0602	A2RIV5	DOWN
GNAT family N-acetyltransferase CDS	-1.453806601	1.57E-12	llmg_1669	A2RLS3	DOWN
LTA synthase family protein CDS	-1.335541859	1.58E-12	llmg_1751	A2RLZ6	DOWN
helix-turn-helix transcriptional regulator CDS	-1.168879154	2.14E-12	llmg_0353	A2RI65	DOWN
MerR family transcriptional regulator CDS	-1.054548839	2.66E-12	llmg_1020	A2RK06	DOWN
hypothetical protein CDS	-1.006819548	3.14E-12	llmg_1344	A2RKW8	DOWN
DUF3042 family protein CDS	-1.078026546	5.11E-12	llmg_1050	A2RK33	DOWN
DUF4395 domain-containing protein CDS	-1.784459873	5.25E-12	llmg_1066	A2RK49	DOWN
Rgg/GadR/MutR family transcriptional regulator CDS	-1.0176188	1.65E-11	llmg_1804	A2RM48	DOWN
SDR family oxidoreductase CDS	-1.049310942	1.85E-11	llmg_0968	A2RJV5	DOWN
dltB CDS	-1.038893698	2.07E-11	llmg_1220	A2RKJ9	DOWN

VanZ family protein CDS	-1.091322543	2.66E-11	llmg_1930	A2RMG9	DOWN
DUF3397 domain-containing protein CDS	-1.12821583	2.88E-11	llmg_0331	A2RI44	DOWN
MerR family transcriptional regulator CDS	-1.587839968	4.59E-11	llmg_0572	A2RIS8	DOWN
sensor histidine kinase CDS	-1.218696879	5.36E-11	llmg_1649	Q7BPI7	DOWN
DUF2177 family protein CDS	-2.158876632	1.32E-10	llmg_1302	A2RKS9	DOWN
arsenic metallochaperone ArsD family protein CDS	-1.33820761	1.62E-10	llmg_1156	A2RKE0	DOWN
cold-shock protein CDS	-1.248417141	1.66E-10	llmg_1238	A2RKL8	DOWN
gap CDS	-1.207572351	2.77E-10	llmg_0530	A2RIN9	DOWN
TIGR02328 family protein CDS	-1.534444103	3.78E-10	llmg_0905	A2RJP6	DOWN
SDR family NAD(P)-dependent oxidoreductase CDS	-1.954719546	4.72E-10	llmg_0087	A2RHF7	DOWN
amino acid permease CDS	-1.176124752	9.77E-10	llmg_1747	A2RLZ2	DOWN
hypothetical protein CDS	-1.070494922	1.49E-09	llmg_0379	A2RI90	DOWN
antibiotic biosynthesis monooxygenase CDS	-1.195003015	1.53E-09	llmg_0971	A2RJV8	DOWN
YhgE/Pip domain-containing protein CDS	-1.190400184	6.33E-09	llmg_0752	A2RJA4	DOWN
cystathionine gamma-synthase CDS	-1.014934915	1.17E-08	llmg_1776	A2RM21	DOWN
arsD CDS	-1.293500303	1.85E-08	llmg_1247	A2RKM6	DOWN
cold-shock protein CDS	-1.199584146	1.85E-08	llmg_1846	A2RM90	DOWN
pyridoxamine 5'-phosphate oxidase family protein CDS	-1.343101371	2.58E-08	llmg_2395	A2RNR7	DOWN
phosphatase PAP2 family protein CDS	-1.063106579	3.11E-08	llmg_1517	A2RLC6	DOWN
YlbF family regulator CDS	-1.031511844	5.24E-08	llmg_0377	A2RI88	DOWN
hypothetical protein CDS	-3.138421917	5.46E-08	llmg_0086	A2RHF6	DOWN
arsC CDS	-1.259489433	5.57E-08	llmg_0902	A2RJP3	DOWN
argF CDS	-1.424121217	6.86E-08	llmg_1754	A2RLZ9	DOWN
hypothetical protein CDS	-1.006148387	7.53E-08	llmg_0800	A2RJE8	DOWN
tryptophan-rich sensory protein CDS	-1.877317029	7.54E-08	llmg_1303	A2RKT0	DOWN
ABC transporter ATP-binding protein CDS	-1.103216093	9.59E-08	llmg_1553	A2RLG1	DOWN
YdbC family protein CDS	-1.041039976	2.02E-07	llmg_0327	A2RI40	DOWN
CopY/TcrY family copper transport repressor CDS	-1.000517187	2.26E-07	llmg_1731	A2RLX7	DOWN
glucosamine-6-phosphate deaminase CDS	-1.000816152	2.82E-07	llmg_0928	A2RJR7	DOWN
VOC family protein CDS	-1.735729717	3.85E-07	llmg_1652	A2RLQ6	DOWN
MFS transporter CDS	-1.12460053	4.25E-07	llmg_1104	A2RK88	DOWN
M50 family metallopeptidase CDS	-1.465756832	4.63E-07	llmg_0889	A2RJN1	DOWN

amino acid permease CDS	-1.122339269	5.08E-07	llmg_2477	A2RNZ6	DOWN
YxeA family protein CDS	-1.248108611	1.08E-06	llmg_1933	A2RMH1	DOWN
putative DNA-binding protein CDS	-1.043660551	1.29E-06	llmg_1069	A2RK52	DOWN
cation-transporting P-type ATPase CDS	-1.520592351	2.16E-06	llmg_0643	A2RIZ7	DOWN
cold shock domain-containing protein CDS	-1.482582856	2.16E-06	llmg_1255	A2RKN4	DOWN
hypothetical protein CDS	-1.088742476	2.48E-06	llmg_0801	A2RJE9	DOWN
PadR family transcriptional regulator CDS	-1.497919967	2.55E-06	llmg_0709	A2RJ61	DOWN
cold-shock protein CDS	-1.684550265	3.49E-06	llmg_1847	A2RM91	DOWN
zinc ribbon domain-containing protein CDS	-1.129781478	3.51E-06	llmg_1852	A2RM96	DOWN
metalloregulator ArsR/SmtB family transcription factor CDS	-1.421670183	3.94E-06	llmg_1246	A2RKM5	DOWN
hypothetical protein CDS	-1.0641824	4.37E-06	llmg_1848	A2RM92	DOWN
cysK CDS	-1.216441553	4.53E-06	llmg_0508	A2RIL7	DOWN
hpt CDS	-1.147723263	7.39E-06	llmg_0993	A2RJX9	DOWN
NAD(P)-dependent oxidoreductase CDS	-1.128141208	8.20E-06	llmg_2003	A2RMN7	DOWN
DUF421 domain-containing protein CDS	-1.289249696	1.04E-05	llmg_2393	A2RNR5	DOWN
YxeA family protein CDS	-2.108434901	1.90E-05	llmg_1079	A2RK63	DOWN
DUF3883 domain-containing protein CDS	-1.313388698	1.95E-05	llmg_1160	A2RKE3	DOWN
basic amino acid/polyamine antiporter CDS	-1.127755758	2.11E-05	llmg_2307	A2RNI1	DOWN
argB CDS	-1.413186606	4.10E-05	llmg_1755	A2RM00	DOWN
acetylornithine transaminase CDS	-1.458484332	4.10E-05	llmg_1756	A2RM01	DOWN
hypothetical protein CDS	-1.043369934	4.28E-05	llmg_0833	A2RJH7	DOWN
TMEM175 family protein CDS	-1.27866792	7.59E-05	llmg_1684	A2RLT7	DOWN
argJ CDS	-1.415370818	9.35E-05	llmg_1757	A2RM02	DOWN
FAD-dependent oxidoreductase CDS	-1.249787194	0.000106185	llmg_0408	A2RIB7	DOWN
site-specific integrase CDS	-1.320881987	0.000180064	llmg_0594	A2RIU7	DOWN
phnC CDS	-1.454613085	0.000213471	llmg_0313	A2RI26	DOWN
lysozyme CDS	-1.018012341	0.000259074	llmg_2082	A2RMW3	DOWN
ComF family protein CDS	-1.16665846	0.000259134	llmg_1484	A2RL95	DOWN
hypothetical protein CDS	-1.954320511	0.000372019	llmg_0595	A2RIU8	DOWN
lipoprotein BA 5634 family protein CDS	-1.035439407	0.00039932	llmg_0551	A2RIQ8	DOWN
hypothetical protein CDS	-1.053010696	0.00039932	llmg_0686	A2RJ38	DOWN
DUF2089 family protein CDS	-1.974288933	0.000447915	llmg_0708	A2RJ60	DOWN

hypothetical protein CDS	-1.110075864	0.000479797	llmg_0675	A2RJ26	DOWN
hypothetical protein CDS	-1.255605491	0.000525854	llmg_0685	A2RJ37	DOWN
AMP-binding protein CDS	-1.288785431	0.000582591	llmg_1965	A2RMK0	DOWN
nitroreductase family protein CDS	-1.013222481	0.000584181	llmg_2172	A2RN51	DOWN
Abi family protein CDS	-1.333237824	0.000636858	llmg_0852	A2RJJ5	DOWN
ABC transporter ATP-binding protein CDS	-1.812952569	0.00073374	llmg_1675	A2RLS8	DOWN
prolyl-tRNA editing protein CDS	-1.449707297	0.000917888	llmg_2306	A2RNI0	DOWN
MarR family transcriptional regulator CDS	-1.976602443	0.001195377	llmg_1860	A2RMA3	DOWN
Cof-type HAD-IIB family hydrolase CDS	-1.07526791	0.001620054	llmg_2426	A2RNU6	DOWN
hypothetical protein CDS	-1.736589765	0.001869263	llmg_1254	A2RKN3	DOWN
flavodoxin CDS	-1.881005883	0.002018507	llmg_1859	A2RMA2	DOWN
GNAT family N-acetyltransferase CDS	-1.304517693	0.002429282	llmg_1174	A2RKF7	DOWN
SugE family quaternary ammonium compound efflux SMR transporter CDS	-1.042736144	0.002523718	llmg_0132	A2RHK3	DOWN
antibiotic biosynthesis monooxygenase CDS	-1.705149979	0.002766566	llmg_0553	A2RIR0	DOWN
hypothetical protein CDS	-1.276762134	0.002817644	llmg_0673	A2RJ24	DOWN
purN CDS	-1.187181742	0.003373018	llmg_0988	A2RJX5	DOWN
Rha family transcriptional regulator CDS	-1.321475938	0.003373018	llmg_2261	A2RND8	DOWN
Rgg/GadR/MutR family transcriptional regulator CDS	-1.176726868	0.004842964	llmg_1143	A2RKC7	DOWN
purK CDS	-1.571021719	0.005049795	llmg_1000	A2RJY7	DOWN
purF CDS	-1.79829718	0.005436907	llmg_0977	A2RJW4	DOWN
phosphate/phosphite/phosphonate ABC transporter substrate-binding protein CDS	-1.411162666	0.006773121	llmg_0312	A2RI25	DOWN
MazG-like protein CDS	-1.064179341	0.008377289	llmg_0899	A2RJP0	DOWN
HAD-IIB family hydrolase CDS	-1.389609445	0.008976425	llmg_0998	A2RJY5	DOWN
hypothetical protein CDS	-1.138593428	0.009027138	llmg_2136	A2RN16	DOWN
lmrA CDS	-1.512277907	0.009135039	llmg_1856	P97046	DOWN
purL CDS	-1.691035589	0.010808209	llmg_0976	A2RJW3	DOWN
phnE CDS	-1.412780473	0.01103987	llmg_0314	A2RI27	DOWN
helix-turn-helix domain-containing protein CDS	-1.150042763	0.015272068	llmg_0925	A2RJR4	DOWN
helix-turn-helix transcriptional regulator CDS	-1.189892519	0.01727015	llmg_0681	A2RJ32	DOWN
purQ CDS	-1.562674643	0.018225298	llmg_0975	A2RJW2	DOWN
ABC transporter ATP-binding protein CDS	-1.165500671	0.020424491	llmg_0501	A2RIL0	DOWN

purH CDS	-1.357997349	0.022742901	llmg_0994	A2RJY0	DOWN
phosphoribosylaminoimidazolesuccinocarboxamide synthase CDS	-1.462754372	0.02321929	llmg_0973	A2RJW0	DOWN
purE CDS	-1.327886976	0.024610003	llmg_0999	A2RJY6	DOWN
purS CDS	-1.442757785	0.029810436	llmg_0974	A2RJW1	DOWN
hypothetical protein CDS	-1.056833252	0.03080053	llmg_0060	A2RHD1	DOWN
hypothetical protein CDS	-1.512774672	0.033684301	llmg_0597	A2RIV0	DOWN
argC CDS	-1.275506185	0.034908548	llmg_1758	A2RM03	DOWN
sigma-70 family RNA polymerase sigma factor CDS	-1.332031626	0.041181923	llmg_0026	A2RH98	DOWN
hypothetical protein CDS	-1.122201809	0.042345855	llmg_0039	A2RHB1	DOWN